
**A molecular basis of ELF3 action
in the Arabidopsis circadian clock**

Inaugural-Dissertation

zur

Erlangung des Doktorgrades
der Mathematisch-Naturwissenschaftlichen Fakultät
der Universität zu Köln

vorgelegt von

Eva Herrero Serrano
aus Vitoria, Spanien

Köln 2011

Die vorliegende Arbeit am Max-Planck Institut für Pflanzenzüchtungsforschung Köln, in der Arbeitsgruppe von Dr. Seth J. Davis, Abteilung für Entwicklungsbiologie der Pflanzen (Direktor Prof. Dr. George Coupland) angefertigt.

Berichterstatter: Prof. Dr. George Coupland
Prof. Dr. Ute Höcker

Prüfungsvorsitzender: Prof. Dr. Martin Hülskamp
Tag der mündlichen Prüfung 20 Mai 2011

Abstract

The circadian clock anticipates daily environmental changes and optimizes timing of physiological events. Circadian systems are present in most living organisms. In *Arabidopsis*, circadian components are arranged in positive/negative regulatory feed-back loops. The core loop is arranged by the morning transcription factors *LHY* and *CCA1*, and the evening pseudo-response regulator *TOC1*. The morning loop reciprocally connects *LHY* and *CCA1* to the *TOC1*-sequence-related components *PRR9* and *PRR7*. Other genes, when mutated, display a clock phenotype, but not all of such genes have been placed into the clock model. For instance, three evening genes, *ELF3*, *ELF4*, and *LUX*, have been found to be essential for circadian function. Clock- and light-signaling networks are tightly interconnected. Light input to the clock is mediated by photoreceptors, such as the phytochromes. *ELF3* and *ELF4* play a pivotal role in the generation of circadian rhythms and in the integration of light signal to the clock mechanism. Both encoded proteins are reported to be located in the nucleus, and both the *elf3* and the *elf4* mutants display a similarly arrested clock.

In this thesis, *ELF3* was found to be genetically downstream of *ELF4* within the same clock signaling pathway required to sustain circadian rhythms. Moreover, I found that *ELF3* and *ELF4* proteins physically interact. This interaction correlated with an increase of *ELF3* nuclear localization. These observations are consistent with a role of *ELF4* as an effector that promotes *ELF3* activity to lengthen circadian periodicity. A functional complementation approach identified three functional modules in the *ELF3* encoded protein. The N-terminus and middle domains mediate interaction with phyB and *ELF4*, respectively. The C-terminus domain was found to be required for *ELF3* nuclear localization. Thus, *ELF3* is a multifunctional protein that interacts with both light-signaling and clock components.

The molecular function of *ELF3* had previously remained elusive. *PRR9* expression was found to be down-regulated in *ELF3* and *ELF4* over-expressors. Interestingly, I found that *ELF3* physically associated with the same conserved region in the *PRR9* promoter as the transcription factor *LUX*. I found that *LUX* was genetically downstream of *ELF4*, and that *LUX* required *ELF3*. Taken together, I proposed that *ELF3*, *ELF4*, and *LUX* are part of an evening-clock complex required to repress *PRR9* expression, and to sustain circadian oscillations.

ELF3 has been reported to be crucial to buffer light input to the oscillator. Photoreceptors and *ELF3* play an opposite role in light-mediated acceleration of circadian periodicity, where photoreceptors shortens, and *ELF3* lengthens, circadian period under constant light. Interestingly, I found that the N-terminus of ELF3 was not essential for ELF3 circadian function, but that mediated the physical interaction of ELF3 to phyB. An *elf3* complementation line deleted for its N-terminus displayed hyposensitivity to the period-shortening effect induced by constant-red light. Therefore, I hypothesized that phyB interaction to the N-terminus of ELF3 mediates light-repression of ELF3 action in circadian-periodicity.

In chapter 4, further characterization of the weak allele *elf3-12* supported the role of ELF3 as a decelerator of circadian periodicity. The *elf3-12* mutation encodes an amino-acid replacement in a conserved box within the ELF4-binding domain. The *elf3-12* coding region led to robust expression of ELF3-12 protein, and ELF3-12 retained the capacity to bind both ELF4 and phyB. *elf3-12* displayed light-dependent short-period phenotype that was enhanced by phytochrome over-expression. Moreover, *elf3-12* displayed hypersensitive to red-light-resetting pulses. Thus, I found that *elf3-12* is attenuated in its function to repress light input to the clock and/or and increased phy-mediated repression of ELF3 function. *elf3-12* was the first described *elf3* weak allele. My characterization of a collection of *elf3* TILLING alleles led to the identification of novel short- and long-period alleles that I predict will expand current understanding of the role of ELF3 as an integrator of light signals and as a core-clock component.

Taken together, my thesis has placed ELF3 within the circadian mechanism. *ELF3*, *ELF4*, and *LUX* are part of an evening-repressor complex required to sustain circadian function. The genetic interaction of these three genes is consistent with a hierarchy of complex assembly. In this, I propose that ELF4 works as an effector protein that activates ELF3, possibly by increasing the ELF3 nuclear pool. Then, the association of both ELF3 and LUX to the *PRR9* promoter is required for transcriptional repression of *PRR9*. Additionally, I propose that ELF3 function in circadian periodicity is modulated by its interaction partners by a competition between a positive effect of ELF4 and a light-mediated-negative effect of phyB. This is consistent with ELF3 being a multifunctional protein that integrates light signals as a core-oscillator component.

Zusammenfassung

Die innere zirkadiane Uhr antizipiert die täglichen Umweltveränderungen und optimiert die zeitliche Koordinierung physiologischer Abläufe. Zirkadiane Systeme existieren in den meisten lebenden Organismen. In der Modellpflanze *Arabidopsis* sind die Komponenten der zirkadianen Uhr in positiv/negativen Rückkopplungsschleifen arrangiert. Der sogenannte Morgenschaltkreis besteht aus den Transkriptionsfaktoren *LHY* und *CCA1*, sowie dem abends expremierten Pseudo-response Regulator *TOC1*. Der morgendliche Schaltkreis verbindet reziprok *LHY* und *CCA1* mit den Komponenten *PRR9* und *PRR7*, deren Sequenzen mit der von *TOC1* verwandt sind. Andere Gene zeigen bei Mutation ebenfalls einen Phänotyp bezüglich der zirkadianen Uhr, aber nicht alle von ihnen sind bisher in das Modell der inneren Uhr integriert worden. So sind beispielsweise die drei abends expremierten Gene *ELF3*, *ELF4* und *LUX* essentiell für die Funktion der inneren Uhr. Die Netzwerke der inneren Uhr und des Lichtsignalweges sind eng miteinander verbunden. Das Lichtsignal wird über Photorezeptoren, wie beispielsweise die Phytochrome, an die innere Uhr weitergegeben. *ELF3* und *ELF4* spielen dabei eine ausschlaggebende Rolle bei der Erzeugung von zirkadianen Rhythmen, aber auch bei der Integration von Lichtsignalen in das System der zirkadianen Uhr. Von beiden Proteinen wird berichtet, dass sie im Nukleus lokalisiert sind. Mutanten beider Gene zeigen eine ähnlichen Phänotyp, der eine Arretierung der inneren Uhr zur Folge hat.

In dieser Dissertation konnte gezeigt werden, dass *ELF3* genetisch *downstream* von *ELF4* im selben Signalweg der inneren Uhr arbeitet und dazu benötigt wird die zirkadiane Rhythmik aufrecht zu erhalten. Darüber hinaus wurde gezeigt, dass die Proteine *ELF3* und *ELF4* physisch miteinander interagieren. Diese Interaktion korrelierte mit einer vermehrten Lokalisation von *ELF3* im Zellkern. Diese Beobachtungen decken sich mit dem Effekt, dass *ELF4* die Aktivität von *ELF3* fördert und dadurch die zirkadiane Periode verlängert. Mit Hilfe eines funktionellen Komplementierungsansatzes konnten drei funktionelle Abschnitte im *ELF3* Protein identifiziert werden. Der N-Terminus vermittelt die Interaktion mit *PhyB*, während der mittlere Proteinabschnitt für die Interaktion mit *ELF4* verantwortlich ist. Für den C-Terminus konnte festgestellt werden, dass er für die Lokalisierung von *ELF3* im Nukleus verantwortlich ist. Daraus folgt, dass *ELF3* ein multifunktionelles Protein ist, das sowohl mit dem Lichtsignalweg als auch mit Komponenten der inneren Uhr interagiert.

Die molekulare Funktion von ELF3 war bisher unbekannt. Man wusste lediglich, dass die Expression von *PRR9* in Überexpressoren von *ELF3* und *ELF4* verringert war. Interessanter Weise konnte in dieser Arbeit gezeigt werden, dass ELF3 physisch mit der selben konservierten Region im *PRR9* Promotor interagiert wie der Transkriptionsfaktor LUX. Außerdem konnte gezeigt werden, dass *LUX* genetisch *downstream* von *ELF4* arbeitet und dass *LUX* *ELF3* benötigt um zu funktionieren. Zusammenfassend lässt sich daher annehmen, dass *ELF3*, *ELF4* und *LUX* Teil eines abends gebildeten Komplexes der inneren Uhr sind, der benötigt wird um die Expression von *PRR9* zu verhindern und daher für die Aufrechterhaltung von zirkadianen Oszillationen benötigt wird.

Von ELF3 wird berichtet, dass es ausschlaggebend ist für die Abpufferung der Lichtsignale an den Hauptoscillator der inneren Uhr. Die Photorezeptoren und *ELF3* spielen entgegengesetzte Rollen bei der Licht vermittelten Beschleunigung der zirkadianen Periodizität. Während die Photorezeptoren die Periode verkürzen, verlängert ELF3 die Periode unter konstanten Lichtbedingungen. In dieser Arbeit konnte gezeigt werden, dass der N-Terminus zwar für die zirkadiane Funktion von ELF3 entbehrlich ist, dennoch aber die physische Interaktionsebene für ELF3 und PhyB darstellt. Eine *elf3* Komplementationlinie, die keinen N-Terminus mehr besaß, zeigte einen hyposensitiven Phänotyp bezüglich der Verkürzung der zirkadianen Periode unter konstantem Rotlicht. Daraus wurde gefolgert, dass die Interaktion von PhyB mit dem N-Terminus von ELF3 die Licht vermittelte Unterdrückung der zirkadianen Periodizität ermöglicht.

In Kapitel 4 wurde ein schwaches Allel von ELF3, *elf3-12*, charakterisiert. Die durchgeführten Untersuchungen lieferten weitere Anhaltspunkte für eine entschleunigende Wirkung von ELF3 auf die zirkadiane Periode. Die *elf3-12* Mutation sorgt für einen Aminosäureaustausch in einem konservierten Bereich innerhalb der ELF4-Bindedomäne. Die kodierende Region von *elf3-12* erzeugte eine robuste Expression des ELF3-12 Proteins, welches die Fähigkeit ELF4 und PhyB zu binden behielt. *elf3-12* hatte einen lichtabhängigen Phänotyp mit einer verkürzten Periode, welcher durch die Überexpression von Phytochrom B noch verstärkt wurde. Darüber hinaus war *elf3-12* hypersensitiv für Lichtpulse, die den Oszillator zurücksetzen. Daraus lässt sich schließen, dass *elf3-12* nur eine abgeschwächte Funktion bei der Unterdrückung von Lichtsignalen an die innere Uhr hat. Möglich ist auch eine Verstärkung der durch PhyB vermittelte Unterdrückung der ELF3 Aktivität. *elf3-12* war das erste schwache Allel von *ELF3*, das beschrieben wurde. Durch die Charakterisierung weiter sogenannter TILLING Allele von *ELF3* konnten weitere Allele

mit verlängerter oder verkürzter Periode identifiziert werden, die zum künftigen weiteren Verständnisses der Rolle von *ELF3* als Integrator von Lichtsignalen und als Hauptkomponente der inneren Uhr beitragen werden.

Zusammenfassend lässt sich sagen, dass durch die Untersuchungen in dieser Arbeit *ELF3* eine Rolle im Mechanismus der inneren Uhr zugeschrieben werden konnte. *ELF3*, *ELF4* und *LUX* sind Teil eines Abendkomplexes mit reprimierender Funktion, der für die Aufrechterhaltung der zirkadianen Rhythmik von Nöten ist. Die genetische Interaktion dieser drei Gene ist vereinbar mit der Hierarchie der Bildung des Komplexes. Das könnte bedeuten, dass *ELF4* als ein Effektorprotein funktioniert, das *ELF3* aktiviert, was möglicherweise durch eine Erhöhung der im Nukleus befindlichen Menge von *ELF3* bewerkstelligt wird. Darüber hinaus wird der Effekt von *ELF3* auf die zirkadiane Periode vermutlich durch seine Interaktionspartner moduliert. So könnte es zu einem Konkurrieren von *ELF4* mit positivem Effekt auf die innere Uhr und dem negativen, durch Licht vermittelten Effekt von *PhyB* kommen. Dies wiederum wäre vereinbar mit der Rolle von *ELF3* als multifunktionelles Protein, das als eine Kernkomponente der inneren Uhr Lichtsignale integriert.

Table of contents

Abstract	i
Zusammenfassung	iii
Table of contents	vi
List of figure elements	viii
Abbreviations	x
Chapter 1 Introduction	1
1.1 Introduction to circadian rhythms	2
1.2 The Arabidopsis circadian clock	4
1.2.1 Tools to investigate clock function	4
1.2.2 The circadian clock model	6
1.3 Three clock genes are essential for sustained circadian oscillations	9
1.3.1 <i>ELF3</i>	9
1.3.2 <i>ELF4</i>	10
1.3.3 <i>LUX</i>	10
1.4 Outputs of the clock	11
1.5 Photoperiodism and plant development	12
1.6 Light signaling is tightly interconnected with the circadian clock	14
1.6.1 Photoreceptors are not core-clock components	15
1.6.2 Light regulation of gene expression	15
1.6.3 Entrainment	16
1.6.4 Aschoff's rule	18
1.6.5 Gating of light signals by the clock	19
1.7 Conserved mechanisms in circadian systems: chromatin remodeling and regulation of sub-cellular distribution	19
1.7.1 Chromatin remodeling	19
1.7.2 Regulation of sub-cellular distribution of clock proteins	20
1.7.3 Light and clock signaling proteins localize in nuclear bodies	23
1.8 The TILLING approach	24
1.9 Thesis objectives	25
Chapter 2 Material and methods	26
2.1 Materials	27
2.1.1 Mutant lines and genetic markers	27
2.1.2 Chemicals	29
2.1.3 Reagents for each method	31
2.2 Methods	38
2.2.1 Seed sterilization	38
2.2.2 Bioluminescence assays	38
2.2.3 Molecular biology	39
2.2.4 Yeast 2-Hybrid	43
2.2.5 Floral dipping	44

2.2.6	Tobacco agro-infiltration	45
2.2.7	Chromatin immunoprecipitation (ChIP)	45
2.2.8	Confocal imaging	47
2.2.9	Analysis of ELF3 encoded sequence	48
Chapter 3	Characterization of ELF3-ELF4 complex	49
3.1	Introduction	50
3.2	Results	51
3.2.1	ELF3 and ELF4 physically and genetically interact	51
3.2.2	ELF4 constrains ELF3 to nuclear distribution	55
3.2.3	The ELF4 binding site of ELF3 is required for sustaining circadian period	58
3.2.4	ELF4 is localized preferentially in the nucleus in Arabidopsis	64
3.2.5	ELF3 represses <i>PRR9</i> by physical association to its promoter	65
3.2.6	<i>LUX</i> is a component of <i>ELF3/ELF4</i> signaling	68
3.3	Discussion	70
Chapter 4	An insight of ELF3 function in the light input to the clock	73
4.1	Introduction	74
4.2	Results	75
4.2.1	Characterization of <i>elf3-12</i> allele	75
4.2.2	Identification of novel <i>elf3</i> alleles	81
4.3	Discussion	96
Chapter 5	Final discussion and perspectives	99
5.1	Summary	100
5.1.1	ELF4 acts as an effector for ELF3	100
5.1.2	The N-terminus of ELF3 is involved in Aschoff's rule	102
5.1.3	ELF3 localizes in nuclear bodies	102
5.1.4	<i>ELF3</i> , <i>ELF4</i> , and <i>LUX</i> form a transcriptional repressor complex	103
5.1.5	Activation and repression in the <i>PRR9</i> promoter	105
5.1.6	<i>elf3-12</i> in the middle of phyB-ELF4 competition	106
5.2	Perspectives	107
5.2.1	ELF3-ELF4 interaction	107
5.2.2	Functional analysis of ELF3 nuclear bodies	108
5.2.3	ELF3-ELF4 as transcriptional repressors	109
5.2.4	Mechanism of cooperative LUX and ELF3 action	110
5.2.5	ELF3 biochemical activity	112
5.2.6	Towards a mechanism for Aschoff's rule	113
5.2.7	ELF4-phyB competition for ELF3	113
Chapter 6	References	115
Appendix 1		125
Acknowledgments		132
Erklärung		133
Curriculum vitae		134

List of figure elements

Figures

Figure 1.1.	The plant circadian clock system.	3
Figure 1.2.	Analysis of circadian rhythms.	5
Figure 1.3.	One Arabidopsis circadian clock model.	7
Figure 1.4.	Clock components are interconnected by transcriptional loops of activation and repression.	8
Figure 1.5.	Phase response curve (PRC).	17
Figure 1.6.	Sub-cellular localization dynamics are at the core of circadian systems.	22
Figure 3.1.	The middle domain of ELF3 mediates the physical interaction with ELF4.	52
Figure 3.2.	<i>ELF3</i> is genetically downstream of <i>ELF4</i> .	54
Figure 3.3.	<i>ELF3-OX ELF4-OX</i> double over-expressor retains circadian rhythms.	55
Figure 3.4.	ELF3 fragments have different sub-cellular distribution and ELF4 is nuclear localized.	56
Figure 3.5.	ELF4 constrains ELF3 to nuclear distribution.	57
Figure 3.6.	Complementation of <i>elf3-4</i> with <i>YFP-ELF3</i> fragments.	58
Figure 3.7.	Bioluminescence of <i>LHY:LUC</i> under LL.	60
Figure 3.8.	The N-terminus of ELF3 mediates interaction with phyB.	61
Figure 3.9.	ELF3N accelerates circadian periodicity under Rc and in DD.	62
Figure 3.10.	Constitutive expression of YFP-ELF4 is localized preferentially in the nucleus.	64
Figure 3.11.	<i>PRR9</i> is down-regulated in <i>ELF3-OX</i> , and <i>ELF4-OX</i> .	65
Figure 3.12.	ELF3 associates with conserved region of <i>PRR9</i> promoter.	67
Figure 3.13.	<i>YFP-LUX</i> nuclear localization is not affected in the <i>elf3-4</i> and <i>elf4-1</i> .	68
Figure 3.14.	<i>LUX</i> is downstream of <i>ELF4</i> action.	69
Figure 4.1.	ELF3-12 protein is nuclear localized, and can bind to ELF4 and phyB	76
Figure 4.2.	Mutant clock-period properties are light-dependent in <i>elf3-12</i>	77
Figure 4.3.	<i>PHY-OX</i> enhances the <i>elf3-12</i> short period phenotype under LL.	79
Figure 4.4.	ELF3-12 is hypersensitive to RL resetting pulses.	80
Figure 4.5.	Distribution of the residue changes on the <i>elf3</i> TILLING lines within the encoded ELF3 protein.	82
Figure 4.6.	<i>elf3-225</i> is a loss of function allele.	84
Figure 4.7.	Circadian rhythms of <i>GI:LUC</i> in <i>elf3</i> -TILLING-lines under LL after LD entrainment.	87
Figure 4.8.	Circadian rhythms of <i>GI:LUC</i> in <i>elf3</i> -TILLING-lines under LL after WC entrainment.	88
Figure 4.9.	Circadian rhythms of <i>GI:LUC</i> in <i>elf3</i> -TILLING-lines in DD after LD entrainment.	89
Figure 4.10.	Circadian rhythms of <i>GI:LUC</i> in <i>elf3</i> -TILLING-lines in DD after WC entrainment.	90
Figure 4.11.	Circadian rhythms of <i>GI:LUC</i> in <i>elf3</i> -TILLING-lines Rc.	91
Figure 4.12.	Circadian rhythms of <i>GI:LUC</i> in <i>elf3</i> -TILLING-lines under Bc.	92
Figure 4.13.	Allelic test for <i>er105</i> and <i>elf3-225</i> .	94

Figure 4.14.	Allelic test of <i>elf3</i> lines 210, 211, 212 and 218.	95
Figure 5.1.	ELF3 is a multifunctional protein.	100
Figure 5.2.	Model of the assembly of ELF3, ELF4, and LUX repressor complex.	104
Figure 5.3.	Activation and repression in the <i>PRR9</i> promoter.	105
Figure 5.4.	ELF4-phyB competition hypothesis.	106
Figure 5.5.	ELF3-ELF4 interaction essential for circadian function.	108
Figure 5.6.	Understanding <i>LUX-ELF3</i> cooperative action.	111

Tables

Table 2.1.	Luciferase lines.	27
Table 2.2.	Mutant and transgenic lines in the Ws background	28
Table 2.3.	Genotyping of mutant lines in the C24 background.	28
Table 2.4.	Primers for genotyping transgenic lines	29
Table 2.5.	Antibiotics for plant selection	31
Table 2.6.	Plasmid used for molecular cloning	32
Table 2.7.	Primers for cloning cDNAs into pDONR 201/207 (Invitrogen)	33
Table 2.8.	Primers for cloning ELF3 into pDONR 201/207 (Invitrogen)	33
Table 2.9.	Primers for Multi-gateway cloning	34
Table 2.10.	Primer for <i>elf3-12</i> mutagenesis	34
Table 2.11.	Antibiotics for bacteria selection	34
Table 2.12.	ChIP buffers. All buffers made in sterile ddH ₂ O	36
Table 2.13.	Primers for amplification of <i>PRR9</i> and <i>PRR7</i> promoters for ChIP	37
Table 2.14.	Light and entrainment conditions in the growth cabinets.	38
Table 2.15.	Gateway [®] reactions set up.	41
Table 2.16.	Site-directed mutagenesis set up.	42
Table 3.1	Period and RAE values of <i>LHY:LUC</i> rhythms in DD, under R+Bc, Rc, and Bc.	63
Table 4.1	<i>elf3</i> -TILLING lines	83
Table 4.2	Summary of period and phase phenotypes of <i>elf3</i> -TILLING lines under different entrainment and free-running conditions.	93
App1 Table 1	Period and phase values of <i>G1:LUC</i> for <i>elf3</i> -TILLING lines under LD to LL.	126
App1 Table 2	Period and phase values of <i>G1:LUC</i> for <i>elf3</i> -TILLING lines under WC to LL.	127
App1 Table 3	Period and phase values of <i>G1:LUC</i> for <i>elf3</i> -TILLING lines under LD to DD.	128
App1 Table 4	Period and phase values of <i>G1:LUC</i> for <i>elf3</i> -TILLING lines under WC to DD.	129
App1 Table 5	Period and phase values of <i>G1:LUC</i> for <i>elf3</i> -TILLING lines under LD to Rc.	130
App1 Table 6	Period and phase values of <i>G1:LUC</i> for <i>elf3</i> -TILLING lines under LD to Bc.	131

Abbreviations

ACE	ACGT- containing element
ATP	Arabidopsis TILLING Project
Bc	Continuous Blue Light
bHLH	Basic-Helix-Loop-Helix
BL	Blue Light
BMAL	BRAIN AND MUSCLE ARNT-LIKE
bZIP	Basic-Region Leucine-Zipper
CAB	CHLOROPHYLL A/B BINDING PROTEIN
CAPS	Cleaved Amplified Polymorphic Sequence
CAT3	CATALASE 3
CCA1	CIRCADIAN CLOCK ASSOCIATED 1
CCG	Clock-control gene
CCR2	COLD AND CLOCK REGULATED 2
CLK	CLOCK
CO	CONSTANS
COP1	CONSITITUTIVELY PHOTOMORPHOGENIC 1
CRY	CRYPTOCHROME
CT	Circadian time
CYC	CYCLE
dCAPS	Derived Cleaved Amplified Polymorphic Sequence
DD	Continuous dark
DET1	DAMAGED DNA-BINDING PROTEIN 1
EE	Evening Element
ELF3	EARLY FLOWERING 3
ELF4	EARLY FLOWERING 4
EMS	ETHYL METHANESULFONATE
FAR1	FAR-RED IMPAIRED RESPONSE 1
FBS	FHY3 Binding Site
FHY3	FAR-RED ELONGATED HYPOCOTYL 3
FRL	Far-Red Light
FRc	Continuous Far-Red Light
FRQ	FREQUENCY
FT	FLOWERING LOCUS T
GCN5	SAGA Complex Histone Acetyltransferase Catalytic Subunit Gcn5
GI	GIGANTEA
H	HISTONE

Abbreviations

H3K27me3	Tri-methylation on Lysine of N-terminus tail of HISTONE 3
H3Lys14	Acetylation on Lysine 14 of N-terminus tail of HISTONE 3
H3Lys9	Acetylation on Lysine 9 of N-terminus tail of HISTONE 3
HAD6	HISTONE DEACETYASE 6
HAT	HISTONE-ACETYLTRANSFERASE
HD1	HISTONE DEACETYLASE 1
HMR	HEMERA
HY5	LONG HYPOCOTYL 5
JMD5	JUMONJI DOMAIN CONTAINING 5
LBS	LUX Binding Site
LD	Light/dark cycles
LHY	LATE AND LONG HYPOCOTYL
LL	Continuous light
LOV	LIGHT OXYGEN VOLTAGE
LUC	LUCIFERASE
LUX	LUX ARRHYTHMO
NES	Nuclear Export Signal
NLS	Nuclear Localization Signal
OX	Over-expressor
PER	PERIOD
PHY	PHYTOCHROME
PIF	PHYTOCHROME INTERACTING FACTOR
PLC1	PHYTOCLOCK
PNB	Phytochrome Nuclear Body
PRC	Phase Response Curve
PRR	PSEUDO RESPONSE REGULATOR
Rc	Continuous Red Light
RL	Red Light
sPNB	Stable Phytochrome Nuclear Body
TILLING	Target Induced Local Lesions in Genomes
TIM	TIMELESS
TOC1	TIME OF CAB EXPRESSION
tPNB	Transient Phytochrome Nuclear Body
WC	Warm/cool cycles
WC	WHITE COLLAR
WCC	WHITE COLLAR COMPLEX
ZT	Zeitgeber time
ZTL	ZEITLUPE

Chapter 1 Introduction

1.1 Introduction to circadian rhythms

Diurnal life rhythms are shaped by circadian clocks. The Earth's rotation has been a constant generator of rhythmic oscillations in environmental conditions. These are notably light - dark, warm - cool, and dampness rhythms. Therefore, physiological processes in most organisms have adapted to be rhythmic. Organism evolved circadian clocks to anticipate these predictable diurnal oscillations in environmental conditions. Circadian rhythms are endogenously generated and enable overall optimization of the timing of physiological processes. Circadian oscillations have a periodicity of ≈ 24 hours to match the duration of a day (Dunlap *et al.*, 2004).

Although biological rhythms had been observed for many centuries, the first circadian experiment was performed in the 18th century. The French astronomer DeMarian showed that rhythms of leaf movement persist in constant dark conditions, providing the first evidence that circadian rhythms are endogenously generated. Since that experiment, the existence of circadian rhythms has extended to many diverse organisms, such as cyanobacteria, yeast, insects, birds, mammals, and plants. Hence, circadian clocks are ubiquitous mechanisms in living organism (Dunlap *et al.*, 2004).

Chronobiology studies the occurrence and generation of life rhythms. Circadian oscillations are part of our everyday. For example, they are found in the patterns of sleeping and awaking, mental concentration, hormone levels, and body-temperature homeostasis. In most organisms, core biological processes, such as cell division and changes in gene expression, occur in a circadian fashion (Dunlap *et al.*, 2004). These processes are outputs of the circadian clock. In plants, examples of clock outputs are leaf movement, growth, metabolic pathway, and stress responses [Figure 1.1, (Harmer, 2009)].

The fitness advantage of an endogenous clock has been demonstrated in several model systems. Plants with an internal-clock length matching the day length of the environment had increased fitness through increasing levels of photosynthesis, growth, and survival (Dodd *et al.*, 2005). Similar conclusions have been observed in cyanobacteria (Ouyang *et al.*, 1998). Moreover, plant mutants that loss circadian regulation had increased levels of mortality (Green *et al.*, 2002) and susceptibility to pathogen infections (Wang *et al.*, 2011). Importantly, in man, serious diseases, such as diabetes, cancer, and depression, have been associated to circadian defects (Dunlap

et al., 2004). These observations highlight the biological relevance of internal time-keeping.

Importantly, external cues reset the circadian clock daily, keeping internal and external times synchronized. This process is called entrainment and it is mediated by the so-called *zeitgebers* ('time-givers'). In most organisms, the main *zeitgebers* are light and temperature signals (Jones, 2009). Entrainment is mediated by the clock-input pathways. Notably, these input pathways are simultaneously controlled as clock outputs (Figure 1.1). This enables circadian clocks to modulate the susceptibility for entrainment cues throughout the day. Therefore, entrainment is a complex process that requires interaction of the circadian clock with both input and output pathways.

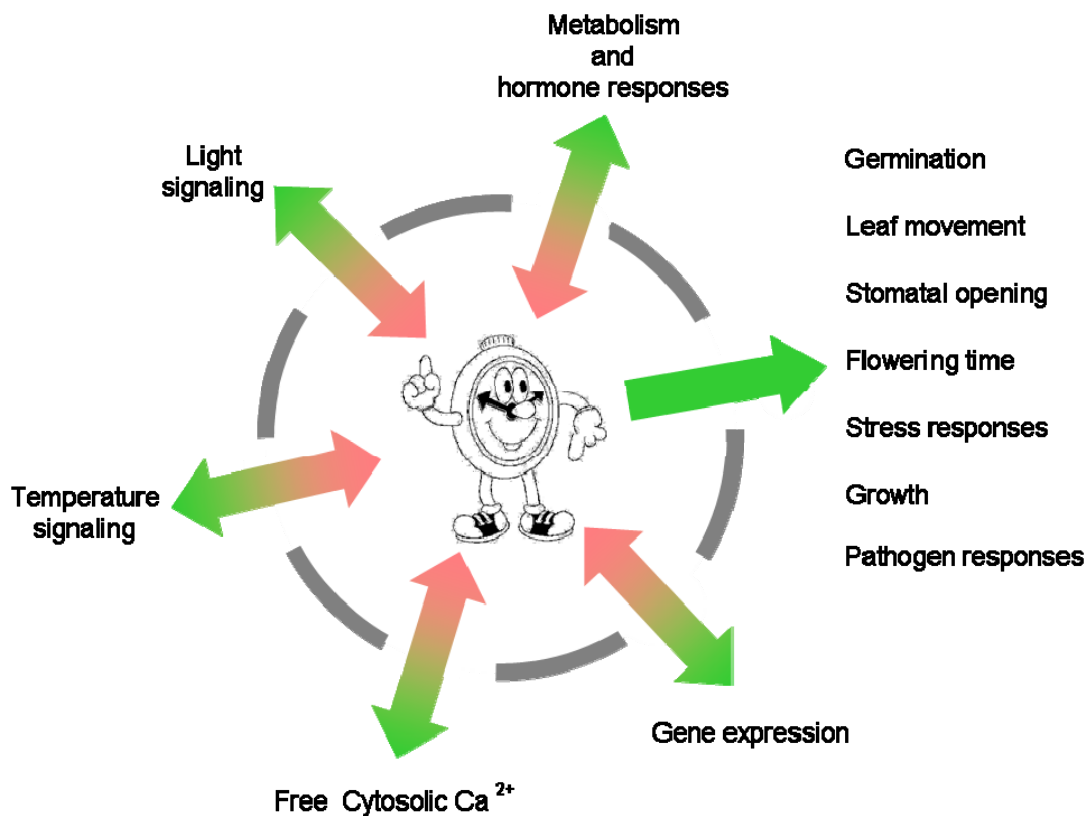


Figure 1.1. The plant circadian clock system. Circadian rhythms are generated by a central oscillator. The timing of many physiological processes is regulated by the circadian clock through the output pathways (green arrows). Moreover, the oscillator is reset daily by the input pathways (pink arrows). Simultaneously, the input pathways are circadian regulated through the output pathways, increasing the robustness of the oscillator to external and internal perturbations.

Entrainment allows circadian clocks to keep track of seasonal changes in day length, in a process termed photoperiodism. Organisms living in extreme latitudes are particularly challenged by seasonal environmental oscillations (Dunlap *et al.*, 2004). Hence, photoperiod is widely used as an external cue to predict the most favorable time for developmental choices. For example, in plants, photoperiod pathways controls flowering time (de Montaigu *et al.*, 2010). Also, photoperiodism controls the timing of bird and monarch butterflies migrations (Gwinner, 2003; Kyriacou, 2009). Photoperiod perception is achieved cooperatively by integrating the timing of the information derived from the circadian clock and light-input pathways (de Montaigu *et al.*, 2010).

The molecular components of the clock are not conserved between kingdoms, suggesting that circadian systems have multiple evolutionary origins. In red-blood cells and the microscopic algae *Ostreococcus tauri*, circadian oscillations persist in the absence of transcription (O'Neill and Reddy, 2011; O'Neill *et al.*, 2011). Nevertheless, the molecular mechanism in most multi-cellular circadian systems involves interconnected transcriptional-translational feedback loops between clock components. Circadian clocks are a fascinating example of convergence evolution (Dunlap *et al.*, 2004). The next sections will focus on the state of the circadian clock in the plant *Arabidopsis thaliana* (*Arabidopsis*).

1.2 The Arabidopsis circadian clock

1.2.1 Tools to investigate clock function

Circadian waves can be mathematically described. Several properties of circadian oscillations are of particular interest. The period is the duration of a single oscillation and defines the speed of the circadian rhythm. The phase describes the timing of specific events within the circadian day. The amplitude is defined as half the difference between the maximum and the minimum value of an oscillation (Figure 1.2). These three properties can be genetically separable (Harmer, 2009). Finally, the accuracy of the circadian oscillation is described by its robustness. Here, the term arrhythmicity is used when circadian rhythms are not sustained. Period, phase, amplitude, and robustness are used to characterize circadian mutants, and to describe input signals that affect the endogenous oscillator.

The main tool to investigate circadian function in plants is the monitoring of circadian oscillations of cotyledon movement and transcript accumulation of clock-

control-genes (CCG). In the early 90s, the use of firefly-luciferase based circadian reporters (*CCG:LUC*) boosted circadian research in *Arabidopsis* (Millar *et al.*, 1992). In these reporters, the promoter of a CCG was fused to the luciferase coding sequence. In the presence of the luciferase substrate (luciferin) plants then emit bioluminescence in a circadian fashion. In such experiments, plants harboring *CCG:LUC* are grown for few days under entraining cycles of light or temperature (Light/Dark, LD or Warm/Cool, WC, respectively), and then they are released to so-called free-running conditions of continuous light (LL) or darkness (DD) (Figure 2A). The bioluminescence emission is acquired by highly sensitive cameras that can detect low intensity light. Then, the obtained data can be analyzed by using mathematical and statistical tools.

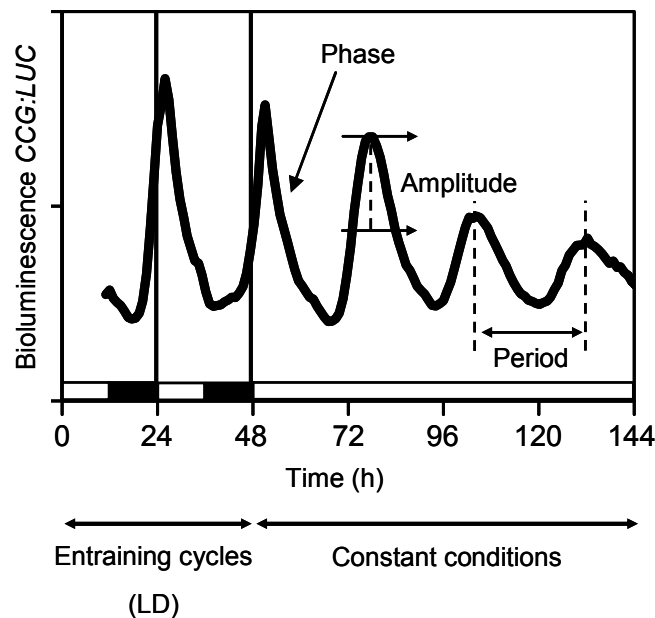


Figure 1.2. Analysis of circadian rhythms.

The figure shows the main features of bioluminescence-based circadian experiments. Under diurnal or entraining cycles of time-givers, such as temperature or light/dark cycles, the period of the clock is about 24 hours. Under constant conditions, circadian period-length deviates from 24 hours. Phase refers to the timing of a physiological event within the circadian cycle. Normally, it refers to the highest luminescence value within the oscillation (peak). Amplitude is half the difference between the highest and the lowest value of the oscillation.

Several CCG promoters have been fused to luciferase to study circadian oscillations. One example is *CHLOROPHYLL A/B BINDING PROTEIN (CAB)*. *CAB* has a complex regulation by both light and the circadian clock. Hence, *CAB:LUC* was the first luciferase reporter to be used for studying the interaction between light and clock (Millar *et al.*, 1995a). Moreover, *CAB:LUC* expression was used to identify

circadian mutants with aberrant reporter expression (Millar *et al.*, 1995b; Millar *et al.*, 1995a). The dampening of *CAB* expression in the dark limits the use of *CAB:LUC* for DD experiments. However, robust rhythmic expression persists in DD for other CCG genes, such as the *COLD AND CIRCADIAN REGULATED* (*CCR2*, also known as *AtGRP7*) (Heintzen *et al.*, 1997; Covington *et al.*, 2001; Hanano *et al.*, 2006; McWatters *et al.*, 2007; Schoning *et al.*, 2007). Finally, most of the core-clock components (see below) are also CCG, and their promoters have also been used within the luciferase platform to build up the complex interconnections of the circadian-clock model.

1.2.2 The circadian clock model

In *Arabidopsis*, the first loop to be defined was the so-called core loop. The core loop connects *LATE AND ELONGATED HYPOCOTYL* (*LHY*) (Schaffer *et al.*, 1998) and *CIRCADIAN CLOCK ASSOCIATED 1* (*CCA1*) (Wang and Tobin, 1998) to *TIME OF CAB EXPRESSION* (*TOC1*) (Strayer *et al.*, 2000) (Figure 1.3). *LHY* and *CCA1* encode two myb-like transcription factors that are expressed in the morning. *LHY* and *CCA1* act additively as transcriptional repressors by associating to the promoter of *TOC1*, confining *TOC1* expression to dusk (Alabadi *et al.*, 2001; Perales and Mas, 2007) (Figure 1.4). Consistently, the over-expression of *LHY* or *CCA1* led to clock arrest with basal levels of *TOC1* expression (Wang and Tobin, 1998; Matsushika *et al.*, 2002b). Conversely, the pseudo response regulator (PRR) *TOC1* promotes the expression of *CCA1* and *LHY* by an unknown mechanism [Figure 1.3, (Alabadi *et al.*, 2001; Pruneda-Paz *et al.*, 2009)]. This thus closes the core of the clock. Notably, in the absence of the core loop the circadian clock arrests (Ding *et al.*, 2007).

Subsequent experimental and mathematical approaches expanded the plant clock to the so-called three-loop-model (Locke *et al.*, 2006; Zeilinger *et al.*, 2006). In this model, a morning and evening loop were added interlocking with the central loop (Figure 1.3). This was extended and confirmed with molecular genetics and biochemical experiments. In here, three *TOC1*-sequence-related clock components, *PRR9*, *PRR7*, and *PRR5*, were placed within the core mechanism. During the day, *PRR9* and *PRR7* associate sequentially with the promoter of *LHY* and *CCA1* to repress their transcription [Figure 1.4, (Nakamichi *et al.*, 2005; Nakamichi *et al.*, 2010)]. Reciprocally, *LHY* and *CCA1* promote the expression of *PRR9* and *PRR7* by direct association to promoter *cis*-elements [Figure 1.4, (Farre *et al.*, 2005; Portoles and Mas, 2010)]. Notably, the function of *TOC1* as an activator of *LHY* and *CCA1* is opposite to the function of *PRR9/7*. Moreover, *PRR5* has been shown to play a dual role within the

oscillator, one as direct repressor of *LHY* and *CCA1* (Nakamichi *et al.*, 2010), and a second one as stabilizer of *TOC1* protein-nuclear pool [Figure 1.4, (Wang *et al.*, 2010)]. This second role of *PRR5* seems to be more prominent since both *toc1* and *prr5* null alleles were shown to have short-period phenotypes, and this was opposite to *prr9*, *prr7*, and the double mutant *prr7 prr9*, all of which displayed a long-period phenotypes (Alabadi *et al.*, 2001; Yamamoto *et al.*, 2003; Farre *et al.*, 2005). Recent mathematical modeling efforts validated the *PRR9*, *PRR7*, and *PRR5* repressor wave to *LHY* and *CCA1* (Pokhilko *et al.*, 2010). Consequently, the triple mutant *prr975* was found to be arrhythmic for all circadian outputs (Nakamichi *et al.*, 2005).

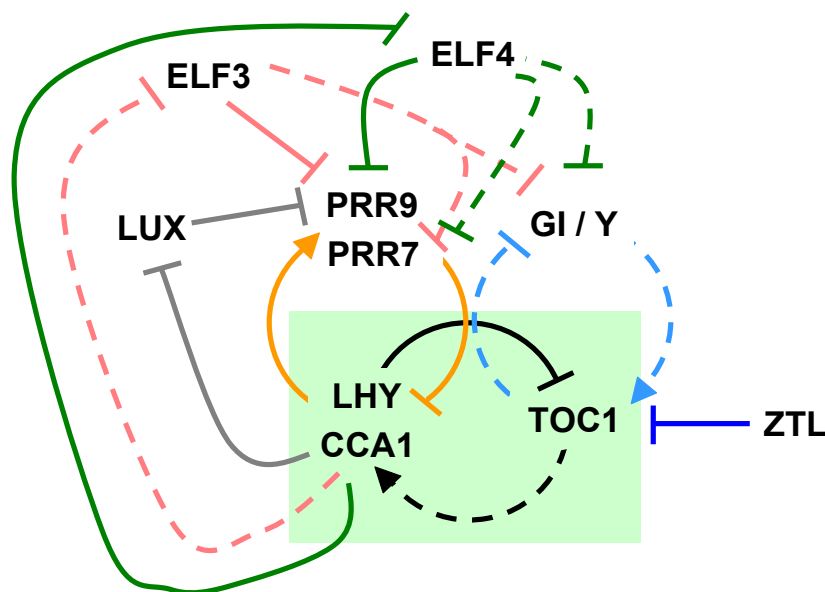


Figure 1.3. One Arabidopsis circadian clock model.

Circadian-clock components are arranged in interconnected feedback loops. In the core loop (black arrows, green box), *LHY* and *CCA1* negatively regulate *TOC1* expression, and feedback from *TOC1* promotes *LHY* and *CCA1*. In the morning loop (orange arrows), *PRR9* and *PRR7* negatively regulate *LHY* and *CCA1*, and *LHY* and *CCA1* feedback to promote *PRR9* and *PRR7*. In the evening loop (light blue arrows), *TOC1* negatively regulates *GI/Y* expression, and *Y* activates *TOC1* expression. *ZTL* promotes *TOC1* protein degradation. *CCA1* and *LHY* represses *ELF3*, *ELF4*, and *LUX* expression (pink, green and blue, respectively). *LUX*, *ELF3*, and *ELF4* repress *PRR9* expression. Additionally, *ELF3* and *ELF4* repress *GI* and *PRR7*. Continuous line indicates regulatory link is direct, dashed line indicates direct link has not been determined.

An evening loop was proposed between an unknown component *Y* and *TOC1* (Figure 1.3). The component *Y* is light induced and acts as a promoter of *TOC1* expression (Locke *et al.*, 2006; Zeilinger *et al.*, 2006). Partial *Y* function was assigned to the evening gene *GIGANTEA (GI)*. However, high levels of *TOC1* found in the *gi* mutants suggested additional components may assist in *Y* function (Martin-Tryon *et al.*, 2007). *GI* encodes for a protein of unknown function and is unique to plants. Different

gi mutants showed pleiotropic defects in flowering time, hypocotyl growth, and stress response (Huq *et al.*, 2000; Cao *et al.*, 2005; Mizoguchi *et al.*, 2005). This suggests that *GI* has a wide role in plant physiology.

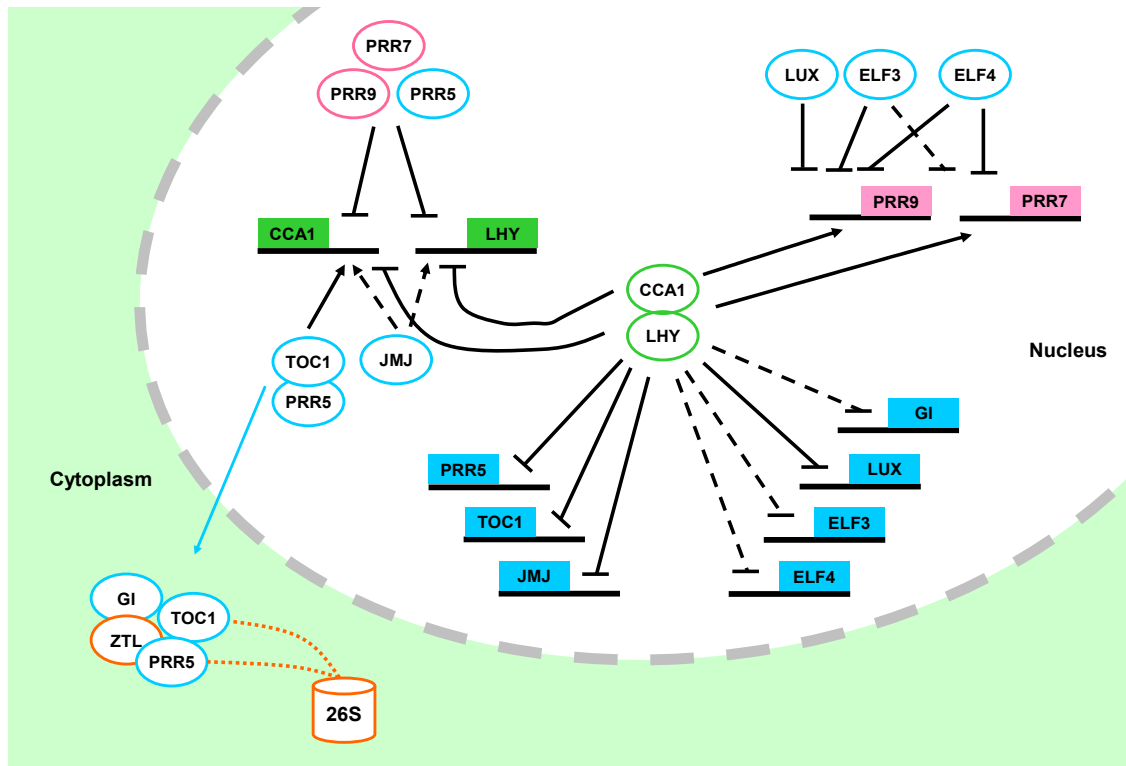


Figure 1.4. Clock components are interconnected by transcriptional loops of activation and repression.

Squares and circles represent clock promoters and clock proteins, respectively. Continuous lines indicate links are direct and have been experimentally validated. Dashed lines refer to indirect or not experimentally confirmed links. Links ending on arrows or horizontal lines represent activation or repression, respectively. Squared line refers to target 26S-proteasome-mediated degradation. The model is explained in the text (Sections 1.2.2 and 1.3).

GI function in the circadian clock is mediated by its physical interaction with ZEITLUPE (*ZTL*) [Figure 1.4, (Kim *et al.*, 2007)]. *ZTL* is a F-box protein that facilitates ubiquitination by E3-ligase of *TOC1* and *PRR5*, targeting them for degradation by the 26S-proteasome [Figure 1.4; (Mas *et al.*, 2003; Kiba *et al.*, 2007; Baudry *et al.*, 2010; Wang *et al.*, 2010)]. Consequently, loss of *ZTL* function lengthened circadian period. *ZTL* protein interactions are mediated by the LOV (Light, Oxygen, or Voltage) domain that also functions as a blue-light photoreceptor. Hence, blue light modulates the affinity of *ZTL* to its protein interactors (Mas *et al.*, 2003; Kiba *et al.*, 2007; Baudry *et al.*, 2010; Wang *et al.*, 2010). For instance, blue light induces *ZTL* and *GI* protein interaction, resulting in stabilization of both proteins. Since *ZTL* protein is localized in

the cytoplasm, the interactions of ZTL, GI, and TOC1 in the cytoplasm is thought to regulate active levels of nuclear TOC1 protein [Figure 1.4, (Kim *et al.*, 2007)]. Therefore, GI negatively regulates TOC1 levels by stabilizing ZTL.

1.3 Three clock genes are essential for sustained circadian oscillations

The function of any individual clock components of the three-loop model is not essential for circadian function (Locke *et al.*, 2006; Zeilinger *et al.*, 2006). To date, only a small group of clock components have been found to be essential for sustained circadian function in Arabidopsis. These three genes are *EARLY FLOWERING-3 (ELF3)*, *EARLY FLOWERING-4 (ELF4)*, and *LUX ARRHYTHMO/PHYTOCLOCK1 (LUX/PCL1)* (Hicks *et al.*, 1996; Doyle *et al.*, 2002; Hazen *et al.*, 2005; Onai and Ishiura, 2005).

1.3.1 ELF3

ELF3 is required for core-clock function since *elf3* loss-of-function mutants are arrhythmic for circadian outputs under LL (Covington *et al.*, 2001) and in DD (Covington *et al.*, 2001; Thines and Harmon, 2010). *ELF3* encodes for an unknown protein unique to plants. It was reported to localize in the nucleus (Liu *et al.*, 2001). *ELF3* protein accumulation is rhythmic and peaks at subjective night (dusk) under LD (Liu *et al.*, 2001). *ELF3* protein possess features of a transcriptional regulator, such as a proline-rich region (residues 440-540), an acidic region (residues 206-320), a threonine-rich region (residues 636-652), a putative nuclear-targeting signal starting at residue 591, and a glutamine-stretch (residues 544-585). The glutamine stretch is polymorphic in length between different Arabidopsis accessions (Hicks *et al.*, 2001; Tajima *et al.*, 2007). The timing of *ELF3* protein accumulation, *ELF3* nuclear localization, and *ELF3* protein features suggest a role in clock-mediated transcriptional regulation at dusk. *elf3* null alleles affect the expression of the core-loop components, with low levels of *LHY* and *CCA1*, and high levels of *TOC1* (Kikis *et al.*, 2005). Moreover, expression levels of *PRR9*, *PRR7*, and *GI* were found to be constantly high in *elf3* loss-of-function mutants (Dixon *et al.*, 2011). Interestingly, *ELF3* protein was recently found to associate to the promoter of *PRR9*, but not to *PRR7* or *GI*, indicating a direct transcriptional repression of *ELF3* on *PRR9* expression [Figure 1.3 and 1.4, (Dixon *et al.*, 2011)]. Plants over-expressing *ELF3 (ELF3-OX)* have rhythmic circadian

oscillations with long period (Covington *et al.*, 2001). Therefore, *ELF3* functions within the core oscillator as a transcriptional repressor of *PRR9*, and a negative regulator of clock periodicity.

1.3.2 *ELF4*

ELF4 is a small homodimeric nuclear protein unique to plants (Khanna *et al.*, 2003; Kolmos *et al.*, 2009). Structural modeling predicts *ELF4* to consist of a single protein-protein interaction domain, and hence, *ELF4* was predicted to function as an effector for a target protein (Kolmos *et al.*, 2009). Similar to *ELF3*, loss of *ELF4* function leads to clock arrest both under LL and in DD, as well as, arrhythmic low levels of *LHY* and *CCA1* expression with high levels of *TOC1* (Doyle *et al.*, 2002; Kikis *et al.*, 2005; McWatters *et al.*, 2007). Hypomorphic alleles of *ELF4* had accelerated circadian rhythms, and a long periodicity resulted by *ELF4-OX*. Hence, *ELF4* decelerated circadian periodicity (McWatters *et al.*, 2007; Kolmos *et al.*, 2009). Additionally, the transcript accumulation of the secondary loop components *PRR9*, *PRR7*, and *GI* was found to be constitutively high in *elf4* loss of function, and this was also found to a lesser extent in weak *elf4* alleles (Kolmos *et al.*, 2009). The expression phenotypes of *LHY*, *CCA1*, and *TOC1* in the *elf4* mutant can be mimicked computationally by the simultaneous increase of the expression levels of *PRR9* and *GI* in the three-loop mathematical model (Kolmos *et al.*, 2009). Taken together, *ELF4* is core-clock component that has two entry points to the oscillator, by repressing both morning and evening secondary loop components [Figure 1.3 and 1.4, (Kolmos *et al.*, 2009)].

1.3.3 *LUX*

The GARP-type transcription factor *LUX* is pivotal to sustain circadian rhythms. *LUX* loss of function is arrhythmic for all tested circadian outputs, and this phenotype is more severe under LL (Hazen *et al.*, 2005; Onai and Ishiura, 2005). *LUX* has been recently found to work as a transcriptional repressor by associating to a DNA motif found in the promoter of *PRR9*, called the LUX BINDING SITE (LBS, nucleotide sequence GATTCG) [(Helfer *et al.*, 2011), Figure 1.3 and 1.4]. Lack of repression of *PRR9* expression is likely to cause abnormal expression levels of core-loop clock components: low expression of *LHY* and *CCA1* and high levels of *TOC1* (Hazen *et al.*, 2005; Onai and Ishiura, 2005), which are also found in *elf3* and *elf4* loss of function mutants (Kikis *et al.*, 2005; McWatters *et al.*, 2007). Since *PRR9* over-expression does not lead to clock arrest (it leads to a short-period phenotype) (Matsushika *et al.*,

2002a), additional lack of repression of other targets of LUX are likely to participate in the *lux* severe clock phenotypes.

Sustained circadian rhythms in *Arabidopsis* require *ELF3*, *ELF4*, and *LUX* function. The three genes act as transcriptional repressors at dusk. Their loss function phenotypes are similar. Therefore, these three genes could act closely in a genetic pathway essential for the circadian-clock mechanism.

1.4 Outputs of the clock

In plants, circadian oscillations can be found in many physiological processes. These include gene expression, hypocotyl growth, photosynthesis, and pathogen responses (Hanano and Davis, 2007; Nozue *et al.*, 2007; Covington *et al.*, 2008; Michael *et al.*, 2008; Roden and Ingle, 2009; Graf *et al.*, 2010). The transcript accumulation of about 40 % of *Arabidopsis* genes is circadian regulated, as shown by microarray analysis (Covington *et al.*, 2008; Hubbard *et al.*, 2009). Such an extensive circadian regulation is achieved by the rhythmic expression of transcription factor families, such as MYB, bHLH, and bZIP (Hanano *et al.*, 2008). Clock regulation extends to hormone production, magnitude of hormone and cold responses, and primary metabolic pathways (Hanano *et al.*, 2006; Covington and Harmer, 2007; Covington *et al.*, 2008; Fukushima *et al.*, 2009). Clock transcriptional regulation of gene expression is extensive in *Arabidopsis*.

Multiple *cis*-elements in the promoter of CCG genes mediate association of positive and negative regulators that shape their circadian oscillation (Michael and McClung, 2002; Harmer and Kay, 2005; Michael *et al.*, 2008; Helfer *et al.*, 2011). Computational analyses have shown the importance of the interplay of the circadian clock with temperature- and light-signaling pathways (Michael *et al.*, 2008). Additionally, several *cis*-elements have found to be over-represented in the promoter of CCG (Covington *et al.*, 2008; Michael *et al.*, 2008). The most studied *cis*-element is the so-called Evening Element (EE, nucleotide sequence AAAATATCT), over-represented in the promoter of genes that peak at dusk, such as *TOC1*, *GI*, *ELF4*, and *LUX* (Harmer, 2009; Li *et al.*, 2011). The binding of LHY and CCA1 to the EE mediates transcriptional repression during the subjective day and confers evening-phase expression. Notably, the EE also mediates activation of the expression of morning phased genes, such as *PRR9*, *PRR7*, and *CAB* (Farre *et al.*, 2005; Lu *et al.*, 2009; Portoles and Mas, 2010). This indicates that LHY and CCA1 can work both as

activators and repressors, possibly by participating in different protein complexes depending on promoter context (Lu *et al.*, 2009). In summary, different clock transcription factors mediate transcriptional activation or repression by associating to the promoters of CCG.

Phylogenetic shadowing of promoter sequences can reveal evolutionary conserved *cis*-elements required for transcriptional regulation (Boffelli *et al.*, 2003). For this, the extent of sequence conservation is examined in an alignment of homologous sequences of related species. Sequence conservation indicates selective pressure to keep DNA motifs of functional importance (Picot *et al.*, 2010), and can be then validated by experimental approaches. The use of this process as a technique is exemplified by the identification of regulatory elements in the *LHY* promoter (Spensley *et al.*, 2009).

1.5 Photoperiodism and plant development

Light- and clock-signaling pathways control diurnal plant growth and the transition from vegetative to reproductive phase (de Montaigu *et al.*, 2010). The regulation of hypocotyl elongation has been studied as a model for diurnal-growth control. Hypocotyl growth rate is controlled by the circadian clock. Hypocotyl growth arrests at the beginning of the day. In arrhythmic mutants, such as *elf3*, hypocotyls are constantly growing. Therefore, these mutants displayed long hypocotyls when grown under LD conditions (Dowson-Day and Millar, 1999; Nozue *et al.*, 2007). Light also inhibits hypocotyl elongation independently of the clock. *long hypocotyl 1 (hy)* mutant displayed rhythmic-hypocotyl elongation, but still had long hypocotyl due to lack of light perception through the phytochrome photoreceptors (Dowson-Day and Millar, 1999). The PHYTOCHROME INTERACTING FACTORS (PIF) *PIF4* and *PIF5* promote hypocotyl growth. These encode bHLH transcription factors that bind to the active form of phytochromes. The clock controls transcript accumulation of *PIF4* and *PIF5* that is highest at the end of the night. *PIF4* and *PIF5* expression peaks coincide with maximal hypocotyl growth rate. In the absence of clock function, *PIF4* and *PIF5* levels are constitutively high leading to continuous growth (Nozue *et al.*, 2007). At dawn, light signaling arrests hypocotyl growth by degrading PIF4 and PIF5. The combined regulation by clock and by light restricts maximal diurnal hypocotyl elongation to the end of the night, when PIFs highest transcript accumulation coincides with protein stability.

Interestingly, loss of *ELF3* or *PHYTOCHROME B (PHYB)* functions were found to lead to similar developmental defects, such as long hypocotyls, elongated petioles, and pale leaves (Zagotta *et al.*, 1996; Liu *et al.*, 2001). The loss of *elf3* had long hypocotyls under constant red light (Rc), and to less extent under constant blue light (Bc), whereas no phenotype was observed under constant far-red light (FRc). This indicates that *ELF3* plays a more important role in phyB mediated red-light signals to inhibit hypocotyl elongation (Reed *et al.*, 2000; Liu *et al.*, 2001). Light inhibition of hypocotyl growth is fluence-rate dependent, *i.e.* increasing light intensities lead to an increase in the inhibition rate. Notably, *elf3 PHYB-OX* mutant responded to increasing red light intensities, but showed longer hypocotyls than *PHYB-OX* (Reed *et al.*, 2000). Overall, *ELF3* affects hypocotyl elongation as a component of the clock mechanism and phyB signaling, whereas phyB role is likely limited to RL signaling.

The circadian clock participates in regulation of the transition from vegetative to reproductive development through the photoperiodic pathway (de Montaigu *et al.*, 2010). In the external coincidence model, the clock controls the phase of *CONSTANS (CO)* expression (Suarez-Lopez *et al.*, 2001). Under short day, *CO* expression occurs in the dark phase, and *CO* protein is targeted to degradation by the E3-ligase *CONSTITUTIVE MORPHOGENIC 1 (COP1)* (Jang *et al.*, 2008). However, under long days, maximal *CO* expression coincides with the light phase. *CO* protein is stable in the light and activates the transcription of *FLOWERING LOCUS T (FT)* (Valverde *et al.*, 2004). Finally, *FT* moves from the leaf to the apex and triggers the transition to flowering (Corbesier *et al.*, 2007).

The *elf3*, *elf4*, and *lux* loss of function mutants are early-flowering mutants regardless of photoperiod (Zagotta *et al.*, 1996; Hicks *et al.*, 2001; Doyle *et al.*, 2002; Hazen *et al.*, 2005). A weaker early-flowering phenotype has been also observed in *phyB* mutants. Notably, *elf3* and *phyB* mutations were additive in reducing flowering time (Reed *et al.*, 2000). This suggests that *ELF3* and phyB delay flowering time by at least partially independent mechanisms.

The *elf3* early-flowering phenotype was shown to be independent of *CO*, and did not require high levels of *FT* expression. This suggest that *ELF3* may repress flowering independently of the *CO*-dependent pathway (Kim *et al.*, 2005). *GI* also posses separable functions in the clock and as a promoter of flowering (Martin-Tryon *et al.*, 2007). *GI* is an activator of *CO* transcription and consequently *gi* mutants are late flowering. Moreover, *elf3 gi* double mutant is late flowering, but displayed a long hypocotyl like *elf3* (Chou and Yang, 1999). This suggests the existence of separate

genetic pathways for hypocotyl elongation and flowering time. In the flowering-time control, *GI* is downstream of *ELF3*, whereas in the hypocotyl-elongation control, *ELF3* is downstream of *GI*.

1.6 Light signaling is tightly interconnected with the circadian clock

Light is the primary source of energy for plants through photosynthesis. In addition, light signals are important modulators of plant development through a process called photomorphogenesis. Light is also a major input signal to the circadian clock through the action of three different types of photoreceptors: phytochromes (phys) for red light (RL) and far-red light (FRL), and cryptochromes (crys), and the *ZTL* family for blue light (BL). Interestingly, *PHYs* and *CRYs* transcript accumulation is regulated as an output of the circadian clock with different phases of maximum expression during the subjective day (Toth *et al.*, 2001). Therefore, clock modulates light input by the photoreceptors.

In *Arabidopsis*, the phytochrome family has five members: *PHYA* to *PHYE* (Sharrock and Quail, 1989). Functional phytochromes form homodimers, and each monomer has a chromophore covalently attached. In dark grown seedlings, cytosolic localization is exclusive for *phyA* and predominant for *phyB* to *phyE*. Upon specific irradiation, activated phytochromes are translocated to the nucleus where they localize in distinct phytochrome-nuclear bodies (PNB). Under light dark cycles, PNB formation precedes the lights on signal, indicating both diurnal and circadian regulation (Kircher *et al.*, 2002). Thereby, the circadian clock optimizes phytochrome signaling by enabling dawn anticipation.

Phytochromes control the responses to RL and FRL. *phyA* controls FR responses mediated by short pulse of low fluence FRL and FRc (Hiltbrunner *et al.*, 2007). *phyA* also participates in the response to low intensities of Rc in etiolated seedlings. *phyB* mediates the response to Rc, and here also *phyC*, *phyD*, and *phyE* participate to a minor extent (Hiltbrunner *et al.*, 2007). Hence, phytochromes play redundant and complementary roles in FRL and RL signaling.

In *Arabidopsis*, *cry1* and *cry2* play the major role on BL light induced changes in gene expression, that can be separable in immediate and in long-term BL responses (Batschauer *et al.*, 2007). Similarly to *phyA*, *cry2* levels rapidly decreased upon exposure to BL (Ahmad *et al.*, 1998a; Lin *et al.*, 1998), whereas *cry1* was stable under

BL (Ahmad *et al.*, 1998a). Cross-talk and interdependence between phytochrome and cryptochrome signaling pathways are directly mediated by physical interaction between phyA and cry1 (Ahmad *et al.*, 1998b), and phyB and crys (Jarillo *et al.*, 2001). Cry1 are the main BL photoreceptors and they also participate in phy signaling.

1.6.1 Photoreceptors are not core-clock components

In mammalian clocks, cryptochromes are essential to sustain circadian oscillations (Kume *et al.*, 1999). In plants, phy and crys seem to play a pivotal role only in light-input signaling into the clock, but not in the core-clock mechanism. For instance, the *quintuple-phy* mutant was found to retain circadian rhythms of leaf movement under LL. However, the *quintuple-phy* mutant was arrhythmic under Rc, indicating that phy function is required for sustain oscillations under Rc (Strasser *et al.*, 2010). Moreover, *phy* mutations does not affect clock function in the dark (Devlin and Kay, 2000b). More strikingly, a quadruple photoreceptor mutant *phyA phyB cry1 cry2* displayed robust circadian rhythms of leaf movement (Yanovsky *et al.*, 2000). Still, the three remaining phytochromes phyC-E and the ZTL family may contribute to this function. In this line, *hy1* has low amount of phytochromes, still showed robust rhythms of *CAB* (Millar *et al.*, 1995a). In plants, photoreceptors are not required for generating a functional oscillator.

1.6.2 Light regulation of gene expression

Downstream of phy, and crys several transcriptional regulators participate in gene expression changes that lead to photomorphogenesis. PIFs function as repressors of photomorphogenesis. Although PIF3 binds to the G-box of *LHY* and *CCA1* promoters, no clock phenotype has been found in *pif3* loss of function mutants or in *PIF3* over-expression plants (Oda *et al.*, 2004; Viczian *et al.*, 2005). This indicates that *PIF3* does not participate in the clock mechanism or in light-input-signaling pathway to the clock.

The bZIP transcription factor *LONG HYPOCOTYL 5 (HY5)* is an important component of light signaling. HY5 binds to the promoter of many light responsive genes, including clock components, through ACGT-containing elements (ACE) (Lee *et al.*, 2007). HY5 physical interaction with CCA1 and LHY (Andronis *et al.*, 2008) is a possible mechanism of HY5-mediated light input to the clock. The loss of *HY5* function shortens the period of *CAB* circadian oscillations (Andronis *et al.*, 2008), but it has no effect on the periodicity of other CCG such as *CATALASE3 (CAT3)* and *ELF4*

(Andronis *et al.*, 2008; Li *et al.*, 2011). FAR RED-ELONGATED HYPOCOTYL 3 (FHY3) and FAR-RED-IMPAIRED RESPONSE 1 (FAR1) induce gene expression by binding to the FHY3 binding site (FBS), present in the promoter of light regulated genes (Lin *et al.*, 2007; Li *et al.*, 2011). The FHY3 direct activation of clock components may explain circadian phenotypes in *fhy3* mutants (Allen *et al.*, 2006). Hence, *HY5* and *FHY3* act in the light input pathways to the circadian clock.

A recent study on the regulation of *ELF4* gene expression nicely illustrates the direct interaction between circadian and light-regulation pathways (Li *et al.*, 2011). *ELF4* transcript accumulation followed circadian oscillations under LL (Doyle *et al.*, 2002). The amplitude of *ELF4* expression was found to be phyB-dependant (Khanna *et al.*, 2003). In DD, *ELF4* expression rhythms dampened (Doyle *et al.*, 2002). Notably, the precise peak of *ELF4* expression changed under different photoperiods (Doyle *et al.*, 2002; McWatters *et al.*, 2007). In the *ELF4* promoter there are FBS boxes, and EE and ACE elements that mediate association with FHY3/FAR1, CCA1, and HY5, respectively (Li *et al.*, 2011). In the *fhy3 far1* double mutant, the amplitude of *ELF4* transcript accumulation was found to be severely reduced, and resembled that of *ELF4* expression in the dark. A less dramatic reduction of amplitude was also observed for *ELF4* expression in the *hy5* mutant (Li *et al.*, 2011). Therefore, FHY3, FAR1, and HY5 act as transcriptional activators on the *ELF4* promoter. Conversely, CCA1 binding to the EE mediates transcriptional repression of *ELF4*. Moreover, CCA1 and FHY3 physically interact, and this interaction reduces the binding of FHY3 to the FBS, leading to transcriptional repression. The combination of *cis*-elements in the *ELF4* promoter is also present in other promoters, suggesting a similar mode of regulation (Li *et al.*, 2011). Taken together, through the repressor activity of CCA1, the circadian clock delimits light-mediated transcriptional activation of *ELF4* to the end of the day, when CCA1 levels decay.

1.6.3 Entrainment

An essential property of circadian systems is the ability to be reset by external or internal cues allowing synchronization to changing conditions, such as day length. In plants, entrainment is mainly mediated by light and temperature *zeitgebers*. Overall, entrainment is achieved by a change in the phase of the oscillator (Devlin, 2002). Phase resetting is studied by constructing a phase response curve (PRC). *Zeitgeber* cues lead to different resetting depending on when they are applied. Resetting pulses applied at the end of the night or after dusk lead to phase advances or phase delays,

respectively. Additionally, a “dead zone” without phase changes is commonly observed at the subjective day (Figure 1.5). Light and temperature pulses produce similar PRCs.

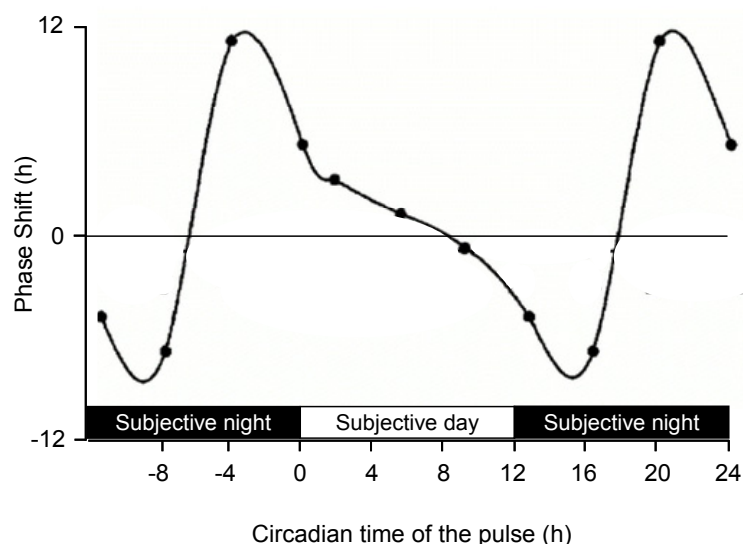


Figure 1.5. Phase response curve (PRC).

Entrainment pulses reset the circadian clock differently depending of the circadian time (CT) of the pulses. Pulses applied around dusk (\approx CT 10-16) or around dawn (\approx CT 20-4) induce phase delays or phase advances, respectively. There is a dead zone during the subjective day (\approx CT 4-10) when pulses do not reset the oscillator. Modified from (Devlin and Kay, 2001)

In *Arabidopsis*, BL and RL pulses both confer similar PRCs, indicating that both *phys* and *crys* are involved in entrainment. The *elf3* loss of function mutant could not be entrained by RL and BL pulses given at subjective night, possibly because *ELF3* is required for overall circadian function. On the contrary, *ELF3-OX* reduced the magnitude of phase advances and delays caused only by RL pulses (Covington *et al.*, 2001), confirming a repressor role of *ELF3* to RL signals to the core oscillator. However, the PRC constructed for temperature pulses was similar for *ELF3-OX* and wild type (Thines and Harmon, 2010), indicating that *ELF3* is not directly involved in temperature input to the clock. *FHY3* is involved in both phyA and phyB signaling pathways. Loss of function of *FHY3* had aberrant red light resetting, with increase phase delays during the subjective day (Allen *et al.*, 2006). In a separate work, pulses of *LHY* and *CCA1* transcription driven by an ethanol-inducible promoter were able to shape a normal PRC, whereas similar *TOC1* pulses cannot (Knowles *et al.*, 2008). Hence the expression timing of these morning genes was sufficient for clock resetting. In summary, photoreceptors, *ELF3*, *FHY3*, *LHY*, and *CCA1* are components of the light-entrainment mechanism.

1.6.4 Aschoff's rule

Diurnal organisms are subjected to the Aschoff's rule: continuous-light input accelerates circadian-oscillator speed leading to shortening of periodicity (Aschoff, 1979). The light acceleration effect is thought to account for the sum of phase advances and delays induced by light throughout the circadian cycle (Devlin, 2002). In plants, light pulses predominantly produce phase advances. Hence, continuous light leads to an overall speeding of the oscillator.

Phys and crys contribute to Aschoff's rule at different fluence rates and light qualities. Under low fluence of Rc, the *phyA* mutant displayed a longer period. Under medium and high fluence Rc, *phyB* mutant displayed long period (Somers *et al.*, 1998; Devlin and Kay, 2000b). The double mutant *phyA phyB* displayed a long period under all fluence of Rc. Under Rc, the effects of loss of the *phyD* and the *phyE* were found to be additive to those of the loss *phyB* (Devlin and Kay, 2000b). Consistently, over-expression of PHYA (*PHYA-OX*) or PHYB (*PHYB-OX*) shortened the circadian period of *CAB*, with larger effects observed in *PHYA-OX* (Anderson *et al.*, 1997). Overall, phytochromes have both complementary and redundant roles on periodicity under Rc.

Under BL, *cry1* mutants displayed long period under low- and high-light intensities. However, *cry2* period was found to be similar to that of the wild type (Somers *et al.*, 1998; Devlin and Kay, 2000b). The double mutant *cry1 cry2* displayed a pronounced long period under all light intensities (Devlin and Kay, 2000b). Interestingly, *phyA* mutants resulted in similar long period to the *cry1* under low fluence Bc, showing that *phyA* is required for *cry1* signaling at this fluence. In this BL response, *phyB* mutant was not affected (Somers *et al.*, 1998; Devlin and Kay, 2000b). Conversely, *cry1* is also required for period shortening under low to medium intensities of Rc. *cry1* and *cry2* function is partially redundant, since *cry1 cry2* double mutant showed larger period lengthening effects under low and medium fluence of Rc (Devlin and Kay, 2000b). Taken together, photoreceptors are collectively required for Aschoff's rule.

Downstream of photoreceptors, several clock-components display abnormal fluence-rate responses when mutated or over-expressed. *ELF3-OX* lengthens circadian period under all intensities of BL and at high intensities of RL (Covington *et al.*, 2001), indicating that *ELF3* works as a repressor of light signals to the central oscillator. Interestingly, *ELF3* was found to physically interact with *phyB* (Liu *et al.*, 2001). The period lengthening effect of *ELF3-OX* (Covington *et al.*, 2001) and *phyB* (Somers *et al.*, 1998; Devlin and Kay, 2000a) mutant is similar under high RL

intensities, suggesting direct repression of phyB to *ELF3*. For Aschoff's rule, *ELF3* plays an opposite role to photoreceptors.

1.6.5 Gating of light signals by the clock

The circadian clock modulates sensitivity to external and internal inputs throughout the day. Such a mechanism is called gating. For example, the transcript accumulation of *CAB* has a characteristic RL acute induction that is limited to the early subjective day (Millar and Kay, 1996). Therefore, *CAB* induction has been extensively used to study the clock-gating mechanism. This acute induction of *CAB* is mediated by phyA and phyB. In *phyA phyB* double mutant the acute induction of *CAB* by light was greatly attenuated while circadian oscillation of *CAB* persists. Consistently, *PHYA-OX* and *PHYB-OX* led to dramatic increase of *CAB* acute peak and amplitude of *CAB* oscillations in etiolated seedlings (Anderson *et al.*, 1997). Two major components of the gating of acute *CAB* induction are *ELF3* and *ELF4*. In their respective loss of function mutants *CAB* was induced by light regardless of the time of the day (McWatters *et al.*, 2000; McWatters *et al.*, 2007). Lack of gating response may be caused by arrhythmia in *elf3* and *elf4* (McWatters *et al.*, 2000; Covington *et al.*, 2001; McWatters *et al.*, 2007). In *ELF3-OX* the acute peak of *CAB* was attenuated, but showed normal gating response (Covington *et al.*, 2001). *ELF3* and *ELF4* are thus critical for processing light information to the oscillating mechanism.

1.7 Conserved mechanisms in circadian systems: chromatin remodeling and regulation of sub-cellular distribution

Although the core components of circadian systems are specific to plants, animals, or fungi, several molecular mechanisms seem to be conserved or they have been recruited for the oscillator function in different kingdoms (Rosbash, 2009). This section focuses on chromatin remodeling, and regulation of sub-cellular distribution of clock proteins that have been found in several clock systems.

1.7.1 Chromatin remodeling

DNA in eukaryotes is wrapped around highly conserved basic proteins called histones to form nucleosomes. These are the basic structural units of chromatin and they play a pivotal role in the regulation of transcription (Pfluger and Wagner, 2007). In each nucleosome, two turns of DNA are wound to a histone (H) octamer containing two

H2A-H2B dimers and one H3-H4 tetramer (Pfluger and Wagner, 2007). Nucleosomes are connected by linker DNA. Chromatin remodeling uses three major classes of proteins: histone chaperones, DNA and histone modifying enzymes, and ATP-dependent chromatin remodeling enzymes.

The histone code comprises a wide array of post-translational modifications of the N-terminal tails of histones termed histone marks (Pfluger and Wagner, 2007). Different histone marks are correlated to transcriptional activation or transcriptional repression depending if they confer a more relaxed or a more compacted conformation of the nucleosomes, respectively. On one hand, histone-hyperacetylation marks, such as H3Lys14 and H3Lys9, lead to an opening of the nucleosomes, and they correlate with transcriptional activation (Lee and Workman, 2007). On the other hand, histone-methylation marks, such as H3K27me3, mediate nucleosome compaction, and transcriptional repression (Pfluger and Wagner, 2007).

Histone acetylation is involved in the core-clock mechanism. In animal clocks, the core-clock component CLOCK has intrinsic histone acetyltransferase (HAT) activity. CLOCK HAT-activity is mediated by its glutamine-rich domain (Doi *et al.*, 2006). In *Arabidopsis*, rhythms of H3 acetylation and deacetylation at the promoter of *TOC1* were found to be essential for rhythmic expression of *TOC1*. Moreover, CCA1 association to *TOC1* promoter precedes the transition from a permissive to a repressive transcriptional state of *TOC1* (Perales and Mas, 2007). Therefore, rhythmic histone-acetylation changes are important for clock transcriptional regulation.

Recently, histone methylation function has been implicated in the circadian clock. The *JUMONJI DOMAIN CONTAINING 5 (JMD5)* is co-expressed with evening-clock components, such as *TOC1*. Loss of function and over-expression of JMD5 caused shortening of the circadian period under LL, but no periodicity phenotype was observed in DD (Jones *et al.*, 2010; Lu *et al.*, 2010). The clock function of JMD5 and its human orthologue is conserved between plants and humans (Jones *et al.*, 2010).

1.7.2 Regulation of sub-cellular distribution of clock proteins

In animals and fungi, the core-clock mechanism consists of a positive-negative feedback loop. A transcriptional activator complex promotes the expression of negative factors. In turn, these negative factors act to repress the activator complex (Mehra *et al.*, 2009). Nuclear import and export events regulate the activity of the components of the core loop in several circadian systems. Some examples are discussed below (Figure 1.6).

In *Drosophila*, the activator complex is arranged by CLOCK (CLK) and CYCLE (CYC). These two proteins interact both in the cytoplasm and the nucleus. CLK-CYC interaction is required for nuclear import of CLK and stabilization of CLK in the nucleus (Hung *et al.*, 2009). CLK-CYC complex activates the transcription of the negative factors PERIOD (PER) and TIMELESS (TIM) (Hung *et al.*, 2009). Newly synthesized PER and TIM proteins bind in the cytoplasm, and their nuclear import is delayed several hours by an unknown mechanism (Meyer *et al.*, 2006). Once in the nucleus, PER disrupts association of the CLK-CYC complex with DNA, and displaces CLK to protein complex that does not associate to DNA (Menet *et al.*, 2010)

In mice, the core activator complex is formed by the homologues of CLK and CYC that are CLK and BMAL, respectively (Gekakis *et al.*, 1998). When BMAL and CLK proteins were ectopically expressed, they preferentially accumulated in the nucleus and cytoplasm, respectively. BMAL-CLK co-expression did not change BMAL nuclear localization, but it dramatically changed CLK sub-cellular distribution to be nuclear. In *Bmal1* mutant fibroblast, CLK protein was constitutively cytoplasmic (Kondratov *et al.*, 2003). The BMAL-CLK complex activates the expression of the negative factors PER and CRY (Gekakis *et al.*, 1998). PER and CRY interact both in the nucleus and cytoplasm. The nuclear-cytoplasm shuttling of PER and CRY is regulated by nuclear import signal (NLS) and nuclear export signal (NES) present in PER protein (Loop *et al.*, 2005). Target mutagenesis of the PER NES leads to arrhythmicity of clock-controlled gene expression (Loop *et al.*, 2005). In the mammalian clock, dynamic nuclear-cytoplasm partitioning of core clock proteins is essential for clock function.

In *Neurospora*, the WHITE COLLAR (WC) transcription factors WC-1 and WC-2 form the WCC transcriptional activator complex (Cheng *et al.*, 2002). Whereas the WCC complex is concentrated in the nucleus, WC-2 protein localizes both in the nucleus and the cytoplasm (Schwerdtfeger and Linden, 2000). WC-1 protein is the limiting factor of the WCC complex and only accumulates in the nucleus in the presence of WC-2 (Cheng *et al.*, 2002). The WCC complex activates the expression of *FREQUENCY (FRQ)*. FRQ protein shuttles to the nucleus where it binds WC-1, and inactivates WCC. This inactivation involves nuclear export of WC-1 (Kondratov *et al.*, 2003; Tamaru *et al.*, 2003; Loop *et al.*, 2005; Hong *et al.*, 2008). Hence, nuclear import-export dynamics are essential for the *Neurospora* clock mechanism.

In Arabidopsis, the nuclear localization of TOC1 is stabilized by its interaction with PRR5 (Figure 1.4). The disruption of this interaction in weak alleles of *TOC1* and

PRR5 decrease TOC1 nuclear pool, and makes TOC1 susceptible for degradation mediated by ZTL in the cytoplasm (Mas *et al.*, 2003; Wang *et al.*, 2010). Taken together, dynamic sub-cellular distribution of clock components is at the core of eukaryotic circadian systems.

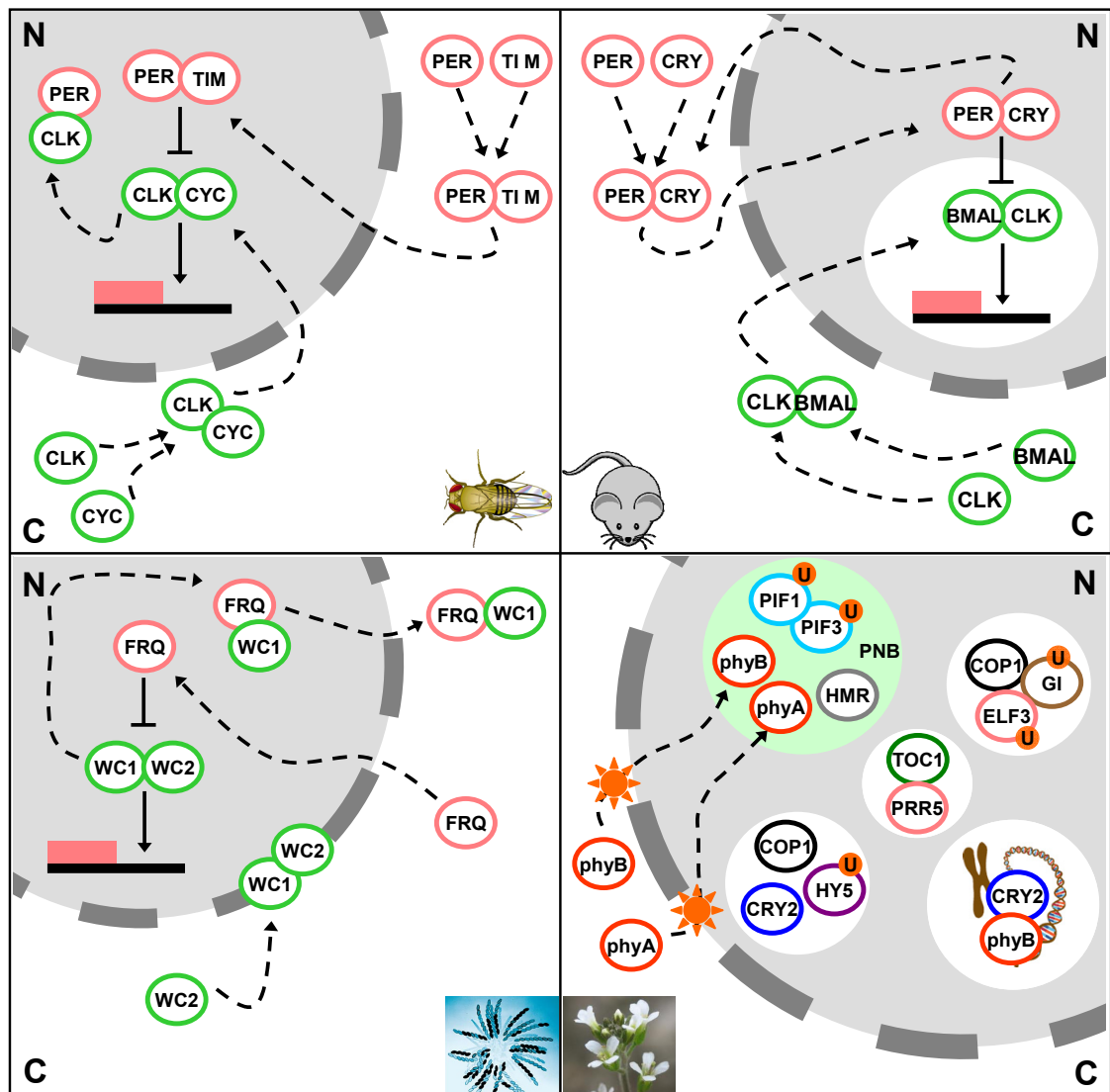


Figure 1.6. Sub-cellular localization dynamics are at the core of circadian systems. Circadian clock systems of *Drosophila* (top left), Mouse (top right), and *Neurospora* (bottom left). Clock- and light-signaling components localize in nuclear bodies (NB) in Mouse (top right) and in Arabidopsis (bottom right). Mouse and plant NB are colored in white. Phytochrome nuclear bodies (PNB) are colored in green. Abbreviations: N (nucleus), C (cytoplasm), U (ubiquitination). The models are explained in sections 1.3.2 and 1.3.3.

1.7.3 Light and clock signaling proteins localize in nuclear bodies

The eukaryotic nucleus is a complex tridimensional structure organized in numerous sub-domains and compartments. Nuclear compartments are generically termed nuclear bodies (NB). Examples of NB are the nucleoli, the Cajal bodies, and the spliceosome. Essential nuclear processes such as RNA transcription and processing occur within these NB (Matera *et al.*, 2009).

Notably, several clock proteins have been shown to localize in NB. In *Drosophila*, the localization of CLK in NB, have been postulated as an storage pool for excess of CLK protein (Hung *et al.*, 2009). In the mammalian clock, sumoylation of BMAL relocates BMAL in transcription-related NB (Figure 1.6). In this NB, CLK-BMAL mediate transcriptional activation, and the CLK-BMAL complex is rapidly targeted to proteasome-mediated degradation (Lee *et al.*, 2008; Kalamvoki and Roizman, 2010). In animal clocks, NB are associated to transcriptional regulation and protein degradation.

In *Arabidopsis*, a common feature of numerous light and clock signaling proteins is the localization within NB (Figure 1.5). Phy nuclear bodies (PNBs) formation is light and circadian regulated. In etiolated seedlings, phytochromes are mainly in the cytoplasm. FRL and RL pulses induce nuclear translocation of phyA (Bauer *et al.*, 2004). In the nucleus, phyAs localize in transient PNBs (tPNBs). In these tPNBs several PIFs are phosphorylated, ubiquitinated, and then targeted for proteasome degradation (Bauer *et al.*, 2004; Shen *et al.*, 2005; Shen *et al.*, 2007; Lorrain *et al.*, 2008). Subsequently, under extended light tPNBs diffuse, and, later, stable PNBs appear (sPNBs). Recently, the characterization of the *hemera* (*hmr*) mutant has demonstrated the exceptional importance of PNBs. The *hmr* mutants do not form PNBs and cannot degrade phyA, PIF1, and PIF3. Thereby, *hmr* mutants are impaired in many phy-mediated responses. HMR protein structure indicates that it could possess a proteolysis activity (Chen *et al.*, 2010). Thus, PNBs seem to be sub-nuclear structures involved in protein degradation.

The photoreceptors cry2 and phyB also co-localize in nuclear bodies (Mas *et al.*, 2000). Interestingly, cry2 and phyB have been implicated in light-mediated changes in chromatin compaction (Tessadori *et al.*, 2007; van Zanten *et al.*, 2010). Therefore, phyB and cry2 may associate to a Chromatin-Protein Complex that maintains chromatin compaction. Potential members of such a complex are HISTONE DEACETYLASE 6 (HDA6), COP1, and DETIOLATED 1 (Tessadori *et al.*, 2009; van Zanten *et al.*, 2010). Hence, PNB may be involved in light-induced changes in chromatin compaction.

Interestingly, COP1 co-localizes in nuclear foci with the clock components ELF3, and GI, where ELF3 recruits GI to such foci. This co-localization could mediate ELF3 and GI targeting for degradation (Yu *et al.*, 2008). Moreover, co-localization in NB COP1 with HY5 and CRY2 (Chen, 2008). Other clock proteins, such as TOC1 and PRR5, also co-localized in NB (Fukamatsu *et al.*, 2005; Perales *et al.*, 2006; Wang *et al.*, 2010). In plants, nuclear bodies may mediate protein degradation and chromatin remodeling.

1.8 The TILLING approach

Reverse genetics is a powerful tool to identify new signaling components and understand the function of genes. A good example is the use of T-DNA lines in Arabidopsis. Such T-DNA lines most often lead to loss of function of the target gene. However, in some cases the severity given by the loss of a given gene can be an obstacle to understand gene function. In here, two relevant examples are *ELF3* and *ELF4*. Both *elf3* and *elf4* null alleles are arrhythmic, and this has precluded placement of these genes into the clock network. TILLING (Targeting Induced Local Lesions in Genomes) has emerged as more subtle reverse genetics approach that generates a series of alleles with point mutations in the coding sequence of the target gene (McCallum *et al.*, 2000). The TILLING approach has been used successfully for many plant and animal model systems (Stemple, 2004).

In Arabidopsis, TILLING alleles have been obtained by ethyl methanesulfonate (EMS) mutagenesis of seeds. Then, mutations in the gene of interest in the mutagenized population are identified by gene specific PCR amplification followed by mismatch-specific enzymatic digestion (CELI) of the PCR products (McCallum *et al.*, 2000). The Arabidopsis TILLING Project (ATP) has automated all of this process in Arabidopsis, and TILLING alleles can be obtained from the seed stock center (Greene *et al.*, 2003). The TILLING approach has been successfully applied to a diverse list of genes in Arabidopsis (Van Norman *et al.*, 2004; Finkelstein *et al.*, 2005). In particular, the isolation of missense alleles provides essential information about gene function and functional domains. For instance, the analysis of a collection of *elf4* missense alleles provided with a model of *ELF4* action within the circadian clock (Kolmos *et al.*, 2009). Hence, TILLING can be a powerful genetic tool for the functional characterization of clock genes.

1.9 Thesis objectives

Circadian clock and light-signaling networks have a complex interconnection. Previous studies have shown the phenotypic similarities between *elf3* and *elf4* mutants that include clock arrest, aberrant expression of core clock components, light-gating defects, and light-resetting defects (Covington *et al.*, 2001; Kikis *et al.*, 2005; McWatters *et al.*, 2007; Kolmos *et al.*, 2009; Thines and Harmon, 2010). Therefore, *ELF3* and *ELF4* play an essential role to sustain circadian function, and they are also required for correct light-input signaling into the clock. Additionally, *LUX* function is also pivotal for circadian rhythms (Hazen *et al.*, 2005; Onai and Ishiura, 2005). The severity of the clock phenotypes of *elf3*, *elf4*, and *lux* has hindered the molecular characterization of their function. Notably, *ELF3*, *ELF4* and *LUX* are the only three clock-components known that lead to clock arrest when mutated, suggesting that they may act within the same genetic pathway. In particular, an insight on the genetic interaction of the *ELFs* indicated that *ELF3* is genetically downstream of *ELF4* (Kolmos, 2007).

This PhD thesis aimed to expand the genetic and molecular characterization of *ELF3*. For this, I studied the biological relevance of *ELF3-ELF4* interaction. Then I dissect functionality of distinct domains of the *ELF3* protein. To address role of *ELF3* in transcriptional regulation I tested the association of *ELF3* to clock promoters. Finally, I examined the genetic interaction of *ELF3*, *ELF4*, and *LUX*.

In Chapter 4, I expanded the investigation of the role of *ELF3* as an integrator of light signaling to the clock. For this, I further characterized the *elf3* missense allele *elf3-12*. Additionally, I investigated circadian phenotypes of a previously established collection of *elf3* TILLING alleles in the context of light-input signaling to the clock.

Chapter 2 Material and methods

2.1 Materials

2.1.1 Mutant lines and genetic markers

Arabidopsis *LUC* markers used in this thesis are listed in table 2.1 (*LUC* markers). Mutant lines were in three different Arabidopsis accession: *Wassilewskija-2* (*Ws-2*, Table 2.2), *C24* (Table 2.3), and *Columbia-0* (*Col-0*, see below). When used, markers for genotyping transgenic lines are specified in Table 2.4.

In the *Col-0* background, the *elf3* TILLING lines were previously described (Kolmos, 2007). All lines were crossed to *Col-0 GI:LUC*, and homozygous plants were selected in the F3 generation. Most of TILLING alleles co-segregate with the linked *erecta* mutation. Hence, when possible, selection of homozygous lines was first via visual inspection of the *erecta* phenotype. Then, the presence of homozygous *elf3* alleles was confirmed by genotyping. Cleave Amplified Polymorphic Sequence (CAPS) and derived CAPS (dCAPS) were used for genotyping. The CAPS and dCAPS markers were previously described (Kolmos, 2007).

In the *C24* background (Table 2.3), the *elf3-12* (*elf3-G12*), and the *elf3-1* mutations genotyping were previously described (Kolmos, 2007).

Table 2.1. Luciferase lines.

LUC marker	Background	Reference source	Selection marker
<i>LHY:LUC+</i>	<i>Ws-2</i>	(McWatters <i>et al.</i> , 2007)	Hygromycin
<i>GI:LUC+</i>	<i>Col-0</i>	This study	PTT
<i>LHY:LUC+</i>	<i>C24</i>	(Kolmos, 2007)	Hygromycin
<i>CCR2:LUC+</i>	<i>C24</i>	(Hall <i>et al.</i> , 2003)	Hygromycin
<i>CCA1:LUC+</i>	<i>C24</i>	(Kevei <i>et al.</i> , 2006)	Hygromycin

Table 2.2. Mutant and transgenic lines in the Ws background

Stable lines previously generated	Reference	
<i>elf3-4 LHY:LUC</i>	(Hicks <i>et al.</i> , 1996)	
<i>elf4-1 LHY:LUC</i>	(Doyle <i>et al.</i> , 2002; McWatters <i>et al.</i> , 2007)	
<i>35::ELF3-CFP LHY:LUC</i>	(Kolmos, 2007)	
<i>35S::ELF4 LHY:LUC</i>	(McWatters <i>et al.</i> , 2007)	
<i>elf4-1 35S::ELF3-CFP LHY:LUC</i>	(Kolmos, 2007)	Crossed
<i>elf3-4 35S::ELF4 LHY:LUC</i>	(Kolmos, 2007)	Crossed
<i>35::ELF3-CFP 35S::ELF4 LHY:LUC</i>	This study	Crossed
Stable lines obtained by floral dipping for this study		
Background	T-DNA insertion	
<i>elf3-4 LHY:LUC</i>	<i>35S::YFP-ELF3F</i>	
<i>elf3-4 LHY:LUC</i>	<i>35S::YFP-ELF3N</i>	
<i>elf3-4 LHY:LUC</i>	<i>35S::YFP-ELF3NM</i>	
<i>elf3-4 LHY:LUC</i>	<i>35S::YFP-ELF3M</i>	
<i>elf3-4 LHY:LUC</i>	<i>35S::YFP-ELF3MC</i>	
<i>elf3-4 LHY:LUC</i>	<i>35S::YFP-ELF3C</i>	
<i>elf3-4 LHY:LUC</i>	<i>35S::YFP-LUX</i>	
<i>elf4-1 LHY:LUC</i>	<i>35S::YFP-ELF4</i>	
<i>elf4-1 LHY:LUC</i>	<i>35S::YFP-LUX</i>	
Ws <i>LHY:LUC</i>	<i>35S::YFP-LUX</i>	Crossed ^a

^a Ws *LHY:LUC YFP-LUX* lines were obtained from crossing *elf4-1 LHY:LUC YFP-LUX* to Ws *LHY:LUC*. The Ws *YFP:LUX* lines were found in the segregating population.

Table 2.3. Genotyping of mutant lines in the C24 background.

Line	Primers		PCR Product	Restriction enzyme
<i>elf3-12</i>	F	gataaatgaagaggcaagtgatga	197 bp; cuts mutant band to 99 and 98 bp	<i>MboI</i>
	R	gaaagagcggagaataaataacca		
<i>elf3-1</i>	F	gtgactctgtttctccattacaatcga	133 bp; cuts mutant band to 111 and 22 bp	<i>ClaI</i>
	R	cagctcgagaagaaacaaataactcat		

Table 2.4. Primers for genotyping transgenic lines

Transgenic line	Primers		PCR band
<i>YFP ELF3</i>	<i>F</i>	GGGCATCGACTTCAAGGAGGAC	1307
	<i>R</i>	ACAAAGCCACCTGACCTTGCA	
<i>YFP ELF3N</i>	<i>F</i>	GGGCATCGACTTCAAGGAGGAC	890
	<i>R</i>	CAACTGTGTAATAATCAGTTTC	
<i>YFP ELF3NM</i>	<i>F</i>	GGGCATCGACTTCAAGGAGGAC	1567
	<i>R</i>	CTTCTCCGAGTCACCCCTTTGT	
<i>YFP ELF3M</i>	<i>F</i>	GGGCATCGACTTCAAGGAGGAC	796
	<i>R</i>	CTTCTCCGAGTCACCCCTTTGT	
<i>YFP ELF3MC</i>	<i>F</i>	GGGCATCGACTTCAAGGAGGAC	1418
	<i>R</i>	ATGGCCGAAAGGACTTGCTACC	
<i>YFP ELF3C</i>	<i>F</i>	GGGCATCGACTTCAAGGAGGAC	746
	<i>R</i>	ATGGCCGAAAGGACTTGCTACC	
<i>YFP ELF4</i>	<i>F</i>	GGGCATCGACTTCAAGGAGGAC	568
	<i>R</i>	AATGTTTCCGTTGAGTTCTTGAATC	
<i>YFP LUX</i>	<i>F</i>	GGGCATCGACTTCAAGGAGGAC	959
	<i>R</i>	CCGAAGCAGAGGGACCTTCATT	

2.1.2 Chemicals

Tris (hydroxymethyl) aminomethane Hydrochloride, Tris HCl (Roth, #5429.3)

Ethylenediaminetetraacetic acid, EDTA (Merck, #944)

KLORIX®, commercial sodium hypochlorite solution

Triton-X100 (Roth, #3051)

Murashige and Skoog media, MS (Sigma, #M5524 and Duchefa, #M0221)

2-(N-morpholino)ethanesulfonic acid, MES (Duchefa, #M1503)

Sucrose (Roth, #4621)

Phytoagar (Duchefa, #P0001)

Bacto-tryptone (BD, #211705)

Yeast extract (BD, #212750)

Sodium chloride, NaCl (Merck, #1.37017)

Bactoagar (BD, #214040)

Beef extract (BD, #212303)

Peptone (Difco, #0122-17-4)

Magnesium sulphate, MgSO₄ (Duchefa, #110513)

Gentamicin sulfate (Sigma, #G-3632)

Carbenicillin (Sigma, #C-1389)

Kanamycin sulfate (Duchefa, #K4378)
Chloramphenicol (Sigma, #C-0378)
Rifampicin (Sigma, #83907)
Spectinomycin (Sigma, #S-9007)
Streptomycin (Sigma, #S-9137)
DL-Phosphinothricin, PPT (Duchefa, #P0159)
Hygromycin (Duchefa, #H0192)
D-Luciferin (Synchem, #S039)
Na₂HPO₄ (Sigma, #S0876)
NaH₂PO₄ (Merck, #1.06346)
Adenine hemisulfate (Sigma, #A-9126)
Sodium dodecyl sulfate, SDS (Roth, #23.26.2)
Boric acid (Merck, #1.00165)
Bromophenol blue (Sigma, #47522)
Glycerol (Roth, #7530.1)
Ethidium bromide (Sigma; #46067)
Glycine (Roth, #3908.2)
Formaldehyde (Merck, #1.040003)
β-mercapthoethanol (Sigma, #47522)
Protease Inhibitors (PI):

- Protease Inhibitors Cocktail for plant cell and tissue extracts (Sigma, #P9599)
- cOmplete® EDTA-free tablets (Roche, #11873580001)
- cOmplete® Mini EDTA-free tablets (Roche, #11836170001)

Phenol /Chloroform (Roth, #A156.1)
Chloroform (Merck, #1.02445)
Isopropanol (Appli. Chem., #A0900)
Ethanol (J.T.Baker, #8006)
Sodium Acetate (Merck, #1.06268)
Lithium chloride (Li Cl) (Roth, #3739.1)
Nonyl phenoxyethoxyethanol (NP-40) (Fluka, #74385)
Sodium deoxycholate (Fluka, #30970)
3',5'-Dimethoxy-4'-hydroxyacetophenone, Acetosyringone (Sigma, # D134406)
Silwet L-77 (Lehle seeds, #Vis-02)
Lithium Acetate (Sigma, #L-5750)
Polyethylene glycol, PEG 3350 (Sigma, # P-3640)
Dimethyl sulfoxide, DMSO (Sigma, #P8418)
3-amino-1,2,4-triazole (3-AT; Sigma, #A-8056)

2.1.3 Reagents for each method

General use

TE buffer: 10 mM Tris HCl pH 8 and 1 mM EDTA

Seed sterilization

Bleach solution: 33% KLORIX®, 0.02% (v/v) Triton-X100 in ddH₂O

0.01% agar in sterile ddH₂O

Growth media for plants

MS1 (1% sucrose)	MS1(1% sucrose) 3% agar	MS3 (3% sucrose)
4.4 g/L MS	4.4 g/L MS	4.4 g/L MS
0.5 g/L MES	0.5 g/L MES	0.5 g/L MES
10 g/L Sucrose	10 g/L Sucrose	30 g/L Sucrose
1.5% Phytoagar	3% Phytoagar	1.5% Phytoagar
pH 5.7	pH 5.7	pH 5.7

Table 2.5. Antibiotics for plant selection

Antibiotic	Stock	Plants
Gentamicin	100 mg/mL in ddH ₂ O	125 µg /mL
Kanamycin	100 mg/mL in ddH ₂ O	100 µg /mL
PPT	12 mg/mL in ddH ₂ O	12 µg/mL
Hygromycin	30mg/mL in ddH ₂ O	15 µg/mL

Bioluminescence analysis

50 mM D-luciferin stock

1 g Firefly D-Luciferin

71.3 mL 1M Triphosphate buffer (Na₂HPO₄ / NaH₂PO₄) pH 8

5 mM D-luciferin working solution

1.5 mL 50 mM D-Luciferin stock

13.5 mL 0.01% (w/v) Triton-X100

Plant DNA extraction

DNA Extraction Buffer (DEB)

200 mM Tris pH 8.0

240 mM NaCl

25 mM EDTA

1% (w/v) SDS

PCR and molecular cloning

Primers (Invitrogen or Sigma)

dNTP Set, 100 mM Solutions (Fermentas, # R0182)

Taq-DNA polymerase (Genaxxon Bioscience : PeqLab, #01-1000)

Pfu II Ultra® II Fusion HS DNA polymerase (Stratagene, # 600670)

Restriction enzymes (New England BioLabs)

GATEWAY® BP Clonase II enzyme mix (Invitrogen, 11789-020)

GATEWAY® LR Clonase II enzyme mix (Invitrogen, 11791-020)

30% PEG 8000/30 mM MgCl₂. (Invitrogen, #P/N59890)

QIAquick Gel extraction kit (Qiagen, #28704)

QIAprep® Spin Miniprep kit (Qiagen, #27104)

10 mg/mL Ethidium bromide

2X TBE Electrophoresis buffer

67.23 g/L Tris HCl

34.31 g/L Boric acid

37.22 g/L EDTA

pH 8.0

6X DNA loading buffer (Fermentas, # R1151)

Table 2.6. Plasmid used for molecular cloning

Plasmid	Antibiotic	Source
pDONR201	Kanamycin	Invitrogen
pDONR207	Gentamicin	Invitrogen
pDONRP4-P1R	Kanamycin	Invitrogen
pDONRP2R-P3	Kanamycin	Invitrogen
pDEST22	Gentamicin	Invitrogen
pDEST32	Carbenicillin	Invitrogen
35S::GW::CFP	Carbenicillin	This study
35S::YFP::GW	Carbenicillin	This study
35S::GW::BIO	Kanamycin	(Qi and Katagiri, 2009)
pPZP211R4R3	Spectinomycin Streptomycin	Darrah, unpublished

Table 2.7. Primers for cloning cDNAs into pDONR 201/207 (Invitrogen)

<i>ELF4</i>	<i>F</i>	GGGGACAAGTTTGTACAAAAAAGCAGGCTTAATGAAGAGGAACGGCGAG
	<i>R</i>	GGGGACCACTTTGTACAAGAAAGCTGGGTAAGCTCTAGTTCCGGCAGC
<i>PHYB full</i>	<i>F</i>	GGGGACAAGTTTGTACAAAAAAGCAGGCTTAGAAGGAGATAGAACCATGGTTCCGGA GTCGGG
	<i>R</i>	GGGGACCACTTTGTACAAGAAAGCTGGGTAATATGGCATCATCAGCAT
<i>PHYB C</i>	<i>F</i>	GGGGACAAGTTTGTACAAAAAAGCAGGCTTAGAAGGAGATAGAACCATGATTGATGAGT TAGGTGCA
	<i>R</i>	GGGGACCACTTTGTACAAGAAAGCTGGGTAATATGGCATCATCAG
<i>LUX</i>	<i>F</i>	GGGGACAAGTTTGTACAAAAAAGCAGGCTTAATGGGAGAGGAAGTACAAATG
	<i>R</i>	GGGGACCACTTTGTACAAGAAAGCTGGGTCTTAATTCTCATTGCGCTTCCACCTC
<i>RFP</i>	<i>F</i>	GGGGACAAGTTTGTACAAAAAAGCAGGCTTAATGGGTCTTCCAAGAATGTTAT
	<i>R</i>	GGGGACCACTTTGTACAAGAAAGCTGGGTATTAAGGAACAGATGGTGGCGTC (stop)
	<i>R</i>	GGGGACCACTTTGTACAAGAAAGCTGGTAAAGGAACAGATGGTGGCGTC (no stop)

Table 2.8. Primers for cloning ELF3 into pDONR 201/207 (Invitrogen)

<i>ELF3 F</i> full-length cDNA	<i>F</i>	GGGGACAAGTTTGTACAAAAAAGCAGGCTTCGAAGGAGATAGAACCATGGGGAAAGAT GAGGAGAAGAT
	<i>R</i>	GGGGACCACTTTGTACAAGAAAGCTGGGTATTAAGGCTTAGAGGAGTCATAGCG
<i>ELF3N</i>	<i>F</i>	GGGGACAAGTTTGTACAAAAAAGCAGGCTTCGAAGGAGATAGAACCATGGGGAAAGAT GAGGAGAAGAT
	<i>R</i>	GGGGACCACTTTGTACAAGAAAGCTGGGTAATATGGCATCATCAGCAT
<i>ELF3NM</i>	<i>F</i>	GGGGACAAGTTTGTACAAAAAAGCAGGCTTCGAAGGAGATAGAACCATGGGGAAAGAT GAGGAGAAGAT
	<i>R</i>	GGGGACCACTTTGTACAAGAAAGCTGGGTGCTAGTATATCAGTCCTTCCGAGGGA
<i>ELF3M</i>	<i>F</i>	GGGGACAAGTTTGTACAAAAAAGCAGGCTTCGAAGGAGATAGAACCATGGCAACGGAA AATCATTAC
	<i>R</i>	GGGGACCACTTTGTACAAGAAAGCTGGGTGCTAGTATATCAGTCCTTCCGAGGGA
<i>ELF3MC</i>	<i>F</i>	GGGGACAAGTTTGTACAAAAAAGCAGGCTTCGAAGGAGATAGAACCATGGCAACGGAA AATCATTAC
	<i>R</i>	GGGGACCACTTTGTACAAGAAAGCTGGGTATTAAGGCTTAGAGGAGTCATAGCG
<i>ELF3C</i>	<i>F</i>	GGGGACAAGTTTGTACAAAAAAGCAGGCTTCGAAGGAGATAGAACCATGAAGCCTCAC CCAGGTATGG
	<i>R</i>	GGGGACCACTTTGTACAAGAAAGCTGGGTATTAAGGCTTAGAGGAGTCATAGCG
<i>ELF3F genomic</i>	<i>F</i>	GGGGACAAGTTTGTACAAAAAAGCAGGCTTAATGAAGAGAGGGAAAGAT
	<i>R</i>	GGGGACCACTTTGTACAAGAAAGCTGGGTAAGGCTTAGAGGAGTCATA

Table 2.9. Primers for Multi-gateway cloning

<i>ELF3 promoter</i> <i>pDONR4-1R</i>	<i>F</i>	GGGGACAACCTTTGTATAGAAAAGTTGCTAAAAACCCAATAAAAACCAC
	<i>R</i>	GGGGACTGCTTTTTTGTACAAACTTGCCACTCACAATTCACAACC
<i>ELF3 genomic</i> <i>pDONR201</i>	<i>F</i>	GGGGACAAGTTTGTACAAAAAAGCAGGCTTAATGAAGAGAGGGAAAGAT
	<i>R</i>	GGGGACCACTTTGTACAAGAAAGCTGGGTAAGGCTTAGAGGAGTCATA
<i>YFP</i> <i>pDONR23R</i>	<i>F</i>	GGGGACAGCTTTCTTGTACAAAGTGGCTGGTATCGATAAGCTTATAATGGTG
	<i>R</i>	GGGGACAACCTTTGTATAATAAAGTTGCTTACTTGTACAGCTCGTCCATGCC

Table 2.10. Primer for *elf3-12* mutagenesis

<i>F</i>	GATGTTGTGGGTATATTAGATCAAAAACGTTTCTGGAGAG
<i>R</i>	CTCTCCAGAAACGTTTTTGTCTAATATACCCACAACATC

Growth media bacteria

Luria Bertani (LB)

10 g/L Bacto-tryptone
5 g/L Yeast extract
5 g/L NaCl
1% Agar
pH 7.5

YEBS

5 g/L Beef extract
5 g/L Peptone
5 g/L Sucrose
1 g/L Yeast extract
0.5 g/L MgSO₄
1% agar
pH 7.0

Table 2.11. Antibiotics for bacteria selection

Antibiotic	Stock	Bacteria
Gentamicin	100 mg/mL in ddH ₂ O	10 µg /mL
Carbemicilin	100 mg/mL in ddH ₂ O	100 µg /mL for <i>E. coli</i> 50 µg/mL for <i>Agrobacterium</i>
Kanamycin	100 mg in ddH ₂ O	50 µg /mL
Chloramphenicol	10 mg/mL in ethanol	30 µg /mL
Rifampicin	50 mg/mL in methanol	25 µg /mL
Spectinomycin Streptomycin	30 mg/mL in ddH ₂ O	30 µg /mL

Yeast two-hybrid

SD media

6.7 g/L Yeast nitrogen base without amino acids (Clontech, #8602-1)

Aminoacid Dropout Solution

- -Leu (Clontech, #630414)
- -Trp (Clontech, #630413)
- -Leu His (Clontech, #630418)
- -Leu Trp (Clontech, #630417)
- -Leu Trp His (Clontech, #630419)
- -Leu Trp His Ade (Clontech, #630428)

20 g Bacto-agar (for plates only)

YPAD

20 g/L Peptone

10 g/L Yeast extract

15 mL/L 0.2% Adenine hemisulfate

20 g/L Bacto-agar (for plates only)

DNA salt salmon testes (Sigma, # D1626)

1X TE / 1X LiAc solution (for 10 mL)

1 mL 10X TE pH 8

1 mL 1M Li Ac

8 mL ddH₂O

PEG/ Li Ac (for 10 mL)

8 mL 50% PEG 3350

1 mL 10X TE pH 8

1 mL 1M Li Ac

1 M 3-AT in sterile ddH₂O

96 well Suspension Culture Plate sterile, F-bottom, with lid CELLSTAR® (Greiner Bio-One, #655185)

Chromatin immunoprecipitation (ChIP)

2 M Glycine

GammaBind™ Plus Sepharose™, protein G beads (GE Healthcare, #17-0886-01)

Anti-GFP antibody (Roche, #11814460001)

Miracloth (Calbiochem, #475855)

3M Sodium acetate

Glycogen mol. grade (Fermenas, #R0561)

Tris HCl pH 7.5

iQ™ SYBR® Green Supermix (BioRad, # 170-8882)

Non-stick Rnase-free 1.5 ml microcentrifuge tubes (Ambion, #AM12450)

Proteinase K (Roche, #13085800)

Table 2.12. CHIP buffers. All buffers made in sterile ddH₂O

<p style="text-align: center;">Cross-linking</p> 1 % formaldehyde 0.4 M sucrose 10 mM Tris HCl	<p style="text-align: center;">Extraction 1</p> 0.4 M sucrose 10 mM Tris-HCl pH 8 10 mM MgCl ₂ 5 mM β-Mercaptoethanol Protease inhibitors	<p style="text-align: center;">Extraction 2</p> 0.25 M sucrose 10 mM Tris-HCl pH 8 1% Triton X-100 5 mM β-Mercaptoethanol Protease inhibitors
<p style="text-align: center;">Extraction 3</p> 1.7 M sucrose 10 mM Tris HCl pH 8 0.15% Triton X-100 2 mM MgCl ₂ 5 mM β-Mercaptoethanol Protease inhibitors	<p style="text-align: center;">Nuclei lysis</p> 50 mM Tris HCl pH 8 10 mM EDTA 1% SDS Protease inhibitors	<p style="text-align: center;">ChIP dilution</p> 1.1 % Triton X-100 1.2 mM EDTA 16.7 mM NaCl Protease inhibitors
<p style="text-align: center;">Low-salt wash</p> 150 mM NaCl 0.1 % SDS 1 % Triton X-100 2mM EDTA 20mM Tris HCl pH 8 Protease inhibitors	<p style="text-align: center;">High-salt wash</p> 500 mM NaCl 0.1 % SDS 1 % Triton X-100 2mM EDTA 20mM Tris HCl pH 8 Protease inhibitors	<p style="text-align: center;">LiCl wash</p> 0.25 M LiCl 1% NP-40 1% Sodium deoxycholate 1mM EDTA 10mM Tris-HCl pH 8 Protease inhibitors

Protease inhibitors were added just before use

Table 2.13. Primers for amplification of *PRR9* and *PRR7* promoters for ChIP

<i>PRR9 promoter</i> PCR1	<i>F</i>	GATTGAACCTTTTTGATAATTATTTTG
	<i>R</i>	TGAAATATTATCCATTGACGAAGAA
<i>PRR9 promoter</i> PCR2	<i>F</i>	TGGATTCCAAAGGGGATCTT
	<i>R</i>	CCTTAGATTTTCAAAGCCCATA
<i>PRR9 promoter</i> PCR3	<i>F</i>	TGGGCTTTTGAAAATCTAAGG
	<i>R</i>	TGCTTTGCGTGGAAGAATA
<i>PRR9 promoter</i> PCR4	<i>F</i>	CGCACTGTCCACATCATAGA
	<i>R</i>	CGTTAGTGGCCGCGTAAAT
<i>PRR9 promoter</i> PCR5	<i>F</i>	CCAATTTTTCATTTGGAGTCG
	<i>R</i>	TTCAAATTGGATGGCTTTTT
<i>PRR9 promoter</i> PCR6	<i>F</i>	TGAATGATACATAGAGCAGCTGAA
	<i>R</i>	AATCGCTCTACGGAAGTGGA
<i>PRR9 promoter</i> PCR7	<i>F</i>	TCCACTTCCGTAGAGCGATT
	<i>R</i>	GTAACAAAGCGGGCCTTCAC
<i>PRR9 promoter</i> PCR8	<i>F</i>	GCCGCGATACAGAGAAAATC
	<i>R</i>	CTTTCGATCACAAACCACGAA
<i>PRR9 promoter</i> PCR9	<i>F</i>	GAGTTTAACTTTCTTCTCCTTCTTCT
	<i>R</i>	GACTCAGACCTCAAACAAACTGA
<i>PRR7 promoter</i> PCR1	<i>F</i>	TTGAAATCTATTGGGCTTCG
	<i>R</i>	GGCGGAAGAGACTAGCGTTT
<i>PRR7 promoter</i> PCR2	<i>F</i>	GAATGGCCCATATGGTAAGC
	<i>R</i>	GTCGTTCAGGAGGCTAGTGG
<i>PRR7 promoter</i> PCR3	<i>F</i>	ATATCCGCTCTGACGTGGAA
	<i>R</i>	GGAAATCGGAGACGACCATA
<i>PRR7 promoter</i> PCR4	<i>F</i>	CTCCGATTTCCACTCTCTGG
	<i>R</i>	GCTCCAGAAGTTGCATCAATC
<i>PRR7 promoter</i> PCR5	<i>F</i>	TCTGGAGCTCGATTCTTCGT
	<i>R</i>	TGAAGAACGACGAATTCTCAAA
<i>PRR7 promoter</i> PCR6	<i>F</i>	TGTATGGTTGGATTTTTATTTGATG
	<i>R</i>	CAGCCATAAACCCCTAATTTTCG

Tobacco Agro-infiltration

Infiltration solution: 1 mM MgCl₂ and 1 mM MES in sterile ddH₂O

1M acetosyringone

1 mL Syringe (BD Plastipak™, #300013)

3-week old *Nicotiana benthamiana* plants

2.2 Methods

2.2.1 Seed sterilization

Seed aliquots were placed in clean 1.5 mL microcentrifuge tubes. Seeds were rinsed with 500 µl of 100% ethanol for 2 min. Then, ethanol was removed and seeds were rinsed with 500 µl of bleach solution for 2 min. The bleach solution was removed and seeds were washed with 1mL of sterile water. The washing step was repeated 2-3 times. Finally the seeds were suspended in sterile 0.01 % Agar.

Seeds were plated on the appropriate MS agar plate supplemented with antibiotics (if required), according to Table 2.5. Seed were stratified at 4 °C for 2-3 days in the dark, and then transferred to the appropriate growth cabinet (see Table 2.14).

Table 2.14. Light and entrainment conditions in the growth cabinets.

Condition	Light	Temperature
LD	12h light / 12h dark	Constant 22 °C
SD	8h light / 16h dark	Constant 22 °C
LL WC	Constant light	12h 22 °C/ 12h 16 °C

2.2.2 Bioluminescence assays

After stratification, seedlings were grown under entrainment cycles for 7 days. On day 7, seedlings were transferred to black 96-well Microplates (OPTIPLATE™-96F, PerkinElmer) containing 200 µl of MS3 agar. Plants of the same genotype were arranged in rows. Then, 15 µl of 5mM Luciferin was added to each well and plates were sealed with transparent film (Packard Topseal). Finally, each well was perforated using a needle. An additional day of entrainment in the growth cabinet was applied before plates were transferred to the TOPCOUNT® scintillation counter (PerkinElmer), at subjective dusk. Luminescence values were recorded as the average count of

5 second and monitored every 30-60 min for 4-5 days. When using constant-light conditions, reflector plates were placed in between the seedling plates, and an additional count delay of one minute was applied before the start of the luminescence measurements. The light source was tri-chromatic LED panels (Mark Darby, MD Electronics, UK) attached to the TOPCOUNT® stackers. A minimum of 24 plants per genotype was used for each experiment.

Circadian rhythms of luminescence were analyzed by using Biological Rhythms Analysis Software System (BRASS) macro in EXCEL (Southern and Millar, 2005). For period analysis, a 72 h window was considered starting within the free-running conditions. Period values weighted by real amplitude error (RAE) were considered. The RAE describes the error of the oscillation amplitude in relation to the most probable amplitude that fits the actual data to a theoretical circadian curve. Hence, the RAE is one estimate of rhythmicity, ranging from 0 (perfect fit of data to theoretical curve) to 1 (arrhythmic oscillation). Phase values were corrected to circadian time. Luminescence traces were visualized with the EXCEL macro TOPTEMP II (<http://millar.bio.ed.ac.uk/Downloads.html>).

The phase response curve (PRC) was constructed according to (Covington *et al.*, 2001). Plants were grown for 7 days under LD and then transferred to DD for one full day before 1h red light pulses ($40 \mu\text{mol m}^{-2}\text{s}^{-1}$) were applied every 3h to replicate plant populations. The time of the first peak after each pulse was calculated for the pulsed and non-pulsed populations. The circadian period of each population after the pulse was calculated and used to transform phase values to circadian time (CT). Phase advances were plotted as positive and phase delays as negative values with error bars that represent pooled S.E.M. (y-axis). The time of the pulse was corrected to circadian time (CT; x-axis).

2.2.3 Molecular biology

Genomic DNA and cDNA sequences were obtained from TAIR. All primers were designed using Vector NTI (Invitrogen), Lasergene (DNASTAR®) software, and Primer3Plus (<http://www.bioinformatics.nl/cgi-bin/primer3plus/primer3plus.cgi>, (Rozen and Skaletsky, 2000))

Plant DNA extraction

DNA extractions were performed according to the protocol from Michaels and Amasino (Michaels and Amasino, 2001) in Qiagen collection microtubes (96-format).

Plant material was ground using metal beads in 400 μ L DEB and 60 μ L chloroform with a mixer mill (Retsch MM 301, Qiagen). The material was then centrifuged at 2500 g for 10 min. In a fresh 96-well microplate, 75 μ L of supernatant were mixed with 75 μ L of isopropanol, and then centrifuged at 2500g for 10 min. DNA pellets were washed once with 70 % ethanol and let to air dry at \approx 20 °C. Finally, DNA was resuspended in sterile ddH₂O and stored at -20 °C.

PCR for genotyping

For plant genotyping, PCR was performed using Taq-polymerase (Genaxxon or Peqlab). A given PCR product was typically resolved in 1% agarose in TBE buffer, and visualized by ethidium bromide staining fluorescence. For CAPS and dCAPS markers restriction of PCR product was performed according to manufacturer's protocol and resolved in a 4 % agarose gel.

PCR and purification for cloning

All PCR for subcloning were made using proof-reading enzyme Pfu II Ultra HF DNA polymerase (Stratagene). PCR was resolved in 1% agarose. The appropriate band was excised, and purified using QIAquick Gel Extraction Kit (Qiagen). Purified product was resuspended in TE. Additionally, purification of PCR product was performed with 30% PEG8000/ 30mM MgCl₂ (Invitrogen) according to manufacturer's protocol. Primers used for obtaining PCR are listed in Table 2.8 for *ELF3* amplicons, and in Table 2.7 for other amplicons.

Cloning with Gateway[®]

All Gateway[®] empty vectors were propagated in *Escherichia coli* (*E. coli*) *DB3.1* cells, and LB media was supplemented with 10 μ g/mL of Chloramphenicol. *E. coli* *DH5 α* cells were used to propagate transformed vectors.

BP reaction was performed to recombine PCR products into pDONR201, pDONR207, pDONR4R-1PR, and pDONR2-3PR (Invitrogen). The BP reaction was set up in a fresh 1.5 mL microcentrifuge tube as indicated in Table 2.15, and gently mixed. The reaction was left \approx 12 h at 20 °C. Then, 0.5 μ L of Proteinase K (Invitrogen) was added to the BP reaction followed by incubation for 10 min at 37°C. Tubes were then kept on ice until transformation. Finally, 1 to 4 μ L of BP reaction were used for transforming 50 μ L cells.

LR reaction was performed to recombine cloning cassette from pDONR to pDEST vectors. LR reaction was set up in a fresh 1.5 mL microcentrifuge as indicated in table 2.16, and gently mixed. The reaction was left ≈ 12 h at 20 °C. Then, 0.5 μ l of Proteinase K (Invitrogen) was added to the LR reaction followed by incubation for 10 min at 37°C. Tubes were then kept on ice until transformation. Then, 1-4 μ l of LR reaction were used for transforming 50 μ l cells. The destination vectors used for yeast and plant expression are listed in Table 2.6.

The Gateway[®] cassette of the pDESTR4R3 vector (Invitrogen) was cloned into the binary vector pPZP211 (Hajdukiewicz *et al.*, 1994) to obtain the modified pPZP211R4R3 vector. The MultiGateway[®] LR reaction was set up in a fresh 1.5 mL microcentrifuge tube as indicated in Table 2.15, and gently mixed. The reaction was incubated ≈ 12 h at 20 °C. Then, 1 μ l of Proteinase K (Invitrogen) was added to the LR reaction followed by incubation for 10 min at 37°C. Tubes were then kept on ice until transformation. Then, 4-8 μ l of the reaction volume was used for transforming 50 μ l cells.

Table 2.15. Gateway[®] reactions set up.

BP reaction	LR reaction	LR reaction MultiGateway
≈ 100 fmol ^a pure PCR 0.5 μ l pDONR (≈ 100 fmol) TE pH 8 to 4 μ l final volume 1 μ l BP Clonase Enzyme mix	0.5 μ l pDONR 0.5 μ l pDEST 3 μ l TE pH 8 1 μ l LR Clonase Enzyme mix	1 μ l 200 fmol pDONR 4-1R 1 μ l 200 fmol pDONR 201 1 μ l 200 fmol pDONR 2-3R 1 μ l 40 fmol pPZP211R4R3 4 μ l TE pH 8 2 μ l LR Clonase Enzyme mix

^a The following formula was used to calculate the appropriate amount of PCR or Plasmid.
 $\text{ng} = (\text{n fmol}) (\text{n bp PCR or plasmid}) \times (660/10^6)$

Site-directed mutagenesis

The point mutation in the *ELF3* genomic sequence present in the *elf3-12* allele was introduced into pDONR vectors containing *ELF3* coding sequences, in order to obtain *ELF3-12* constructs. Site-directed mutagenesis was performed using the primers listed in Table 2.10. First, primer extension was performed according to Table 2.16. Then, 1 μ l of *DpnI* restriction enzyme was added to the reaction and incubated for 2 hours at 37 °C. Finally, 10 μ l of the reaction were used to transform *E. coli*. This is analogous to the Quickchange protocol (Stratagene).

Table 2.16. Site-directed mutagenesis set up.

Primer extensin	Cycling conditions	
2 µl Pfu buffer	1X	95 °C 30 sec
1 µl Plasmid template	18X	95 °C 30 sec
2 µl Primer mix		55 °C 1 min
1 µl dNTPs		68 °C 10-15 min
0.5 µl Pfu II Ultra HS		
13.5 µl with ddH ₂ O		

***E. coli* transformation**

For *E. coli* transformation, an aliquot of chemical-competent *E. coli* cells was thawed on ice and 1- 8 µl of plasmid or BP/LR reaction was added to the cells. After 20 minutes on ice, cells were submerged in a 42 °C water bath for 45 sec. Immediately after, 900 µl of LB media was added to the cells, and they were incubated for at least 1 hour at 37 °C, with gentle shaking. After incubation, the cells were plated on LB agar plate supplemented with appropriate antibiotics (see Table 2.11). Plates were sealed with parafilm and incubate for ≈12 h in a 37 °C growth cabinet.

Isolation of Plasmid DNA

Bacterial clones (colonies) that grew on the selective plate were propagated on 3 ml of selective LB media o/n. Plasmid miniprep was performed using the Qiaprep® Spin Miniprep Kit (Qiagen) following manufacturer's protocol. DNA was resuspended in 50 µl sterile ddH₂O.

***Agrobacterium* transformation**

Agrobacterium tumefaciens (*Agrobacterium*) strains GV3101 (Koncz and Schell, 1986) and ABI (Schomburg *et al.*, 2001) were used. An aliquot of chemically competent cells was thawed on ice. Then, 1 µl of plasmid miniprep (100-200 ng), and 80 µl of sterile ddH₂O were gently added to the cells. Cells were transferred to an electroporation cuvette. Electric pulse was applied with Gene Pulser (Bio-Rad). After electroporation, cells were diluted with 900 µl of LB media, and incubated for at least 2 h at 28 °C while shaking at 250 rpm. Then, 80 µl of the culture was plated in YEBs agar complemented with appropriate antibiotics (Table 2.11). Plates were sealed with parafilm and incubated for 2 days at 28 °C.

2.2.4 Yeast 2-Hybrid

Y2-H assay was performed by mating using *Saccharomyces cerevisiae* (yeast) strain *PJ69a/α* (James *et al.*, 1996), and by co-transformation using yeast strain *AH109* (Clontech).

Yeast transformation

Yeast transformation was performed following Small-scale Li Cl Yeast transformation procedure (Clontech Yeast Handbook, # PT-3024-1). Yeast glycerol stock was streaked on a YPAD agar plate and grown for 3 days at 30 °C, until colonies reached 2-3 mm in diameter. Several colonies were resuspended in 1mL of liquid YPAD by vortexing for 5 min. Then, the 1 mL of resuspended yeast was diluted in 50 mL of YPAD, and incubated for 16-18 hrs at 30 °C with shaking at 250 rpm. After 16-18 hrs, the culture was diluted with fresh YPAD to obtain a culture of 300 mL of OD600 ≈0.2-0.3. The 300 mL culture was grown for ≈ 3 hours or until the cell density reached OD600<0.5. Then, the culture was transferred to six 50 mL centrifuge tubes, and centrifuged for 5 min at 1000g at ≈20 °C. The supernatant of each tube was discarded, and the pellet was resuspended in sterile TE. Then, the resuspended pellets were collected into the same centrifuge tube, and the cells were pelleted a second with a centrifugation of 5 min at 1000 g at RT. The supernatant was decanted and the yeast pellet was resuspended in a sterile 1X TE/1X Li Ac solution. For each transformation, a fresh microcentrifuge tube was prepared containing well mixed 100 µg of carrier DNA and 0.1 µg plasmid DNA (for co-transformation, 0.1 µg of each plasmid was added). Then, 100 µl of yeast suspension was added to each tube and mixed by vortexing. Finally, 0.6 mL of PEG/LiAC solution was added to each tube and mixed by 10 sec of vortexing. Tubes were then incubated at 30 °C for 30 min with shaking at 200 rpm. After this incubation, 70 µl of DMSO was added to each tube and mixed by gentle inversion. The tubes were placed in a water bath at 42 °C for 15 min. Immediately after, tubes were chilled for 2 min on ice. Then, tubes were centrifuged for 10 sec at 14,000 rpm. The supernatant was discarded and the yeast cells were resuspended in 200 µl of sterile TE. Cells suspensions were gently distributed on appropriate SD Dropout agar media (for single transformation SD-L and SD -W, and SD-LW for double transformation). Finally, plates were sealed with parafilm and incubated for 2-3 days until colonies with a 2-3 mm diameter resulted.

Yeast mating

Yeast strain *PJ69a* was transformed with pDEST22 and strain *PJ69 α* was transformed with pDEST32 to obtain yeast single-transformants. For the mating, 160 μ l of YPAD was added to each well of a 96-well Suspension Culture plate F-bottom (Greiner Bio-One). For each strain to be mated, several colonies, each about 2-3 mm of diameter, were resuspended in 1.5 mL of YPAD. Then, 20 μ l of each *PJ69a* and *PJ69 α* strains were added to the corresponding well. The plate was incubated for \approx 16 h at 30 °C with 200 rpm. The following day, the cultures of each well were resuspended, and 5 μ l of each suspension was plated onto a SD-LW plate. Plates were sealed with parafilm and incubated for 2-3 days.

Interaction test

Double-transformed yeast strains, obtained by co-transformation or mating, were tested for genetic complementation by growing them on selective media with SD-LWH supplemented with 1 to 10 mM 3AT and SD-LWHA. For the interaction test, 5 colonies of each reporter strain were resuspended in 100 μ l of sterile TE. Then, 5 μ l was plated on the each of the SD plates with selective media. Plates were sealed with parafilm and incubated at 30 °C for 3 days. The interaction results were then collected.

2.2.5 Floral dipping

Arabidopsis floral-dipping transformation was performed by a simplified protocol (Davis *et al.*, 2009). For the starting culture, 2-3 colonies of the *Agrobacterium* strains were grown for 2 days in 25 mL of YEBS with appropriate antibiotics (Table 2.11). On the day of the transformation, the starting culture was diluted in 500 mL of YEBS and grown for 6-8 hours. Then, 80 μ l of Silwet L-77 were added to the culture. For dipping, the culture was transferred to a 500 mL beaker. Arabidopsis flowering plants were submerged for 30 seconds in the bacterial culture. After dipping, plants were wrapped with plastics bags for 12-18 hours. Selection of T1 transgenic plants was made on MS1 plates supplemented with appropriate antibiotics. Surviving plants were propagated in the greenhouse and genotyped for the presence of the transgene (Table 2.4).

2.2.6 Tobacco agro-infiltration

Agro-infiltration of tobacco leaves was performed basically as (Voinnet *et al.*, 2003). Cultures of 5-10 mL YEBS with the appropriate antibiotics of each strain were grown for 2 days at 28 °C at 250 rpm. On the day of the infiltration, bacterial cultures were centrifuged at 4000 rpm for 10 minutes, and the supernatant was discarded. Pellets were resuspended in infiltration buffer. Then, 1 µl of 1M acetosyringone was added and the cultures were left for 3 hours in the dark at ≈20 °C. Cell density was determined by measuring OD600. For the infiltration, bacterial cultures were diluted with infiltration buffer until OD3. Appropriate bacterial strains were mixed with the strain P19 (Voinnet *et al.*, 2003), to a final OD1 for each strain. Bacterial mixtures were infiltrated into *N. bentamiana* leaves with a 1 mL syringe. Plants were watered several hours before the infiltration. After infiltration, plants were kept in the greenhouse for 3 days before microscope observation or sample collection.

2.2.7 Chromatin immunoprecipitation (ChIP)

Seeds were surface sterilize and plated on MS3 3% agar plates. After stratification, seedlings were grown under SD. Buffers composition is listed in Table 2.13. The ChIP protocol was related to these two references (Gendrel *et al.*, 2005; Perales and Mas, 2007)

Sample collection

For each sample 1.5g of 2-week old seedlings was harvested. Seedlings were cross-linked on 65 mL of fixing solution for 10 min by vacuum infiltration. The cross-link reaction was stopped by adding 5 ml of 2M glycine and vacuum-infiltration for an additional 10 min. Then, the seedlings were rinse twice with sterile ddH₂O. Surface liquid on the seedling was removed, by gentle blotting a paper towel. Finally, seedlings were packed into aluminum foil and froze in liquid nitrogen. Fixed samples were stored at -80 °C until further use.

Isolation and sonication of chromatin

Frozen plant material was ground in liquid nitrogen with a pre-cooled mortar and pestle until a fine powder was obtained. The powder was placed in a pre-cooled 50mL centrifuge tube, resuspend in 30 mL extraction-buffer-1, and filtered through four layers of Miracloth. The filtered solution was centrifuged for 20 min at 2880 g at 4°C.

After gently removing the supernatant, the pellet was resuspended in 2 ml of extraction-buffer-2, and transferred to a fresh 2 mL microcentrifuge tube. Samples were incubated for 10 min on ice, and then centrifugated at 12000 g for 10 min at 4°C. The supernatant was discarded and the nuclei pellet was resuspended in 800 µl of nuclei lysis buffer. The chromatin was sonicated to obtain DNA fragments \approx 500 bp (Bioruptor, 30 sec on/ 1 min off, medium power). Then chromatin was centrifuged for 5 min at 14.000 rpm at 4°C to pellet down nuclear debris. The supernatant was transferred to a new tube. To test the efficiency of the sonication, 15 µl of chromatin samples were resolved in 1 % agarose gel and the sonication pattern was visualized by ethidium bromide fluorescence. If required, additional sonication was applied.

Immunoprecipitation

For immunoprecipitation (IP), 150 µl of chromatin was diluted with 1350 µl of ChIP dilution buffer, and the volume was divided to 3 Non-stick Rnase-free 1.5 ml microcentrifuge tubes (Ambion): one tube was kept at -80 °C as the input, the second tube was the no-antibody control, and the third tube was the IP. In the IP tube, 5 µl of Anti-GFP antibody (Roche) was added. IP and no-antibody control tubes were incubated for \approx 12h in a rotor at 4° C.

On the next day, GammaBind Plus Sepharose G Beads (GB HealthCare) were equilibrated with binding buffer and collected by centrifugation 0.8 rpm for 2 min. Washing of beads with binding buffer was repeated 3 times. Then, 100 µl of beads in a 50% slurry with binding buffer were added to the IP and to the no-antibody control tubes. After incubation for 2 hours in a rotor at 4° C, beads were collected by centrifugation at 800 rpm for 2 min. The supernatant was discarded and pelleted bead-complexes were washed with 1 mL of Low-Salt Buffer for 10 min. Beads were collected by centrifugation at 8000 rpm for 2 min. This washing procedure was then repeated with High-Salt Buffer, Li Cl buffer, and twice with TE buffer. For elution, 200 µl of freshly prepared elution buffer was added to the beads and mixed by vortexing. Tubes were incubated at 65°C for 15 min with agitation. Beads were collected by centrifugation for 2 min at 800 rpm and supernatant was transferred to a new tube. The elution was repeated once more, obtaining a final volume of 500 µl.

For the following steps, the tubes with the input were also processed. To reverse the cross-linking, 20 µl of 5M NaCl was added to the eluates from the IP and the no-antibody control, and the input. This was followed by incubation at 65°C for 5 h.

Then, 10 μ l of 0.5 M EDTA, 20 μ l 1M Tris HCl pH 6.5, and 5 μ l of 14 mg/ml Proteinase K were added, and the tubes were incubated at 45 °C for 1 h.

Purification of DNA from the ChIP samples

For DNA purification, equal volume of Phenol/Chloroform was added to the de-cross-linked samples and this was vortexed. Then, the tubes were centrifuged for 2 min at 12,000 rpm at 4 °C. The supernatant was carefully transferred to a clean tube and 1/10 volume of 3M sodium acetate, 2.5 volumes of 100% ethanol, and 1 μ l of 10 mg/mL Glycogen was added. This was vortexed. Afterwards the tubes were placed at -20 °C for DNA precipitation. The next day, tubes were centrifuged for 20 min at 12,000 rpm at 4 °C, and supernatant was discarded. Then 1mL of 0 °C 70% ethanol was carefully added to the DNA pellet, and tubes were centrifuged for 2 min at 12,000 rpm at 4 °C. The supernatant was discarded, and then the tubes were left open to allow evaporation of ethanol. Finally, the dried DNA pellet was resuspended in 50 μ l of 10 mM Tris pH 7.5 and stored at -20 °C.

qPCR

Enrichment of DNA sequences was measured by qPCR. Primers for amplification of promoter fragments were designed using Primer3Plus (Untergasser *et al.*, 2007) to obtain amplicon sizes that ranged from 150-200bp (Table 2.13). Primer efficiencies were calculated for a melting temperature of 58°C. qPCR was performed with IQ SYBR Green Supermix (Bio-Rad) in the iCycler iQ5 Multicolor Real-time PCR Detection System (Bio-Rad). Expression values of ChIP samples were normalized to expression values of input samples to calculate the percent of enrichment.

2.2.8 Confocal imaging

For all experiments, a LEICA TCS SP2 AOBS Confocal laser scanning microscope with an HCX PL APO CS 40.0x1.25 OIL UV objective, and LEICA Confocal Software (Leica Microsystems) was used. *N. benthamiana* leaf excisions and *A. thaliana* seedlings were submerged in water. The spectral settings were as follows: for YFP, excitation 514nm and emission 518-570nm; for CFP, excitation 405nm and emission spectra 460-550nm. The pinhole was set to Airy 1 (optimal for objective). Laser intensity was \approx 40%. For each image, channel voltage and offset was adjusted to obtain a linear LUT of fluorescence intensity.

Fluorescence resonance energy transfer (FRET) was assayed by Acceptor-Photobleaching. The spectral settings before and after bleaching were as follows: for CFP (donor) excitation 405nm and emission 450-505nm, and for YFP (acceptor) excitation 514nm and emission 518-590nm. Laser light-intensity was 40%. For bleaching, 100% laser light-intensity of 405nm was applied until YFP levels were reduced to about 25%. Then, FRET efficiency was calculated with the following formula: $\text{FRET efficiency} = \frac{\text{CFP intensity post-bleaching} - \text{CFP intensity pre-bleaching}}{\text{CFP intensity post-bleaching}}$.

2.2.9 Analysis of ELF3 encoded sequence

The analysis of ELF3 protein sequence was performed using CLC Protein Workbench 5.5.1. Domains with distinct amino-acid composition in ELF3 encoded protein were previously described (Hicks *et al.*, 2001). For the prediction of secondary structure, the CLC Protein Workbench Secondary structure prediction was used. This uses a trained and performance-evaluated hidden-Markov-model (HMM) with extracted protein sequences from the protein databank (<http://www.rcsb.org/pdb/>). This feature of CLC predicts alpha-helices and beta-sheets. Protein-kinase-C phosphorylation sites and N-glycosylation sites were predicted by PROSITE (Sigrist *et al.*, 2010) within the CLC Protein Workbench. Evolutionary conserved regions were identified by a multiple-alignment of 35 ELF3 sequences from different plant species (Saini, personal communication). These regions have an overall conservation of at least 80% of sequence similarity.

Chapter 3 Characterization of ELF3-ELF4 complex

Some of the results in this chapter represent collaborative work:
Elsebeth Kolmos generated the LHY:LUC lines used in Figure 3.2
Nora Bujdoso performed rtPCR in Figure 3.11
Markus Berns performed phylogenetic shadowing in Figure 3.12

3.1 Introduction

ELF3 and ELF4 are essential for sustain circadian function (Doyle *et al.*, 2002; McWatters *et al.*, 2007; Thines and Harmon, 2010). The *ELF3* and *ELF4* transcripts are co-expressed, and both act at dusk to achieve their function (Liu *et al.*, 2001; Doyle *et al.*, 2002; McWatters *et al.*, 2007). For ELF3, it has also been shown that protein accumulation reaches a maximum in the first half of the night (Liu *et al.*, 2001; Yu *et al.*, 2008). Previous studies described similar clock arrest phenotypes for *elf3* and *elf4* loss-of-function plants, including attenuated *LHY* and *CCA1* transcript accumulation and elevated levels of *TOC1* (Kikis *et al.*, 2005). Notably, the arrhythmic phenotype of *elf4* can be mimicked computationally by setting the parameters of the three-loop model to the high levels of expression of *GI* and *PRR9* that are found in *elf4* (Kolmos *et al.*, 2009). This suggests that *ELF4* has a dual entry point into the oscillator to repress morning and evening loop components (Kolmos *et al.*, 2009). High expression of *PRR9*, *PRR7*, and *GI* at dusk has also been reported for *elf3* (Thines and Harmon, 2010; Dixon *et al.*, 2011). Therefore, it is possible that ELF3 and ELF4 act in the same signaling pathway.

The biochemical function of ELF3 and ELF4 remains unclear. Both are nuclear localized proteins, but neither show any known conserved domains. Also, ELF3 and ELF4 protein sequences do not relate to each other. Nevertheless, structural modeling suggested that ELF4 has a single domain involved in protein-protein interactions, and therefore, it is likely to be an effector protein (Kolmos *et al.*, 2009). Interestingly, a genetic-epistasis experiment placed *ELF3* genetically downstream of *ELF4* (Kolmos, 2007). Thus, one attractive hypothesis I explore here is that ELF4 acts as an effector for ELF3.

To expand on the functional characterization of *ELF3*, I conducted a transgenic complementation approach to identify genic regions required to restore the *elf3* null-allele phenotype. Interestingly, I could separate the functional domains of ELF3 required to sustain circadian function and to modulate ELF3 function. This is consistent with ELF3 being a multifunctional protein.

ELF3 and phyB play an opposite role in the regulation of clock speed: *ELF3* lengthens and phyB shortens circadian period, respectively (Anderson *et al.*, 1997; Covington *et al.*, 2001). ELF3 has been proposed as a general repressor of light signals to the oscillator (Carre, 2002). Light-input repression has been proposed to be

mediated by ELF3-phyB physical interaction (Liu *et al.*, 2001). In this Chapter, the functional relevance of ELF3-phyB interaction is explored.

General amino-acid features of ELF3 protein suggest its involvement in transcriptional regulation (Hicks *et al.*, 2001). As explained above, levels of *PRR9* and *PRR7* are constitutively high in the *elf3* mutants. Hence, I hypothesized that ELF3 could act as a transcriptional regulator of *PRR7* and *PRR9* expression. Therefore, in this chapter I tested if ELF3 can associate to the *PRR9* and *PRR7* promoters.

Finally, *lux* mutants show similar phenotypes to those of *elf3* and *elf4* (Hazen *et al.*, 2005; Kikis *et al.*, 2005; Onai and Ishiura, 2005; McWatters *et al.*, 2007). In this chapter, I also tested if *ELF3*, *ELF4*, and *LUX* are components of the same genetic complex required to maintain circadian oscillations.

3.2 Results

3.2.1 ELF3 and ELF4 physically and genetically interact

The overall similarity of *elf3* and *elf4* mutant phenotypes led me to the hypothesis that *ELF3* and *ELF4* act in the same pathway. Therefore, the physical interaction of ELF3 and ELF4 was first tested in a yeast two-hybrid assay (Y2-H). Figure 3.1A shows that full-length ELF4 interacts with ELF3. Moreover, using a series deletion fragments of ELF3, the ELF3 the middle domain (ELF3M, residues 261-484) was found to contain the sequence required for ELF4 associations (Figure 3.1A). Note that only the constructs containing the middle domain (ELF3NM, ELF3M, and ELF3MC) led to viable yeast, whereas ELF3N and ELF3C did not. Subsequently, this interaction was confirmed *in planta* by fluorescence resonance energy transfer (FRET). For this, ELF3-CYAN FLUORESCENT PROTEIN (ELF3-CFP) and YELLOW FLUORESCENT PROTEIN-ELF4 (YFP-ELF4) were co-expressed in *N. benthamiana* leaves. Efficiency of FRET from the CFP to the YFP fluorophores was assayed by YFP photo-bleaching. As negative controls RED FLUORESCENT PROTEIN-CFP (RFP-CFP) and YFP-RFP fusions were used. When YFP-ELF4 and ELF3-CFP were co-expressed, the FRET efficiency was 52.4±10.6%, while for the negative controls YFP-RFP with ELF3-CFP and YFP-ELF4 with RFP-CFP the FRET efficiency was much lower (2.0±2.3% and 3.5±2.6%, respectively; Figure 3.1B). Thus, I concluded that ELF4 physically associates with ELF3.

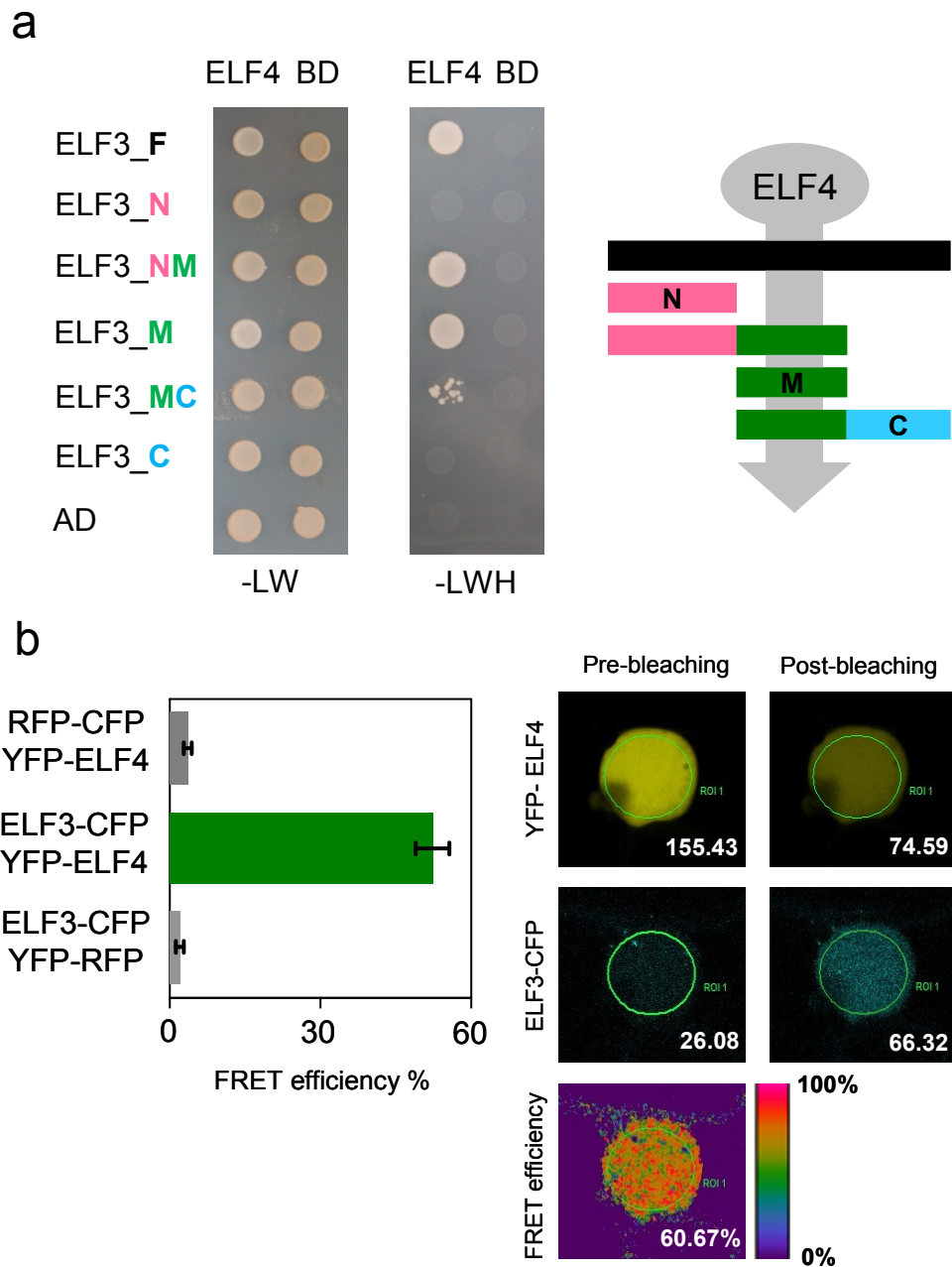


Figure 3.1. The middle domain of ELF3 mediates the physical interaction with ELF4. (a), Y-2H assay of ELF4-BD and ELF3-AD fragments. AD-ELF3 fragments are defined in the right panel. Color code bars: ELF3 F (full-length, black), ELF3N (residues 1-259, blue), ELF3M (residues 261-484, green), and ELF3C (residues 485-695, blue). Abbreviations: AD (activation domain only), BD (binding domain only); - LW and -LWH (drop out for Leu/Trp and Leu/Trp/His, respectively); 3AT (3-Amino-1,2,4-triazole). Y 2-H experiments were performed three times with similar results. (b), ELF3 and ELF4 interact *in planta*. Left panel, FRET assay of ELF3-CFP and YFP-ELF4 in *N. benthamiana*. FRET efficiency \pm SEM: ELF3-CFP YFP-RFP, $2.0 \pm 0.7\%$; ELF3-CFP ELF4-YFP, $52.0 \pm 3.4\%$; RFP-CFP YFP-ELF4, $3.5 \pm 0.8\%$; $n=10$. Error bars indicate Standard Error of the Mean (SEM). Right panel, representative photos of FRET assay by photo-bleaching. The experiment is representative of three independent replicates.

In order to analyze the epistatic relationship between these two *ELF* genes, and "bypass" their arrhythmic mutant phenotypes, double mutants combining the loss-of-function of one and the over-expression of the other were generated. Then, circadian rhythms *LHY:LUC* under LL were assayed. A version of this experiment was previously performed (Kolmos, 2007), and in my extended version, similar results were obtained. In the wild type, *LHY:LUC* expression showed a circadian rhythm with a peak in the early morning (Figure 3.2A-C). Consistent with previous studies (Kikis *et al.*, 2005; McWatters *et al.*, 2007), both *elf3-4* and *elf4-1* single mutants displayed marginal *LHY:LUC* activity and were arrhythmic (Figure 3.2A,B). The over-expression of *ELF3* (*ELF3-OX*) and *ELF4* (*ELF4-OX*) produced a long circadian period (Figure 3.2 A-C), as expected (Covington *et al.*, 2001; McWatters *et al.*, 2007). Similar to *elf3-4*, the double mutant *elf3-4 ELF4-OX* displayed essentially no *LHY:LUC* expression and no circadian rhythms, as seen in the *elf3-4* single mutant (Figure 3.2A). Thus, *ELF4* over-expression has no effect on the *elf3-4* phenotype. In stark contrast, *elf4-1 ELF3-OX* regained overt bioluminescence of the reporter and rhythmic activity, relative to the single *elf4-1* phenotype (Figures 3.2B). Note here that the real amplitude of error (RAE) was similar for wild type, *ELF3-OX*, *ELF4-OX*, and *elf4-1 ELF3-OX*, indicating similar rhythmicity of these backgrounds (Figure 3.2C). Formally, this genetic interaction places *ELF3* and *ELF4* in the same signaling pathway, where *ELF3* acts downstream.

Both the observations that *ELF3* and *ELF4* physically interact and that *ELF3-OX* bypass the *elf4* arrhythmicity phenotype, support the hypothesis that works *ELF4* as an effector (Kolmos *et al.*, 2009), and the *ELF4* target protein is *ELF3*. Both *ELF3-OX* and *ELF4-OX* conferred a long period phenotype, where *ELF4-OX* effect was larger (Figure 3.2 and 3.3). To examine the effect of simultaneously over-expression of *ELF3* and *ELF4*, I introduced *ELF3-OX* and *ELF4-OX* in the same line by crossing, and tested *LHY:LUC* expression under LL. When both *ELF3-OX* and *ELF4-OX* were combined, the *LHY:LUC* period was rhythmic with a long period similar to *ELF4-OX* (Figure 3.3), further supporting that *ELF3* and *ELF4* are in the same pathway within the circadian clock.

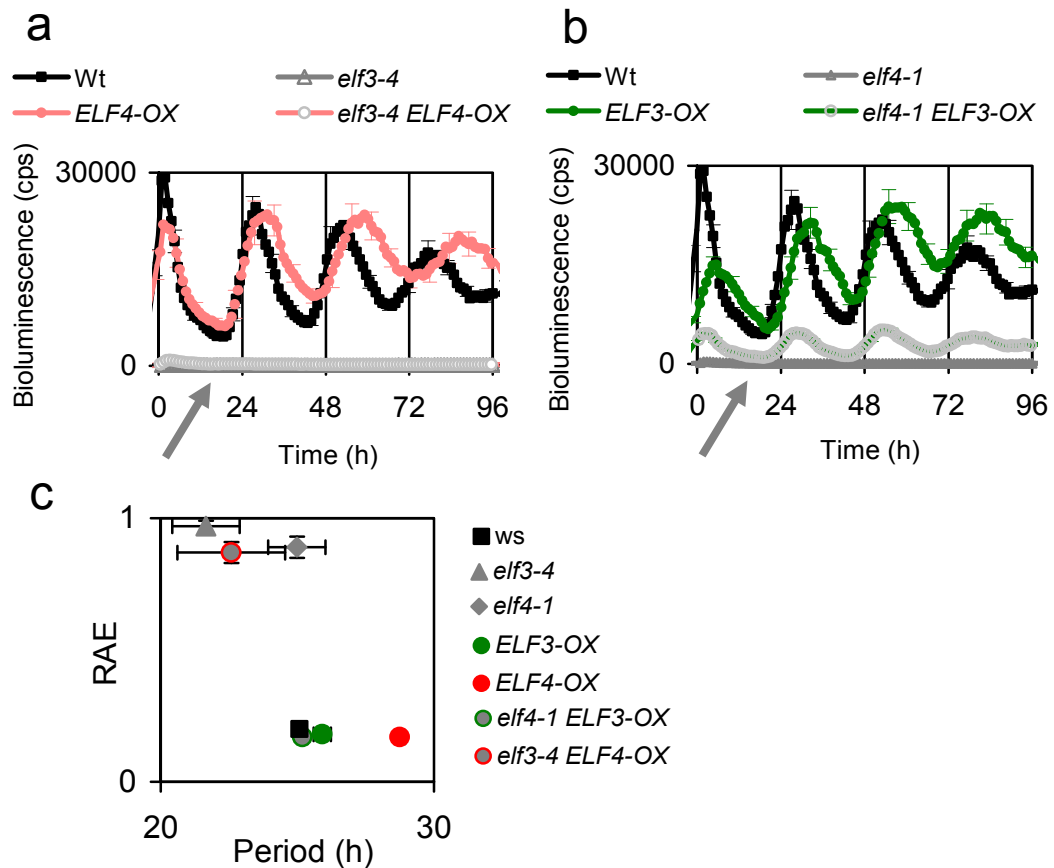


Figure 3.2. *ELF3* is genetically downstream of *ELF4*. (a) and (b), Bioluminescence of *LHY:LUC* under LL. Note that in *elf3-4*, *elf3-4 ELF4-ox* (a), and in *elf4-1* (b) *LHY:LUC* is nearly undetectable (arrow). On the contrary, *elf4-1 ELF3-OX* regains *LHY:LUC* rhythms (b). Wt is the same in both panels. (c) Period vs. RAE of *LHY:LUC* under LL of (a) and (b). Period length \pm SD: (a) Wt, 25.1 ± 1.3 h; *ELF4-OX*, 28.75 ± 0.95 , (b) Wt, 25.1 ± 1.3 h; *ELF3-OX*, 25.9 ± 1.6 h; *elf4-1 ELF3-OX*, 25.2 ± 0.9 h. Error bars indicate SEM, $n=24$. In (a) and (b) errors bars are shown every 6 time point to clarify the curves. cps, count per second. RAE, real amplitude error. This experiment is representative of at least three independent replicates.

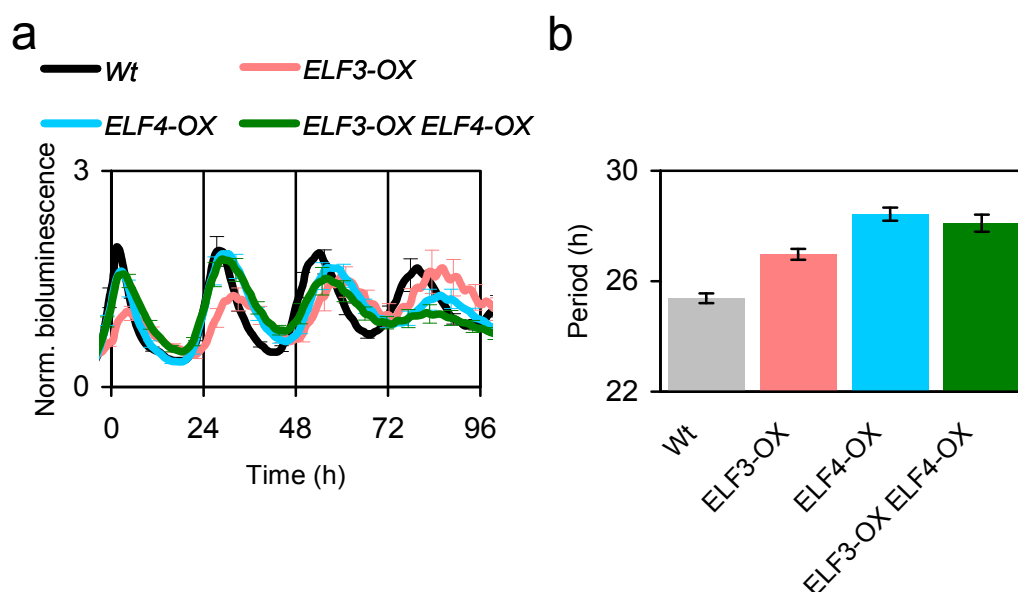


Figure 3.3. *ELF3-OX ELF4-OX* double over-expressor retains circadian rhythms. (a), Bioluminescence of *LHY:LUC* under LL. (b) Period length of *LHY:LUC* under LL: Wt, 25.39±0.17h; *ELF3-OX*, 26.98±0.2h; *ELF4-OX*, 28.43±0.23; *ELF3-OX ELF4-OX*, 28.10±0.31. Error bars indicate SEM, n=24. In (a) errors bars are shown every 6 time point to clarify the curves. This experiment is representative of at least three independent replicates.

3.2.2 ELF4 constrains ELF3 to nuclear distribution

Observations that different domains of ELF3 are required for given protein interactions suggests that the function of ELF3 can be separated [Figure 3.1, (Liu *et al.*, 2001; Yu *et al.*, 2008)]. To further examine this, six different *YFP-ELF3-OX* lines were generated, corresponding to the ELF3 fragments used in the Y2-H experiments (Figure 3.1A and 3.4), and analyzed for their sub-cellular distribution in *N. benthamiana* epidermal cells. Consistent with previous studies (Liu *et al.*, 2001; Yu *et al.*, 2008), full-length ELF3 (*YFP-ELF3F*) was localized in the nucleus and formed distinct nuclear foci (Figure 3.4). On the contrary, the N-terminal fragment of ELF3 (*YFP-ELF3N*) was nearly absent from the nucleus, and accumulated preferentially in the cytoplasm (Figure 3.4). Furthermore, the middle domain (*YFP-ELF3M*) and a longer N-terminal fragment (*YFP-ELF3NM*) were evenly distributed in the nuclear and cytoplasmic compartments (Figure 3.4). Finally, the C-terminal domain of ELF3 (*ELF3C*) was exclusively localized in few, but bright nuclear foci (Figure 3.4). Consistently, the fragment comprising both the middle and C-terminal domains (*ELF3MC*) was preferentially nuclear (Figure 3.4). Thus, the C-terminal domain of ELF3 was required for nuclear localization, which is consistent with the prediction of a nuclear-import signal in the C-terminal of ELF3 (residue 591) (Liu *et al.*, 2001).

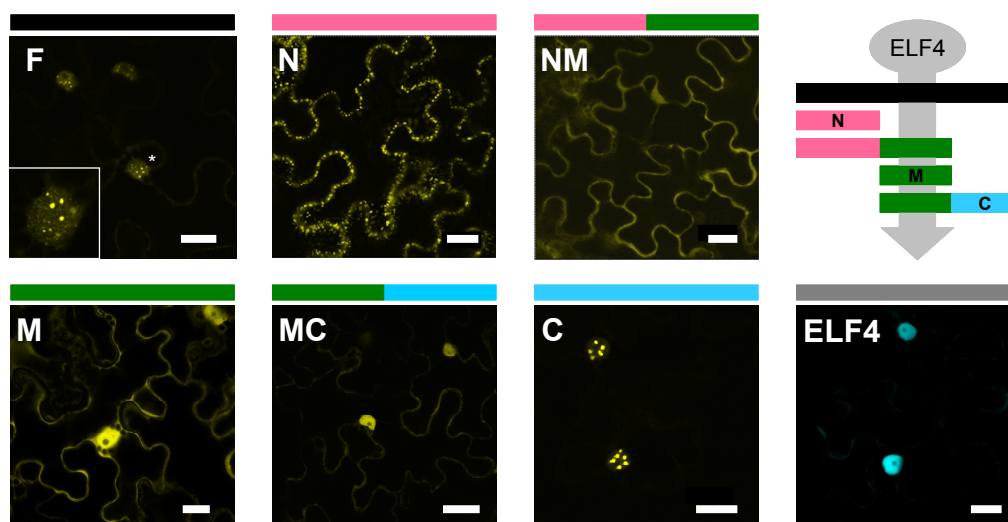


Figure 3.4. ELF3 fragments have different sub-cellular distribution and ELF4 is nuclear localized.

YFP channel of epidermal cells of *N. benthamiana* infiltrated with YFP-ELF3 fragments and ELF4-CFP. Color code bars: ELF3 F (full-length, black), ELF3N (residues 1-259, blue), ELF3M (residues 261-484, green), ELF3C (residues 485-695, blue), and ELF4 (grey). White bar is 20 μ m. YFP-ELF3F (black) and magnification of the nuclei highlighted with a star, YFP-ELF3MC (residues 261-695, green-blue), and YFP-ELF3C (residues 485-695, blue) are all localized in nuclear foci, while YFP-ELF3N (residues 1-260, pink) is cytoplasmic. YFP-ELF3NM (residues 1-484, pink-green) and YFP-ELF3M (residues 261-484, green) have both a cytoplasmic and nuclear distribution. The photos are representative of three independent experiments.

Next, the function of ELF4 as an effector of ELF3 localization was tested. For this, the various YFP-ELF3 fragments were co-expressed with ELF4-CFP and tested if there was a change in the ELF3 cellular distribution. When expressed alone, ELF4-CFP showed a diffuse nuclear localization (Figure 3.4). I did not observe a change in the sub-cellular distribution for the YFP-ELF3 fusions that were already nuclear localized, *i.e.* for ELF3F, ELF3MC and ELF3C; nor for ELF3N, which was found in the cytoplasm. Interestingly, ELF3 co-expression with ELF4 dramatically increased the nuclear accumulation of both YFP-ELF3M and YFP-ELF3NM (Figures 3.5). Note here that the sub-cellular distribution of ELF4-CFP did not change when co-expressed with YFP-ELF3M and YFP-ELF3NM (Figure 3.5). Thus, ELF4 binding to the middle domain of ELF3 constrains it to the nucleus, even in the absence of the ELF3C domain.

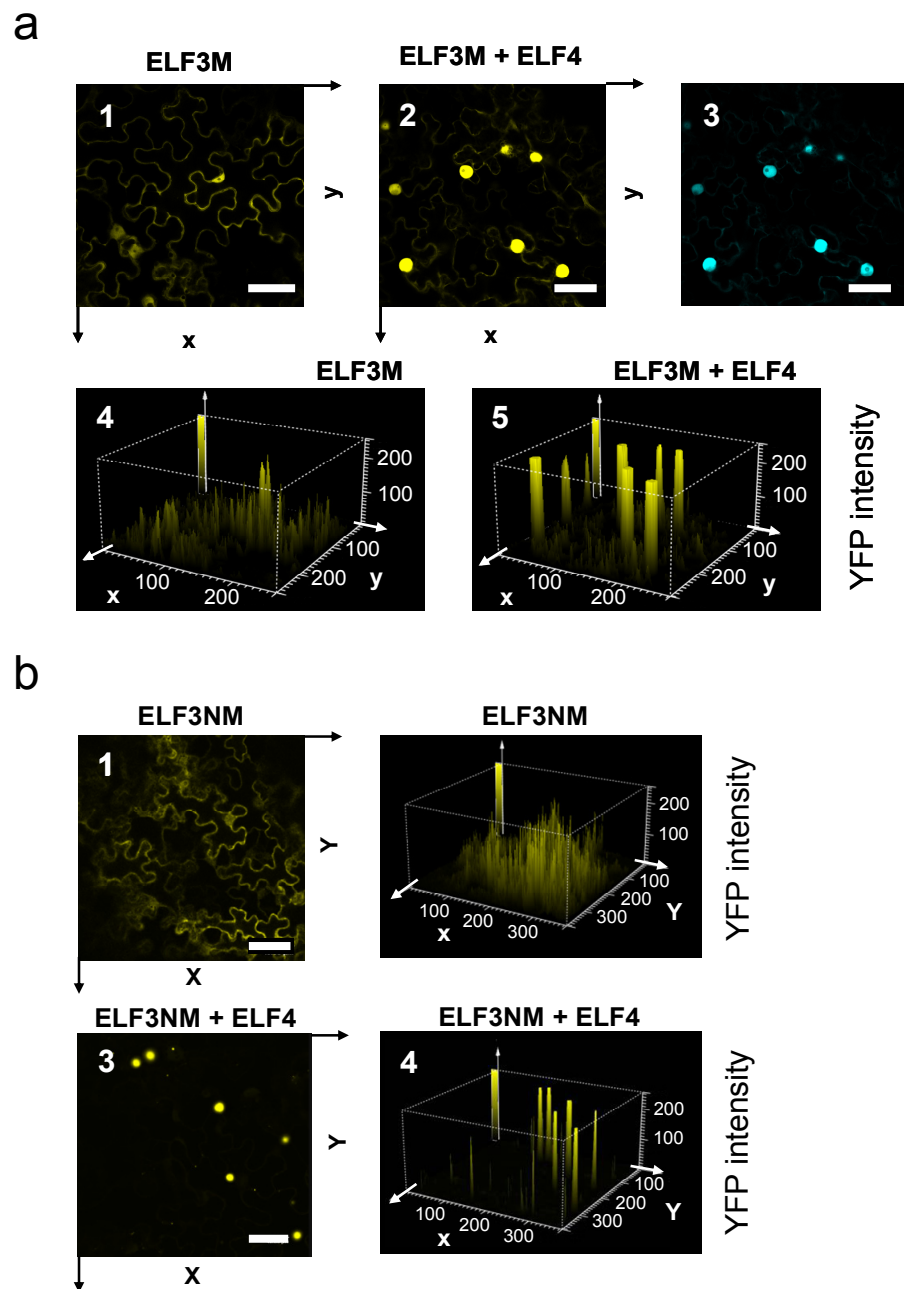


Figure 3.5. ELF4 constrains ELF3 to nuclear distribution.

(a), ELF4 increases ELF3M nuclear localization. Expression of YFP-ELF3M only: (1), YFP channel. Co-expression of YFP-ELF3M and ELF4-CFP: (2), YFP channel and (3), CFP channel. Signal intensity of YFP channel: (4), YFP-ELF3M alone from experiment 1; (5), co-expression of YFP-ELF3M and ELF4-CFP from experiment (2).

b), ELF4 increases ELF3NM nuclear localization. Expression of YFP-ELF3NM only: (1), YFP channel. Co-expression of YFP-ELF3M and ELF4-CFP: (2), YFP channel. Signal intensity of YFP channel: (3), YFP-ELF3MM alone from experiment 1; (4), co-expression of YFP-ELF3NM and ELF4-CFP from experiment (2).

The z, x, and y axes represent YFP intensity, horizontal plane, and vertical plane, respectively. Black arrows (1,2) correspond to white arrows in (4,5). This experiment is representative of two independent replicates.

3.2.3 The ELF4 binding site of ELF3 is required for sustaining circadian period

In order to identify the ELF3 domains required for circadian function, I tested whether each of the YFP-ELF3 fragments described in Figure 3.4 could complement the null allele *elf3-4*. These YFP-ELF3 fragments were expressed under the control of the 35S promoter. The sub-cellular localization of all the YFP-ELF3 fragments in stable Arabidopsis lines was similar to those in transient expression in *N. benthamiana* (Figures 3.4 and 3.6). Thus, these constructs behaved as expected in stable transgenic lines. Interestingly, I observed that the nuclear bodies generated by *YFP-ELF3* full length and *YFP-ELF3C* were different in size and number. The YFP-ELF3 nuclear bodies were smaller, but more abundant than YFP-ELF3C nuclear bodies (Figure 3.6)

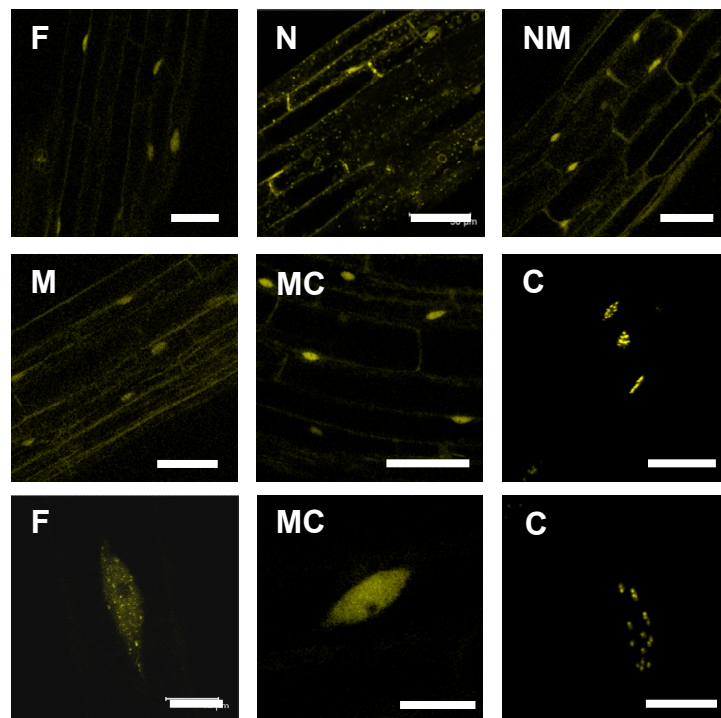


Figure 3.6. Complementation of *elf3-4* with YFP-ELF3 fragments. Confocal microscopy of stable Arabidopsis lines YFP-ELF3 fragments expressed under the 35S promoter. The cellular distribution of YFP ELF3 fragments was similar in *N. benthamiana* (Figure 4) and in Arabidopsis stable transgenic lines. Maximum projection of 6 μm stacks of hypocotyl cells, and 4 μm stacks for single nuclei zoom-in. White bars indicate 50 μm and 10 μm , in hypocotyl cells and nuclei magnification images, respectively.

The complementation capacity of the *elf3-4* phenotype by each *ELF3* transgenic line was tested with the *LHY:LUC* reporter. Consistent with Figure 3.2, and with previous studies (Covington *et al.*, 2001), the over-expression of *YFP-ELF3* conferred a long circadian period of *LHY:LUC* under LL, when compared to the wild type (Figure 3.7). Interestingly, the over-expression of *YFP-ELF3MC* was sufficient to re-establish circadian rhythms in *elf3-4*, albeit with a lower amplitude of *LHY:LUC*, compared to *YFP-ELF3* (Figure 3.7). The rest of the complementation lines did not restore the *elf3-4* phenotype. Thus, both nuclear localization conferred by the ELF3 C-terminal domain, and ELF4-binding mediated by the ELF3 middle domain, are required for ELF3 circadian function.

Interestingly, the amino-terminus of ELF3 (ELF3N) was dispensable for circadian function. Previously, it was shown that a large N-terminal fragment of ELF3 (residues 1 - 440) mediates the physical interaction with the C-terminus of phyB (Liu *et al.*, 2001). Furthermore, using the same ELF3 fragments as in Figure 3.1., the phyB interaction domain of ELF3 was further delineated. The co-expression of ELF3 full length (ELF3) with and PHYB full length (PHYB) or PHY C-terminus domains (PHYBC) led to viable yeast in selective media. Moreover, the fragments containing the ELF3N domain (ELF3N and ELF3NM) also lead to viable yeast when co-expressed with PHYB and PHYBC, whereas, ELF3M, ELF3MC, and ELF3 did not (Figure 3.8). Hence, ELF3N was found to be dispensable for ELF3 circadian function and required for physical interaction with phyB.

The functional relevance of ELF3-phyB interaction is not well understood. Notably, *ELF3* and phyB have opposite effects on the speed of the oscillator (Devlin and Kay, 2000b; Covington *et al.*, 2001). Therefore, it is possible that the amino terminus of ELF3 negatively modulates ELF3 action in period lengthening by interacting with phyB. To physiologically test this hypothesis, the circadian rhythms of *YFP-ELF3* and *YFP-ELF3MC* were measured under different light qualities -continuous red+blue light (R+Bc), continuous red light (Rc), and Bc- and in the darkness (DD). Importantly, all lines were similarly rhythmic under all conditions tested (see R.A.E. in Table 4.1). In diurnal organisms, continuous light shortens circadian period, a phenomena defined as the Aschoff's rule (Aschoff, 1979). Consistently, the period of *LHY:LUC* in the wild type was shorter under R+Bc, Rc, and Bc when compared to DD (Figure 3.9). LL also shortened period length in *YFP-ELF3*, but it had significantly longer period than that of the wild type in DD, under Bc, and under R+Bc (Figure 3.9, Table 3.1). Interestingly, under Rc, the period length of wild type and *YFP-ELF3* was

similar (Figure 3.9). Taken together, *YFP-ELF3* has a significantly longer period than that of the wild type under R+Bc, Bc, and in DD, whereas no significant difference was found in Rc. This suggests that RL, in particular, negatively affects the ELF3 period lengthening effect and that ELF3N is required for Rc shortening of periodicity.

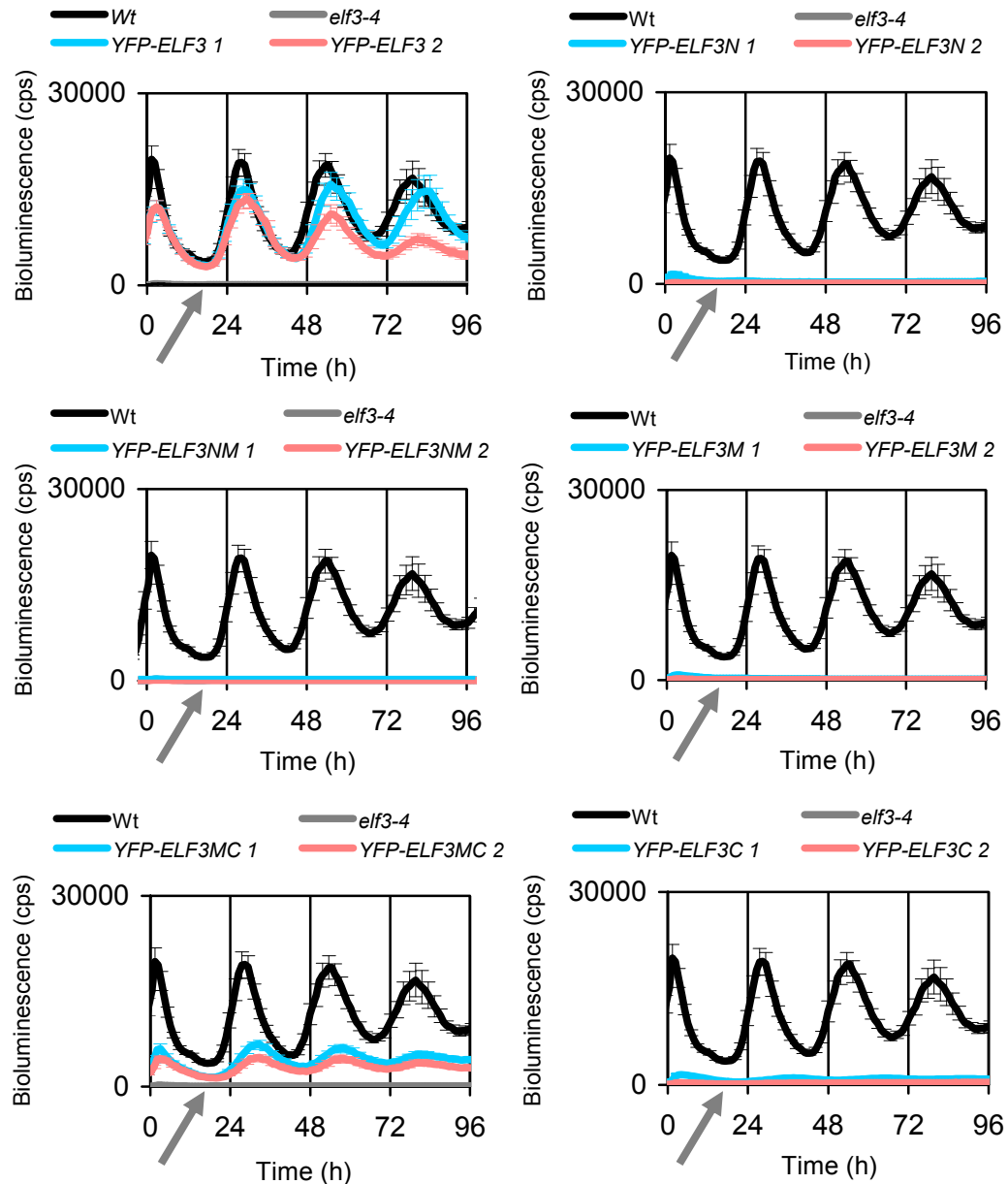


Figure 3.7. Bioluminescence of *LHY:LUC* under LL.

The over-expression of *YFP-ELF3N*, *YFP-ELF3NM*, *YFP-ELF3M*, and *YFP-ELF3C* does not restore *elf3-4* circadian oscillations. However, the over-expression of *YFP-ELF3* and *YFP-ELF3MC* restores circadian rhythmicity. Arrows indicate the position of traces for *elf3-4*. Error bars, SEM and they are placed every two points for clarification of the curves. Wt is the same for the six panels. cps, count per second. These experiment was performed three times with similar results.

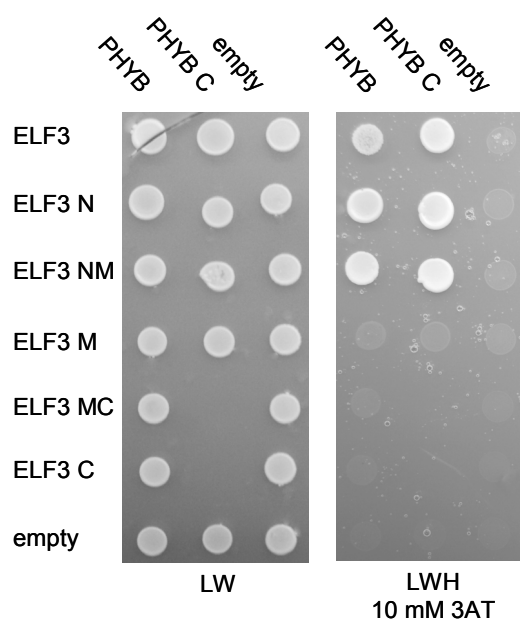


Figure 3.8. The N-terminus of ELF3 mediates interaction with phyB. Y-2H assay of ELF3-BD fragments and PHYB-AD fragments. AD-ELF3 fragments are defined in Figure 3.1 right panel: ELF3 (full-length), ELF3N (residues 1-259), ELF3M (residues 261-484) ELF3C (residues 485-695); PHYB (full length), and PHYBC (residues 646-1172). Abbreviations: AD (activation domain), BD (binding domain); empty (AD or DB only); - LW and -LWH (drop out for Leu/Trp and Leu/Trp/His, respectively); 3AT (3-Amino-1,2,4-triazole). Y 2-H experiments were performed three times with similar results.

Subsequently, I tested the period-lengthening effect on *LHY:LUC* expression of YFP-ELF3MC, which retains circadian function but lacks the phyB-binding domain (ELF3N). For the *YFP-ELF3MC* lines, the period was significantly longer than wild type under all four free-running conditions (Figure 3.9, Table 3.1). Under R+Bc *YFP-ELF3* and *YFP-ELF3MC* displayed similar period length. However, under Bc, *YFP-ELF3MC* had a 2h-longer period than *YFP-ELF3*. Interestingly, both in DD and under Rc, the period length was 3 h longer for *YFP-ELF3MC* than for *YFP-ELF3*. Notably, there was no difference in period length for *YFP-ELF3MC* between DD and Rc conditions (Figure 3.9, Table 3.1), suggesting that *YFP-ELF3MC* does not respond to Rc-period-shortening effect and can lengthen circadian period further in DD. Taken together, the period lengthening effect of *YFP-ELF3MC* under Rc and in DD is consistent with a role of ELF3N as a negative modulator of ELF3 reduction of circadian speed. The shorter period length under R+Bc, and Bc suggests that BL signaling does not require ELF3N for shortening of periodicity.

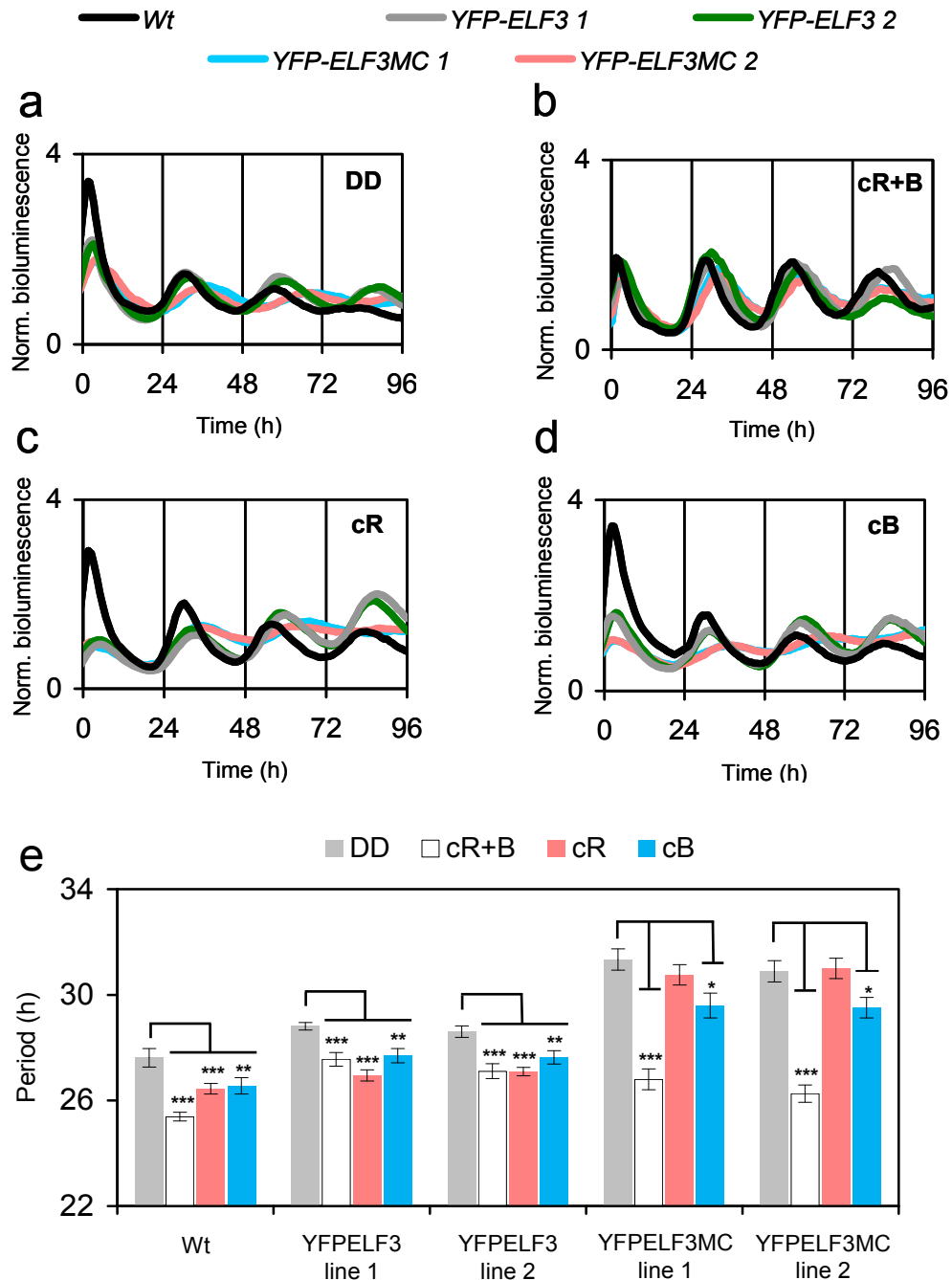


Figure 3.9. ELF3N accelerates circadian periodicity under Rc and in DD. (a) Normalized bioluminescence of *LHY:LUC* in DD (a), under R+Bc (b), Rc (c), and Bc (d). (e) Circadian period length of *LHY:LUC* of Wt, *YFP-ELF3* and *YFP-ELF3MC*. Period and RAE values are listed in table 3.1. Wt and *YFP-ELF3MC* values correspond to panels a-d. Error bars indicate SEM, count 24. In (e) stars depict statistical significance of comparisons: pvalue >0.05 (*), >0.01(**), >0.001 (***). These experiments were performed at least twice with similar results.

	DD		R+Bc	
	Period (h) ± SE	RAE ± SE	Period (h) ± SE	RAE ± SE
Wt	27.6 ± 0.4	0.2 ± 0.04	25.4 ± 0.2	0.2 ± 0.01
<i>YFP ELF3 1</i>	28.8 ± 0.1	0.1 ± 0.01	27.6 ± 0.3ns	0.3 ± 0.02
<i>YFP ELF3 2</i>	28.6 ± 0.2	0.1 ± 0.01	27.1 ± 0.3ns	0.2 ± 0.04
<i>YFP ELF3MC 1</i>	31.3 ± 0.4	0.2 ± 0.04	26.8 ± 0.4ns	0.2 ± 0.01
<i>YFP ELF3MC 2</i>	30.9 ± 0.4	0.2 ± 0.04	26.3 ± 0.3ns	0.2 ± 0.01

	Rc		Bc	
	Period (h) ± SE	RAE ± SE	Period (h) ± SE	RAE ± SE
Wt	26.5 ± 0.2	0.2 ± 0.01	26.6 ± 0.3	0.2 ± 0.01
<i>YFP ELF3 1</i>	27.0 ± 0.2	0.2 ± 0.02	27.7 ± 0.3	0.1 ± 0.01
<i>YFP ELF3 2</i>	27.1 ± 0.2	0.1 ± 0.01	27.6 ± 0.3	0.1 ± 0.01
<i>YFP ELF3MC 1</i>	30.8 ± 0.4	0.2 ± 0.03	29.6 ± 0.5*	0.4 ± 0.08
<i>YFP ELF3MC 2</i>	31.0 ± 0.4	0.2 ± 0.04	29.5 ± 0.5*	0.2 ± 0.01

Table 3.1 Period and RAE values of *LHY:LUC* rhythms in DD, under R+Bc, Rc, and Bc. From Figure 3.9. SE, standard error of the mean. Color code is used to define comparisons of differences in the period-length between genotypes and/or conditions: *YFP-ELF3MC 1* in DD vs. under Rc (Light blue), *YFP-ELF3MC 2* in DD vs. under Rc (Dark blue), *YFP-ELF3MC 1* in DD vs. under Bc (Pink), *YFP-ELF3MC 2* in DD vs. under Bc (Red), Wild type vs. *YFP-ELF3 1* and *YFP-ELF3 2* under Rc (Grey), Wild type vs. *YFP-ELF3MC 1* and *YFP-ELF3MC 2* under Rc (Dark green), *YFP-ELF3MC 1* under Rc vs. under Bc (orange), *YFP-ELF3MC 2* under Rc vs. under Bc (yellow), *YFP ELF3 1* and *YFP ELF3 2* vs. *YFP-ELF3MC 1* and *YFP-ELF3MC 2* under R+Bc (light green). Stars depict statistical significance as follows pvalue >0.05 (*), >0.01(**), >0.001 (***)* p value < 0.05; ns (not significant). Additional statistical comparisons are presented in Figure 3.7.

3.2.4 ELF4 is localized preferentially in the nucleus in Arabidopsis

ELF4 was shown to be a nuclear localized protein in transient expression in epidermal cells of onion (Khanna *et al.*, 2003), and in *N. benthamiana* (Figure 3.4 and 3.10 A1). However, these experiments did not confirm the sub-cellular localization of ELF4 in Arabidopsis. Hence, stable Arabidopsis lines over-expressing *YFP-ELF4* were generated in the *elf4-1* background. Consistent with transient assay YFP-ELF4 localized diffusely in the nuclei of hypocotyl cells (Figure 3.10 A3). Additionally, a portion of YFP-ELF4 signal was found in the cytoplasm (Figure 3.10 A2). The *YFP-ELF4* expression restore the arrhythmic *LHY:LUC* expression of *elf4-1* mutant, and confer a long period (Figure 3.10 B), consistent with previous observation (Figure 3.2, 3.3).

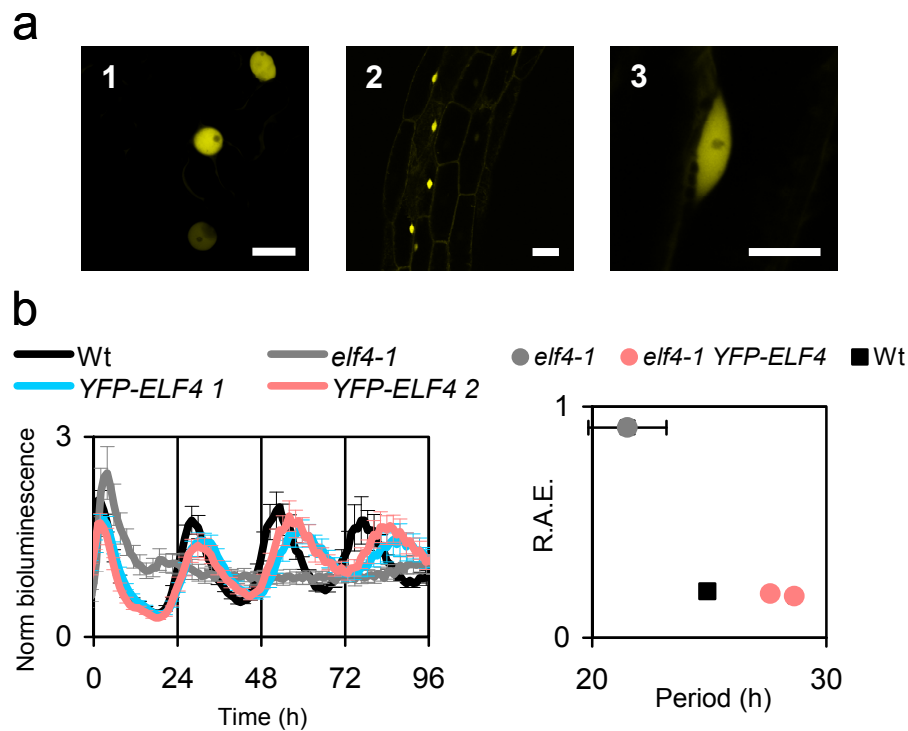


Figure 3.10. Constitutive expression of YFP-ELF4 is localized preferentially in the nucleus.

(a) YFP confocal microscopy of *YFP-ELF4* of epidermal cells in *N. benthamiana* (1), and hypocotyl of *elf4-1 YFP-ELF4* lines (2) and (3) expressed under the 35S promoter. White bars indicate 25 μ M (1) and (2) and 10 μ M in (3). The images are representative of at least two independent *elf4-1 YFP-ELF4* lines. The imaging was performed twice with similar results. (b) Normalized bioluminescence of *LHY:LUC* under LL for Wt, *elf4-1*, and *elf4-1 YFP-ELF4* lines. (c) Period vs RAE plot of panel b. Period and RAE values \pm SEM: Wt, 24.93 \pm 0.20, 0.2 \pm 0.01; *elf4-1*, 21.50 \pm 0.167, 0.91 \pm 0.03; *elf4-1 YFP-ELF4 1*, 28.63 \pm 0.24, 0.18 \pm 0.01; *elf4-1 YFP-ELF4 2*, 27.61 \pm 0.19, 0.19 \pm 0.01. Error bars indicate SEM, n=24.

3.2.5 ELF3 represses *PRR9* by physical association to its promoter

The transcript accumulation of *PRR9* and *PRR7* is elevated in *elf4* (Kolmos *et al.*, 2009) and *elf3* (Thines and Harmon, 2010), implicating that *ELF4* and *ELF3* are genetic repressors of these morning-clock genes. To test whether *ELF* genes are sufficient to mediate *PRR9* and *PRR7* repression, the expression of *PRR9* and *PRR7* was measured in *ELF3-OX* and *ELF4-OX* under LL and SD conditions (Bujdosó, personal communication). Both *ELF3-OX* and *ELF4-OX* alone were genetically sufficient to decrease *PRR9* transcript levels, especially under LL (Figure 3.11). Notably, the over-expression of these *ELF* genes had a much less pronounced effect of *PRR7* accumulation (Figure 3.11). Thus, the *ELF4-ELF3* signaling activity seems to mediate preferentially the repression of *PRR9*.

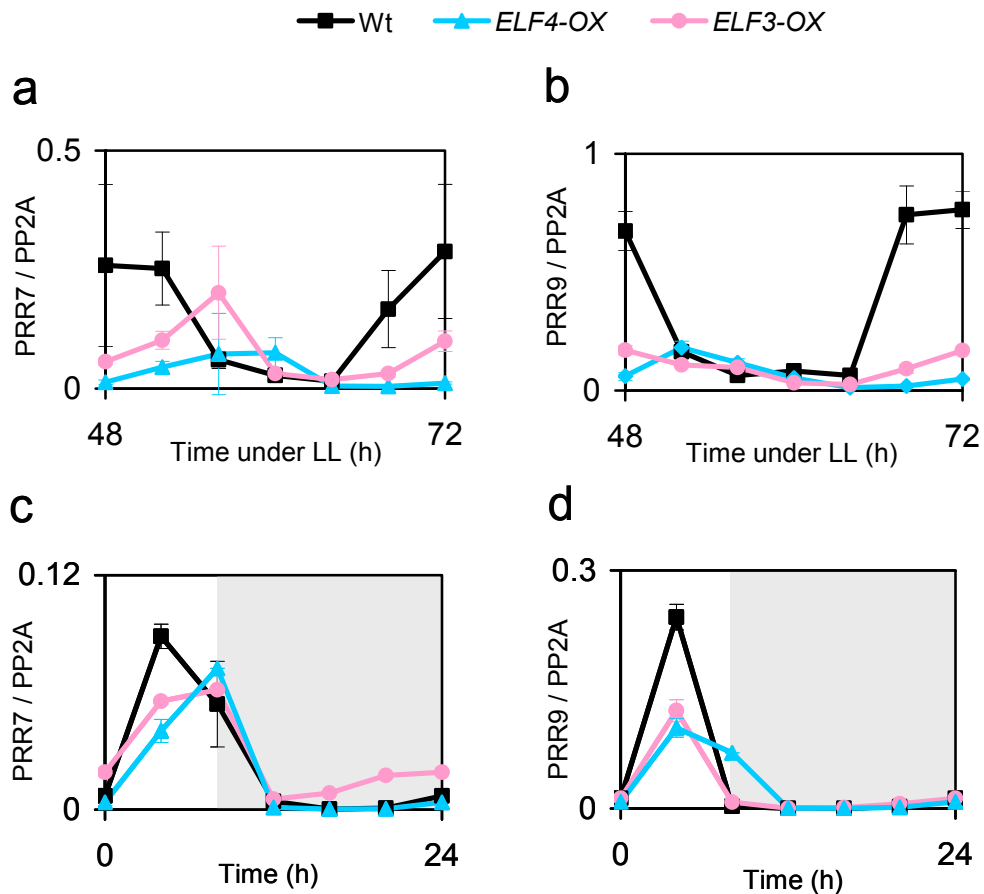


Figure 3.11. *PRR9* is down-regulated in *ELF3-OX*, and *ELF4-OX*. Samples were collected after 48h under LL (a) and (b), and under short days (SD) (c) and (d). Expression values were normalized to *PP2A* and are representative of two biological replicates. Error bars indicate SD. This experiment was performed by Nora Bujdosó.

Aiming to identify conserved elements in the *PRR9* promoter that could mediate repression by an ELF4-ELF3 complex, a phylogenetic shadowing approach was used (Berns, personal communication). The *PRR9* promoter of *Arabidopsis* was compared to orthologous promoters of *Arabidopsis lyrata*, *Capsella rubella*, and *Arabis alpina*. This analysis revealed high conservation upstream of *PRR9* (-556 to -136 bp), and it was called Conserved Region 1 (Figure 3.12A). Notably, this region was found to be crucial for the normal expression of *PRR9* (Ito *et al.*, 2005). Within the Conserved Region 1, there are two fully conserved *cis*-elements: an Evening Element (EE) (Harmer *et al.*, 2000) and a LUX Binding Site (LBS) (Helfer *et al.*, 2011). It is likely that both elements contribute to the rhythmic circadian oscillation of the *PRR9* transcript, as promoter deletion analysis reveals this region to be critical for normal *PRR9* function (Ito *et al.*, 2005).

Using the *YFP-ELF3* line described in figure 3.6, I tested by Chromatin immunoprecipitation (ChIP) if ELF3 associates with the promoter of *PRR9*. For this, both *YFP-ELF3* (Figure 3.6-3.9) and *elf3-4* seedlings were grown for 2 weeks under SD. Samples for ChIP were collected at ZT 16 when *PRR9* levels are lowest (Figure 3.11D). Chromatin fractions were pulled down with anti-GFP antibody and the enrichment of different fragments of the *PRR9* promoter in the *YFP-ELF3* ChIP samples was quantified by qPCR. Interestingly, ELF3 was found to associate specifically to the Conserved Region 1 in the *PRR9* promoter (Figure 3.12B). On the contrary, association of ELF3 to the *PRR7* promoter was not detected, supporting the idea that the ELF4-ELF3 complex acts directly on *PRR9*, but not *PRR7*.

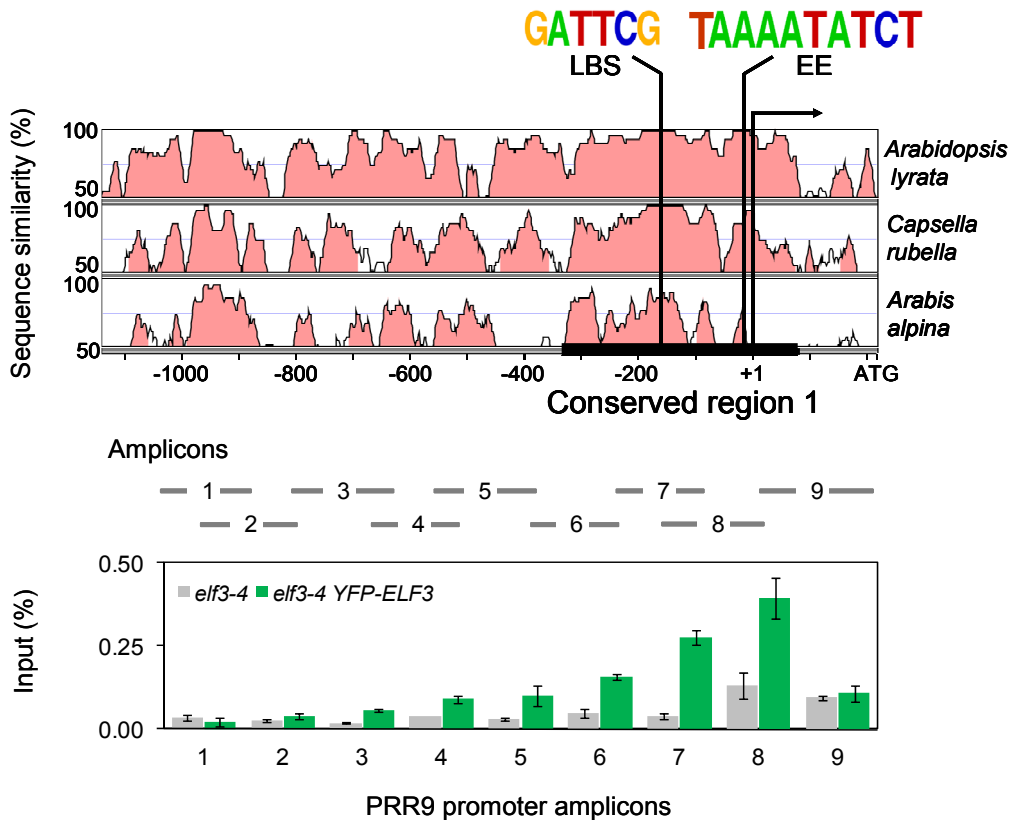


Figure 3.12. ELF3 associates with conserved region of *PRR9* promoter.

(a), Phylogenetically conserved region of the *PRR9* promoter mediates circadian regulation. Pairwise alignments of *Arabidopsis PRR9* promoter to orthologous sequences of *A. lyrata*, *Capsella rubella* and *Arabis alpina*, shown as VISTA plots. Light-red color indicates regions where a sliding window of at least 30bp has >70% identity. Conserved Region 1 (556 to -130bp) is highlighted with a black line. Vertical bars indicate the position of highly conserved LBS, EE, and the translational initiation codon (pointing arrow). Conservation of LBS and EE is shown as WEBLOGO. The phylogenetic shadowing was performed by Markus Berns.

(b), ELF3 associates to Conserved Region 1 of *PRR9* promoter. ChIP of *YFP-ELF3* to the *PRR9* promoter. *elf3-4* and *elf3-4 YFP-ELF3* seedlings were grown under SD (8h-light/16h-dark) and samples collected at ZT16. Chromatin fractions were pulled down with anti-GFP antibody. Enrichment was determined by qPCR and normalized to the input DNA; error bars indicate SEM, n=3 independent experiments. Two biological replicates and two technical replicates were performed with similar results to the values presented here. Grey horizontal bars indicate the position of the ChIP amplicons and are within the same scale as the shadowing regions of panel (a).

3.2.6 *LUX* is a component of *ELF3/ELF4* signaling

Since *ELF3* does not obviously encode a DNA-binding domain (Liu *et al.*, 2001), its association with the *PRR9* promoter could require a coupling component. Interestingly, a recent publication found that the evening-expressed factor *LUX* (Helfer *et al.*, 2011) can associate with the Conserved Region 1 of the *PRR9* promoter (Figure 3.9A). Moreover, the phenotype of the *lux* mutant was reported to be similar of that of *elf3* and *elf4* (Hazen *et al.*, 2005). Thus, it is possible that *LUX* is a component of the *ELF3/ELF4* repressive activity. To test this hypothesis, I generated double mutants that over-expressed *LUX* (*YFP-LUX*) in both *elf3-4* and *elf4-1*, respectively. Since *LUX* is a transcription factor, nuclear localization was expected. Hence, I tested the sub-cellular localization of *LUX* in wild type, *elf3*, and *elf4* backgrounds. *LUX* was localized in the nucleus regardless of the presence of *ELF3* or *ELF4* (Figure 3.13). Therefore, *ELF3* or *ELF4* were not found to be required for *LUX* nuclear localization.

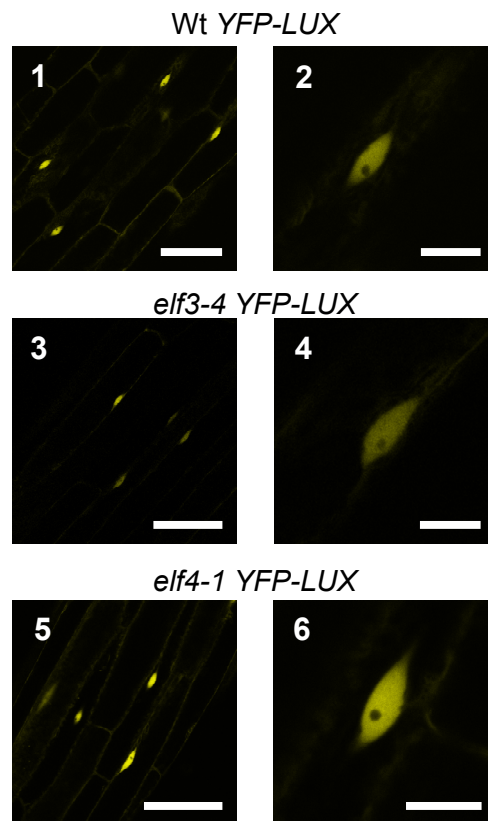


Figure 3.13. *YFP-LUX* nuclear localization is not affected in the *elf3-4* and *elf4-1*. YFP confocal microscopy of hypocotyl epidermal cells in *Arabidopsis YFP-LUX* lines, Wt (1-2), *elf3-4* (3-4), and *elf4-1* (5-6). White bars indicate 50 μ M (1,3,5) or 10 μ M (2,4,6). The images are representative of at least two independent lines for each background. The imaging was performed twice with similar results.

Using the transgenic YFP-LUX lines, I tested if *LUX-OX* could restore *elf3* and *elf4* *LHY:LUC* phenotype (Figure 3.2) Consistent with previous reports (Onai and Ishiura, 2005; Helfer *et al.*, 2011), *LHY:LUC* expression in the *LUX-OX* background was rhythmic under LL, but the oscillations gradually faded to a constitutive level of *LHY* (Figure 3.14). Interestingly, as *ELF3-OX* suppressed the *elf4-1* phenotype (Figure 3.2B), the *elf4-1* *LUX-OX* double mutant resulted in overt *LHY:LUC* rhythmicity (Figure 3.14). Furthermore, *LUX-OX* was ineffective in complementing *elf3-4* (Figure 3.14). Taken together, *LUX* is a downstream component of *ELF4* signaling that requires *ELF3* action.

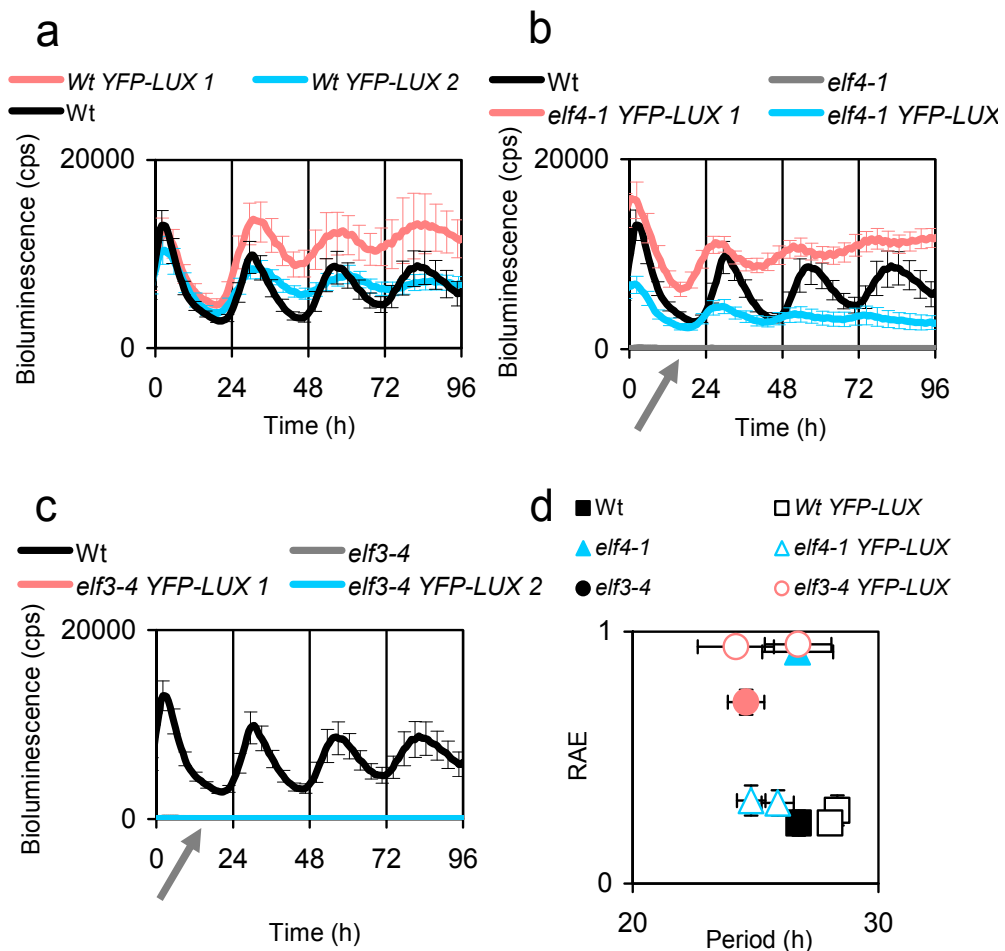


Figure 3.14. *LUX* is downstream of *ELF4* action.

(a)-(c), *LHY:LUC* rhythms of *YFP-LUX* in the Wt (a), *elf4-1* (b) and *elf3-4* (c) backgrounds, respectively, under LL. Arrows indicate the position of traces for *elf4-1* and *elf3-4*. (d) Period vs. RAE of *LHY:LUC* rhythms from (a), (b) and (c). Period length / RAE \pm SEM: Wt, 27.7 \pm 0.4h/0.28 \pm 0.05; *elf3-4*, 23.7 \pm 3.9h/0.94 \pm 0.03; *elf4-1*, 27.9 \pm 2.8h/0.96 \pm 0.03; Wt^o *YFP-LUX*^o1, 26.8 \pm 0.8h/0.36 \pm 0.04; Wt *YFP-LUX* 2, 27.3 \pm 1.1h/0.35 \pm 0.05; *elf3-4*-*YFP-LUX* 1, 24.2 \pm 3.1h/0.96 \pm 0.02; *elf3-4* *YFP-LUX* 2, 28.5 \pm 2.6h/0.93 \pm 0.03; *elf4-1* *YFP-LUX* 1, 26.3 \pm 0.7h/0.38 \pm 0.04; *elf4-1* *YFP-LUX* 2, 26.4 \pm 0.6h/0.32 \pm 0.05. cps, count per second. Error bars indicate SEM, and they were plotted every sixth count to clarify the curves, in a, b, and c.

3.3 Discussion

In this chapter, I showed that three evening components of the circadian clock, *ELF4*, *ELF3*, and *LUX*, cooperatively act to sustain circadian oscillations. This cooperation is consistent with these mutants having similar circadian-arrhythmicity phenotypes (Covington *et al.*, 2001; Doyle *et al.*, 2002; Hazen *et al.*, 2005; Kikis *et al.*, 2005; Onai and Ishiura, 2005; McWatters *et al.*, 2007; Thines and Harmon, 2010).

The physical interaction between ELF3 and ELF4 was demonstrated and the binding interface was mapped (Figure 3.1). Moreover, the over-expression of *ELF3* restored circadian rhythmicity of *elf4* mutants, indicating that is *ELF3* genetically downstream of *ELF4* (Figure 3.2). Both physical and genetic interaction of ELF3 and ELF4 are consistent with the previous hypothesis of ELF4 being an effector protein that binds a target protein (Kolmos *et al.*, 2009), and this target protein was shown to be ELF3. The middle domain of ELF3 (ELF3M) mediated physical interaction with ELF4 (Figure 3.1). The ELF3M (residues 261-484) domain mediates ELF3-GI interaction, whereas ELF3N (residues 1-259) domain is required for both phyB (Figure 3.8) and COP1 binding (Liu *et al.*, 2001; Yu *et al.*, 2008). Therefore, ELF3 has different interaction domains for each of its interaction partners.

The same ELF3 fragments used for Y2-H were fused to YFP to study their sub-cellular distribution. My studies revealed that the C-terminus domain (ELFC) mediates ELF3 nuclear localization. On the contrary, the N-terminal domain of ELF3 (ELF3N) was localized in the cytoplasm (Figure 3.4 and 3.6). In other circadian systems, specific regions of clock proteins have been shown to mediate dynamics of cytoplasmic-nuclear distribution. For example, mouse PER protein has both nuclear import signals (NLS) and nuclear export signals (NES) (Loop *et al.*, 2005). The YFP-ELF3M and YFP-ELF3NM fusion-proteins localized both in the nucleus and cytoplasm. Interestingly, the co-expression of these two ELF3 fragments with ELF4 increased their nuclear distribution (Figure 3.5). This mechanism is analogous to CLK-BMAL in mice, and to CLK-CYC in *Drosophila*. Both BMAL and CYC stabilize CLK nuclear pool (Kondratov *et al.*, 2003; Hung *et al.*, 2009). The stabilization of ELF3 nuclear pool by ELF4 provides a mechanism of ELF4 activation to the ELF3 protein.

Both ELF4 binding (ELF3M) and nuclear-targeting domain (ELF3C) were required for complementation of *elf3-4* arrhythmicity of *LHY:LUC* expression (Figure 3.7, 3.9). Notably, the ELF3N domain that mediates interaction with phyB (Figure 3.8)

was found to be dispensable for *LHY:LUC* rhythmicity (Figure 3.7). *ELF3* and phyB have opposite roles in Aschoff's rule, where *ELF3* decreases and phyB decreases clock periodicity (Devlin and Kay, 2000b; Covington et al., 2001). Hence, it is possible that phyB-ELF3 binding mediates phyB deactivation of ELF3 action, leading to acceleration of circadian speed. The observation that *YFP-ELF3MC* lines had a 3.5 h longer periodicity of *LHY:LUC* than wildtype under Rc is consistent with a phyB-mediated negative-modulation of ELF3 action (Figure 3.9, Table 3.1). This negative modulation could be mediated by phyB-ELF3N binding. However, in the presence of Bc, the period of *ELF3MC* was significantly shorter than in Rc and DD (Figure 3.7, 3.9; Table 3.1), suggesting that Bc acceleration of periodicity is achieved independently of the ELF3 repression through the ELF3N domain. Under all free-running conditions (DD, Rc, Bc, and R+Bc), the expression level of *LHY:LUC* in *YFP-ELF3MC* lines was significantly reduced. This suggests that ELF3N is required for positive induction of *LHY* expression. Taken together, ELF3 is a multifunctional protein where *ELF3MC* mediates circadian function and ELF3N domain may modulate ELF3 activity.

ELF3 nuclear localization and its amino-acid features suggest a role of ELF3 in transcriptional regulation (Hicks *et al.*, 2001). The loss of function of *ELF3* and *ELF4* leads to constitutive elevated levels of *PRR9* and *PRR7* transcripts (Kolmos *et al.*, 2009; Dixon *et al.*, 2011). This indicates that *ELF3* and *ELF4* act as repressors of *PRR7* and *PRR9*. To further test this, *PRR9* and *PRR7* transcript accumulation in the *ELF3-OX* and *ELF4-OX* backgrounds were tested. Under LL, the levels of *PRR9* were severely repressed compared to wild type, whereas the reduction of *PRR7* levels was minor. This indicated that *PRR9* is likely a direct target of ELF3-ELF4 repressor complex.

Phylogenetic shadowing identified a highly conserved region in the *PRR9* promoter (Figure 3.12 A). Notably, the Conserved Region 1 is part of a previously identified region of the *PRR9* promoter required for *PRR9* rhythmic accumulation (Ito *et al.*, 2005). This confirms the functional relevance of the Conserved Region 1. By using ChIP, I tested the association of ELF3 to the *PRR9* promoter. Interestingly, ELF3 associated specifically to the Conserved Region 1 (Figure 3.12 B), suggesting that ELF3 association to the *PRR9* promoter is required for *PRR9* rhythmicity. However, I did not find association of ELF3 to the *PRR7* promoter. My results are consistent with a recent publication, where it was found that ELF3 associates to the promoter of *PRR9*, but not *PRR7* (Dixon *et al.*, 2011).

LUX associates to the *PRR9* promoter through a LBS located in the Conserved Region 1 (Helfer *et al.*, 2011). Loss of any of *ELF3*, *ELF4* or *LUX* leads to similar clock-arrest phenotypes (Covington *et al.*, 2001; Doyle *et al.*, 2002; Hazen *et al.*, 2005). Since ELF3 does not have a DNA-binding domain, *LUX* could act within the *ELF3-ELF4* complex to modulate *PRR9* expression. I tested this hypothesis by examining the genetic interactions of *LUX* with *ELF3* and *ELF4*. Similar to the ability of *ELF3-OX* to bypass the *elf4* phenotype (Figure 4.2), *LUX-OX* restore *LHY:LUC* rhythmicity in the *elf4* mutant, indicating that *LUX* is genetically downstream of *ELF4*. However, *LUX-OX* did not restore *elf3* arrhythmicity (Figure 3.14). The nuclear localization of YFP-LUX was not affected in the *elf4* or *elf3* backgrounds (Figure 3.13). Therefore, an evening repressor complex formed by ELF3, ELF4, and LUX is required to sustain circadian rhythmicity.

Taken together, the genetic interaction of *LUX*, *ELF3*, and *ELF4* reveals a hierarchy of complex assembly (Figures 3.2 and 3.14). Association to the *PRR9* promoter of both ELF3 and LUX is required for clock function [Figure 3.12 and 3.14; (Helfer *et al.*, 2011)]. The over-expression of both *ELF3* and *LUX* can bypass the lack of *ELF4* function. In here, ELF4 appears to work as an effector protein that activates ELF3, possibly by stabilizing the ELF3-nuclear pool (Figures 3.1 and 3.5). Finally, ELF3 function in periodicity may be modulated by its interaction with phyB (Figures 3.8 and 3.9). This latter hypothesis will be further explored in Chapter 4.

Chapter 4 An insight of *ELF3* function in the light input to the clock

Part of the results in this chapter are part of collaborative work

Elsebeth Kolmos generated lines in the C24 background used in Figures 3.2, 3.3 and 3.4.

4.1 Introduction

ELF3 function is essential both for circadian function and to process light-signal inputs to the oscillator (McWatters *et al.*, 2000; Thines and Harmon, 2010). The *elf3* alleles described in the literature are null alleles *eg.* *elf3-1*, or nearly null alleles *eg.* *elf3-7*. In the case of *elf3-7*, it was proposed that a residual ELF3 function enable sustained circadian function in the first day under free-running conditions (McWatters *et al.*, 2000; Reed *et al.*, 2000). This arrhythmicity phenotype of previously described alleles of *elf3* has precluded the understanding of the overall function of ELF3.

ELF3 has been proposed to be a repressor of light signals to the oscillator (Covington *et al.*, 2001). In Aschoff's rule, photoreceptors act to shorten circadian periodicity, whereas ELF3 lengthens circadian period. In particular, under high fluence Rc, both the phyB mutant and *ELF3-OX* displayed long periodicity, when compared to the wild type (Devlin and Kay, 2000b; Covington *et al.*, 2001). In Chapter 3, I proposed that the interaction of phyB to N-terminus of ELF3 (ELF3N, residues 1-259) mediates light-repression ELF3 action in circadian periodicity, in particular by red light (RL). In this case, attenuation of *ELF3* function by light would lead to a reduction of circadian periodicity.

Interestingly, a forward genetic screen led to the isolation of a new *elf3* allele termed *elf3-12* (Kevei *et al.*, 2006; Kolmos, 2007). The *elf3-12* allele causes a weak phenotype as compared to the *elf3* loss of function. Initially, *elf3-12* was found to have an early first-peak of *CAB:LUC* expression in DD. Subsequent analysis revealed that *elf3-12* displayed short periodicity under LL. Unlike loss of function alleles of *elf3*, *elf3-12* displayed wild-type flowering time and normal hypocotyl length (Kolmos, 2007). The *elf3-12* has a missense mutation leading to a change from an evolutionary-conserved glycine at position 236 for an aspartic acid (G326D) (Kolmos, 2007). Since *elf3-12* is not a null allele, I used this allele to test the hypothesis that light represses ELF3 function in periodicity as a component of phytochrome signaling.

The availability of additional new weak *elf3* alleles could assist in the characterization of the ELF3 encoded protein. The TILLING (Targeted Induced Local Lesions in Genomes) approach has been widely used for isolation of new mutant alleles in many plant and animal species. For instance, the phenotypic characterization of new weak *elf4* alleles aided the placement of ELF4 within the clock function (Kolmos *et al.*, 2009). For ELF3, a collection of 31 *elf3*-TILLING alleles was previously described

(Kolmos, 2007). In this Chapter, I characterized circadian rhythms of the *elf3*-TILLING alleles. Circadian phenotypic data was interpreted based on the position of the residue changed of each allele in relation to the functional domains and the amino-acid features of the ELF3 encoded protein.

4.2 Results

4.2.1 Characterization of *elf3-12* allele

ELF3 is proposed to lengthen circadian period (Covington *et al.*, 2001), and thus, a reduction of ELF3 protein levels could explain an attenuated function in *elf3-12* allele leading to the observed a short-period phenotype. To examine this possibility, I tested the capacity of *ELF3-12* coding region to generate cellular-accumulated protein. For this, *ELF3-YFP* and *ELF3-12-YFP* fusion constructions were generated under the control of the native ELF3 promoter, and these constructs were used for transient expression in *N. benthamiana*. Young leaf material was imaged at dusk, the time of maximal ELF3 accumulation (Liu *et al.*, 2001). I found that both ELF3-YFP and ELF3-12-YFP robustly accumulated in the nuclei of epidermal cells during the evening phase of the circadian day (~ZT14) (Figure 4.1 A). More cytoplasmic accumulation could be observed in ELF3-12 YFP compared to ELF3-YFP. Taken together, the phenotypes in *elf3-12* are unlikely to be a result of a failure to accumulate ELF3 protein.

In Chapter 3.1, I showed that ELF4 is likely to work as an effector of ELF3. Moreover, ELF3-ELF4 binding, mediated by ELF3M domain, increased ELF3 nuclear pool. Notably, the ELF3-12 point mutation is located within the ELF3M domain of ELF3. Hence, it was possible that *elf3-12* encodes for a protein with altered ELF4 binding capacity. I tested this possibility in a Y2-H assay, and I found that both ELF3-12 full-length and ELF3M-12 led to viable yeast when co-expressed with ELF4 (Figure 4.1B). This indicates that ELF3-12 allele does not abolish ELF3-ELF4 binding.

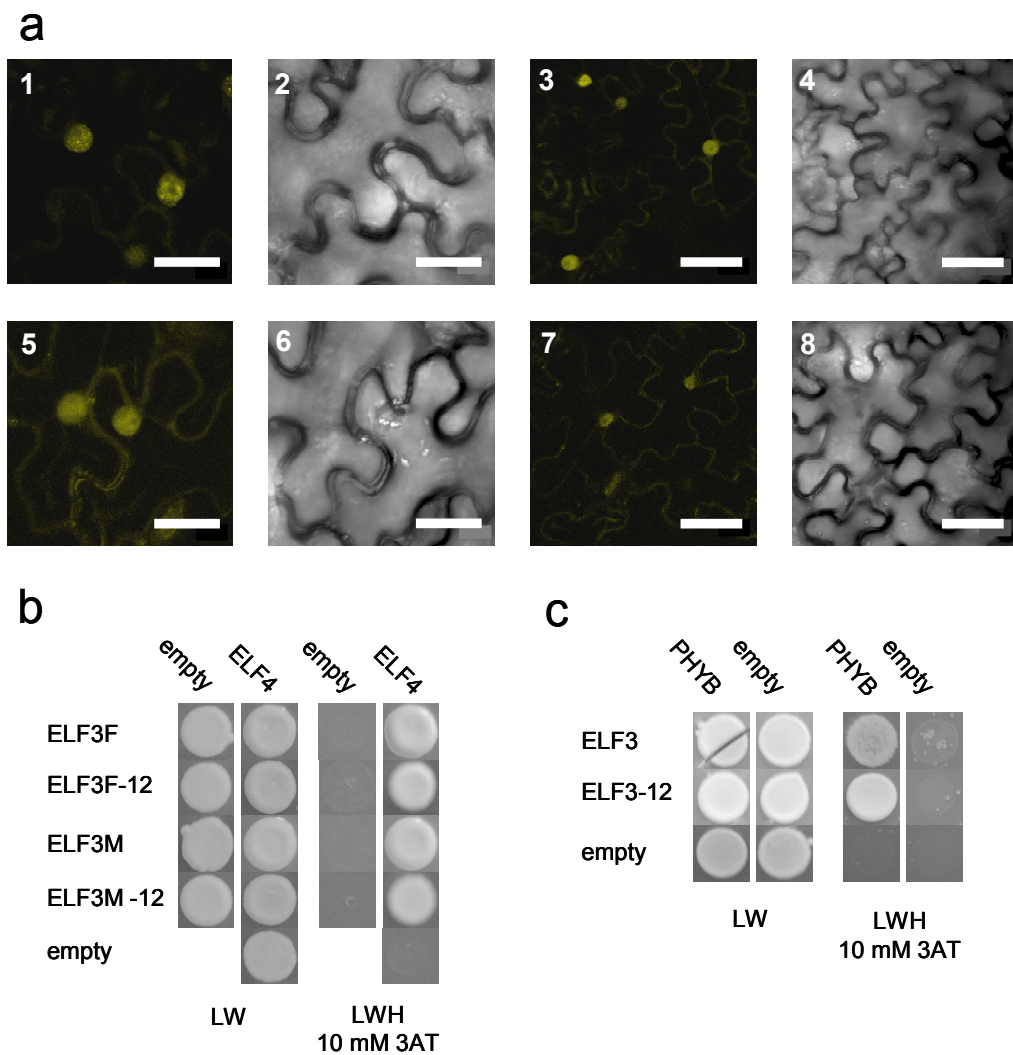


Figure 4.1. ELF3-12 protein is nuclear localized, and can bind to ELF4 and phyB
(a) Confocal microscopy of ELF3-YFP and ELF3-12-YFP. The fusion-proteins ELF3-YFP and ELF3-12-YFP were expressed in *N. benthamiana* leaves under native ELF3 promoter. YFP channel (1,3,5,7) and bright field (2,4,6,8). Maximum projection of 10 μ m stacks (10 stacks, 1 μ m each) White bars indicate 25 μ m (1-2,5-6) and 50 μ m (3-4, 7-8). All photos were made with the same microscope settings.
(b) Y2-H assay of ELF4-BD with ELF3-AD and ELF3-12-AD. ELF3-F (full length), ELF3M (residues 261-484); ELF3-12 and ELF3M 12 has a point mutation (G326D). Abbreviations: empty (AD or BD only); -LW and -LWH (drop out for Leu/Trp and Leu/Trp/His, respectively); 3-AT (3-amino-1,2,4-triazole).
(c) Y2-H assay of ELF3-BD, ELF3-12-BD and phyB-AD. ELF3-12 has a point mutation (G326D). Abbreviations same as in b.

The *elf3-12* allele displayed short periodicity of *CCA1:LUC* and *LHY:LUC* under LL (Kolmos, 2007). To further examine the effect of light on the *elf3-12* phenotype, I tested *LHY:LUC* and *CCR2:LUC* rhythms under LL and in DD. *elf3-12* rhythms were compared to the wild type and to the *elf3-1* loss of function allele. Under LL, *elf3-1* displayed marginal *LHY:LUC* expression and no detectable circadian rhythms (Figure 3.2A). This was previously showed for *elf3-4* null allele in Chapter 3 (Figure 3.2). However, *elf3-12* had rhythmic *LHY:LUC* expression that were shorter in periodicity compared to wild type (Figure 3.2 ,D). In DD, no periodicity phenotype was observed for *elf3-12* (Figure 3.2 D). Under LL and in DD, *elf3-1* displayed arrhythmic high levels of *CCR2:LUC* expression (Figure 4.2C). On the contrary, *elf3-12* had rhythmic expression of *CRR2:LUC* under LL with a short period, when compared to the wild type (Figure 4.2 B, D). Similarly to *LHY*, under DD, *elf3-12* did not display a periodicity phenotype for *CCR2* (Figure 4.2 C,D). Taken together, the *elf3-12* short period phenotype was light-dependent.

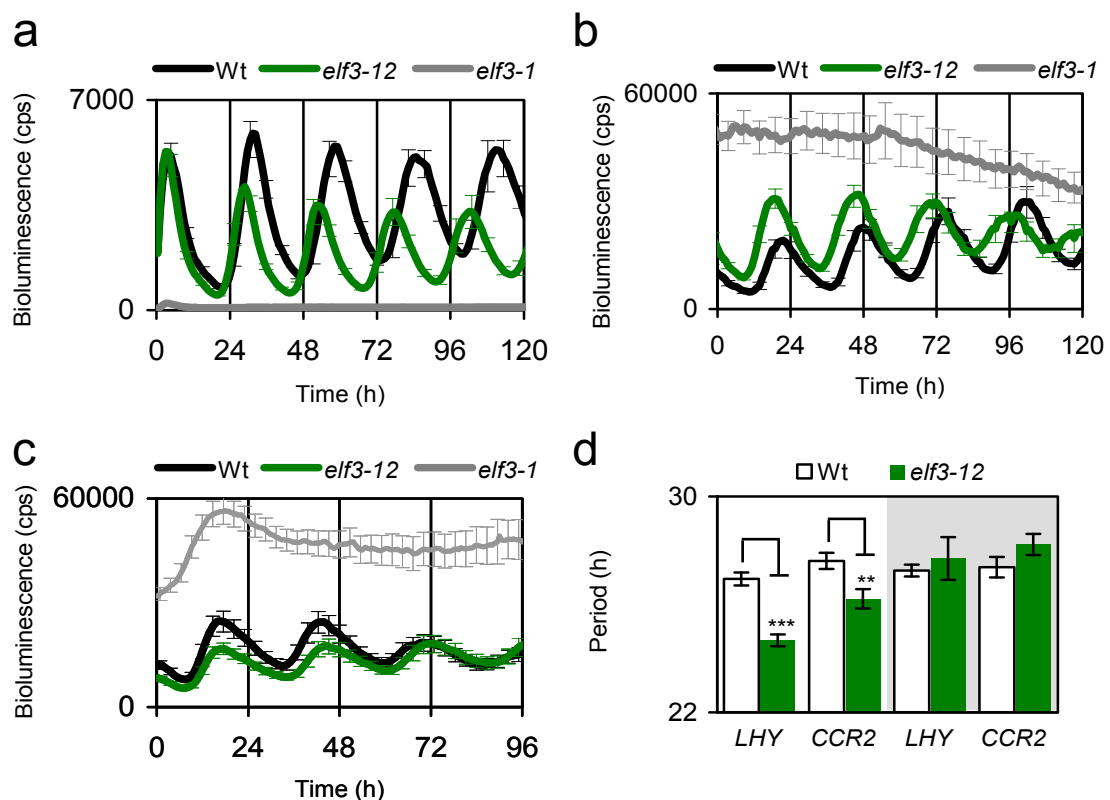


Figure 4.2. Mutant clock-period properties are light-dependent in *elf3-12*
 (a) Free-running profile of *LHY:LUC* expression in the wild type, *elf3-12*, and *elf3-1* under LL. Arrow indicate marginal expression in *elf3-1*. (b) Free-running profile of *CCR2:LUC* in the wild type, *elf3-12*, and *elf3-1* under LL.
 (c) Free-running profile of *CCR2:LUC* in the wild type, *elf3-12*, and *elf3-1* in DD.
 (d) Circadian period length of *LHY:LUC* and *CCR2:LUC* rhythms. Under LL, the period of *elf3-12* was short for *LHY:LUC* and *CCR2:LUC*. In DD, no period phenotype was found for *LHY:LUC* and *CCR2:LUC*. Error bars correspond to SE. Statistical significance: pvalue >0.01 (**), >0.001 (***). cps, count per second.

In Chapter 3, I showed that the interaction of ELF3 and phyB was mediated by the N-terminus of ELF3 (ELF3N). The point mutation of *elf3-12* occurs in the ELF3M domain. Hence, I predicted that ELF3-12 retains phyB-binding capacity. In a Y2-H assay, co-expression of ELF3-12 and phyB protein led to yeast growth on selective media, similarly to the comparison of ELF3 wild type co-expression with phyB (Figure 4.1C). This suggests that ELF3-12 phenotype is not caused by a deficient phyB binding.

The observation that *elf3-12* short periodicity is light dependent suggests a direct repression of light to *ELF3-12* function. If true, then increasing light input should lead to further period shortening of *elf3-12* rhythms. The over-expression of phy (PHY-OX) causes a constant increase of light input to the oscillator (Anderson *et al.*, 1997). I thus generated double mutants *elf3-12 PHY-OX* and used these lines to test *elf3-12* periodicity in the context of increased light-input to the clock. The circadian rhythms of *CCR2:LUC* were assayed under LL. *elf3-12* plants showed rhythmic, but significantly short-period oscillations, compared to the wild type (Figure 4.3). *PHYB-OX* did not cause a statistically-significant period-shortening effect whereas *PHYA-OX* have short period compared to wild type (Figure 4.3). Interestingly, the period of *elf3-12 PHYB-OX* was significantly shorter than the single mutant *elf3-12* and *PHYB-OX*. A similar additive effect was found in *elf3-12 PHYA-OX* plants (Figure 4.3). Therefore, increased light input to the clock caused by PHY-OX led to an enhanced period-shortening effect of *elf3-12*. This is consistent with an attenuated function of *elf3-12* to repress light input to the clock and/or an increased phy-mediated repression of ELF3 function in the *elf3-12* mutants.

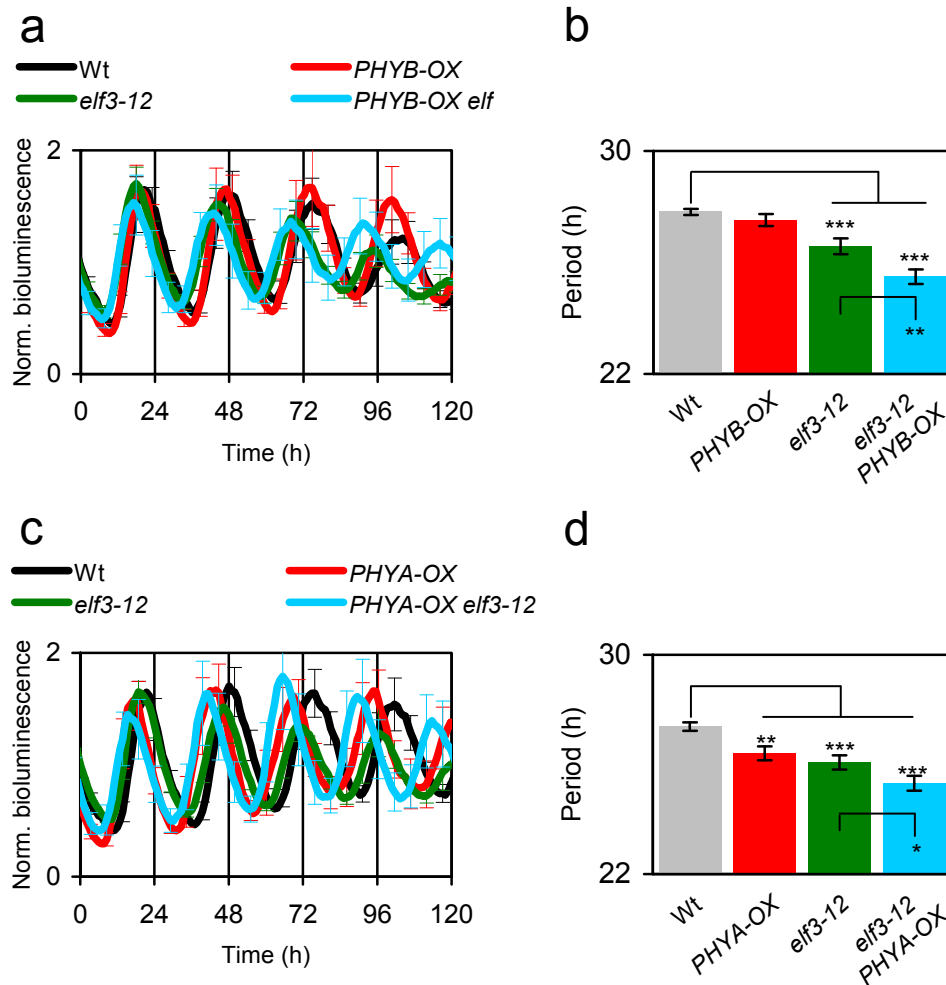


Figure 4.3. *PHY-OX* enhances the *elf3-12* short period phenotype under LL.
(a) Free-running profile of *CCR2:LUC* for the wild type, *PHYB-OX*, *elf3-12*, and *PHYB-OX elf3-12* under LL. Error bars indicate S.E.M, and they are plotted every 6 time points to clarify traces.
(b) Circadian period length of *CCR2:LUC* rhythms under LL, from panel a.
(c) Free-running profile of *CCR2:LUC* for the wild type, *PHYA-OX*, *elf3-12*, and *PHYA-OX elf3-12* under LL. Error bars indicate S.E.M, and they are plotted every 6 time points to clarify traces. Statistical significance: p value >0.05 (*), >0.01 (**) and >0.001 (***)

Light mediates daily resetting of the phase of the oscillator (Jones, 2009). The phase response curve (PRC) recapitulates phase advances and delays caused by entrainment pulses depending on the time of the day when they are applied (Chapter 1 Figure 1.6). *ELF3* is also involved in the clock-resetting mechanism (Covington *et al.*, 2001). I compared the ability of *elf-12* and wild type to reset the oscillator by constructing a PRC curve. For this, *elf3-12* and wild type plants were grown for 7 days under LD cycles and then transferred to DD. After one full day in DD, replicate populations were subjected to 1 hour RL pulse at different times of the day. Then, changes in the circadian phase of the oscillator were calculated and plotted in the PRC. Wild-type plants responded with phase delays at early subjective night (CT 12-18) and with phase advances at the end of the night (CT18-24), as expected. Additionally, an expected “dead zone” with limited phase changes was observed for wild type during the circadian day (CT 3-12) (Figure 4.4). At early subjective night (CT12-18), *elf3-12* responded similarly to the wild type, as it displayed phase delays. However, *elf3-12* responded with increased phase advances to light pulses given at the end of the subjective night and early subjective day (CT 18-3) (Figure 4.4). Therefore, RL-resetting pulses caused increased phase advances on *elf3-12*, indicating that encoded ELF3-12 protein is hypersensitive to RL input to the clock.

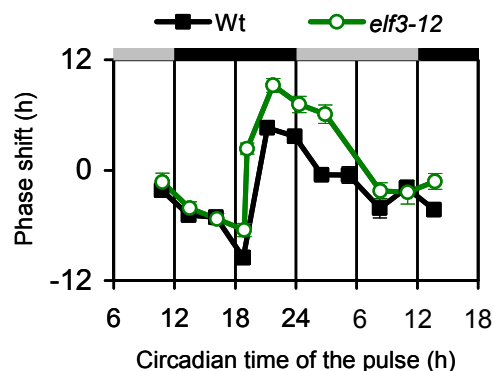


Figure 4.4. ELF3-12 is hypersensitive to RL resetting pulses. Circadian period length of *CCR2:LUC* rhythms under LL, from panel c. Error bars indicate S.E.M. Error bars indicate pooled S.E.M of pulsed and non-pulsed plant populations. Grey bars and black bars depict subjective day and subjective night, respectively.

4.2.2 Identification of novel *elf3* alleles

The characterization of *elf3-12* allele confirmed the essential role of ELF3 as an integrator of light signal to the core mechanism. The availability of additional ELF3 alleles may be useful in deciphering ELF3 functions within the clock mechanism. For this, I further characterized a series of *elf3*-TILLING alleles that were previously generated (Kolmos, 2007). Figure 4.5 depicts the distribution of these 31 *elf3* alleles according to the position of the encoded-residue change within the ELF3 protein. The residue changes on the alleles *elf3-201* to *elf3-213* are located in the ELF3N domain necessary to mediate phyB (Figure 3.8) and COP1 binding (Yu *et al.*, 2008). The residue changes on the alleles *elf3-214* to *elf3-221* are located in the ELF3M domain that is required to ELF4 binding (Figure 3.1). Finally, the residue changes on the alleles *elf3-222* to *elf3-231* are located in the ELF3C domain that mediates ELF3 nuclear localization (Figure 3.4). ELF3 has two regions of special amino acid compositions that suggest a role of ELF3 in transcriptional regulation (Figure 4.5 yellow boxes) (Hicks *et al.*, 2001). The acidic region (residues 206-320) is located between ELF3N and ELF3M domains. The residue changes on the alleles *elf3-208* to *elf3-218* are located within the acidic region. The proline-rich region lies between ELF3M and ELF3C domains. The residue changes on the alleles *elf3-220* to *elf3-224* are located in the proline-rich region. Additionally, four highly-conserved regions of ELF3 protein can be found in the N-terminus (residues 1-53), at the middle part (residues 298-382), within the proline-rich region (residues 470-490) and at the C-terminus end (residues 670-end) (Figure 4.5 grey boxes). From the *elf3*-TILLING collection, the residue changes on the alleles *elf3-219* and *elf3-221* lie within the highly conserved middle, and proline-rich regions, respectively. Hence, the residue changes encoded by the *elf3*-TILLING alleles are distributed throughout different domains of the encoded ELF3 protein.

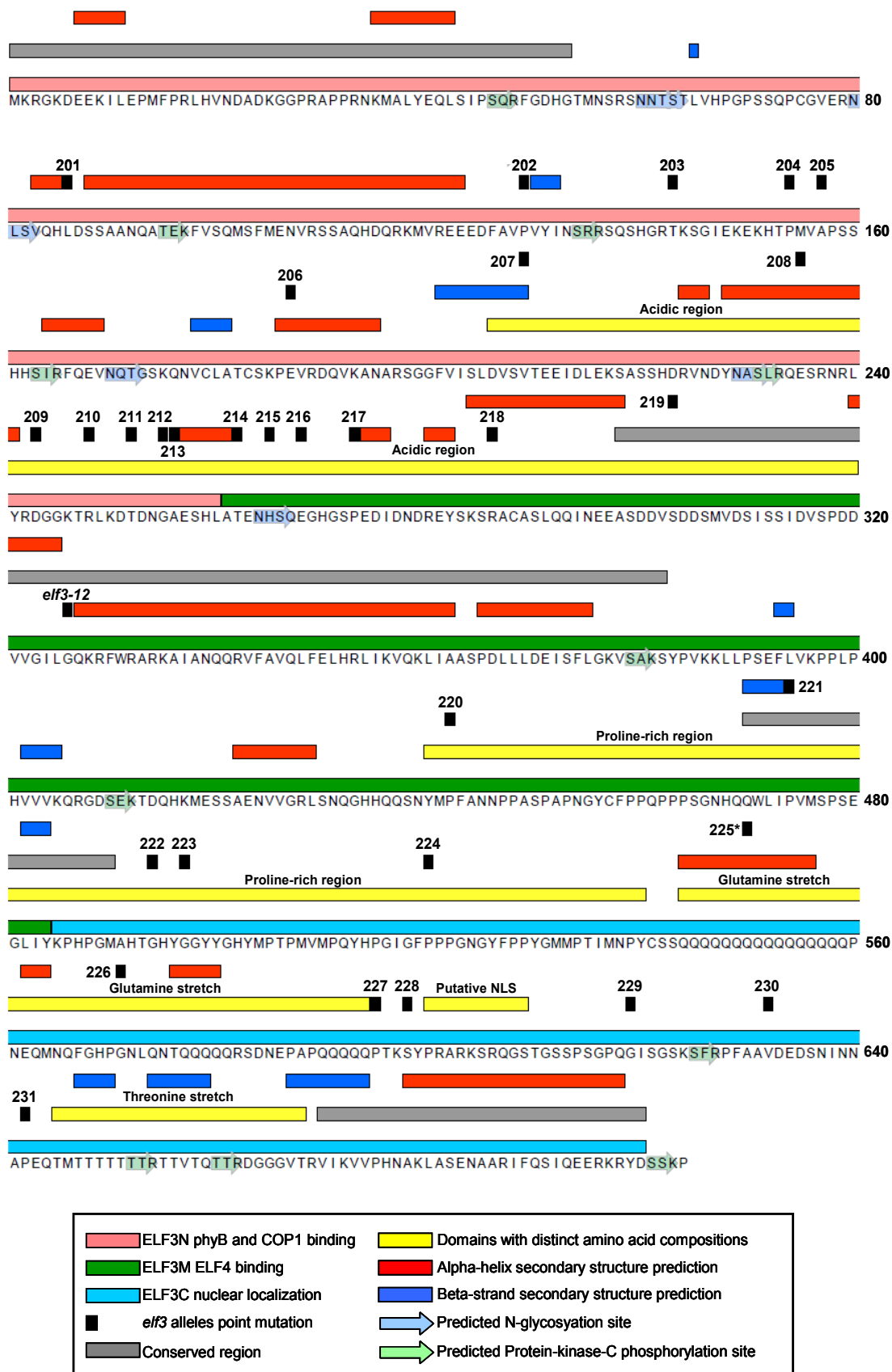


Figure 4.5. Distribution of the residue changes on the *elf3* TILLING lines within the encoded ELF3 protein.

Figure legend continues in the next page.

Scheme of ELF3 protein features and distribution of the *elf3*-TILLING alleles. See legend for color coding of boxes. The domains ELF3N (residue 1-259), ELF3M (residues 261-484), and ELF3C (residue 485-695) are described in Chapter 3. Table 4.1 describes the encoded residue change of each *elf3*-TILLING line. Domains with distinct amino-acid compositions have been previously described (Hicks *et al.*, 2001). Predictions of secondary structure, N-glycosylation sites, and Protein-kinase-C phosphorylation sites were made with CLC software.

Table 4.1 *elf3*-TILLING lines

<i>elf3 allele</i>	ELF3 aa residue	Residue change	% conserved ¥	Features in ELF3 protein
201	86	L to F	22	
202	129	P to S	82	
203	143	I to T	17	
204	154	P to S	44	
205	157	A to T	26	
206	187	E to K	15	
207	209	V to I	23	Acidic region
208	235	E to K	37	Acidic region, alpha helix
209	243	D to N	26	Acidic region
210	248	R to H	11	Acidic region
211	252	T to I	29	Acidic region
212	255	G to E	32	Acidic region
213	256	A to T	50	Acidic region, alpha helix
214	262	T to M	10	Acidic region, alpha helix
215	265	H to Y	26	Acidic region, predicted N-glycosylation site
216	268	E to K	29	Acidic region
217	273	P to L	37	Acidic region, alpha helix
218	286	R to K	26	Acidic region, alpha helix
219	303	S to F	83	Acidic region
220	442	P to L	43	Proline-rich region
221	474	P to S	98	Proline-rich region, beta-strand
222	494	G to R	37	Proline-rich region
223	497	G to E	11	Proline-rich region
224	520	P to L	80	Proline-rich region
225	550	Q to *		Glutamine stretch in Arabidopsis
226	562	G to R	32	Glutamine stretch in Arabidopsis
227	586	P to S	46	Glutamine stretch in Arabidopsis
228	589	S to F	17	
229	610	G to R	58	
230	623	V to I	20	
231	633	P to S	49	

¥ % conserved was calculated according to amino-acid identity in a multiple alignment of 35 ELF3 sequences (Saini, personal communication)

In order to characterize the circadian rhythms of the *elf3*-TILLING collection, I introgressed *Gl:LUC* reporter to each line. In the F3 populations, homozygous lines for the corresponding *elf3* allele, and harboring *Gl:LUC* reporter, were used for circadian analysis. All *elf3*-TILLING alleles, except *elf3-212*, co-segregate with *erecta* mutation, and therefore I used *er-105* as the wild type for these lines. For the line *elf3-212*, Col-0 was used as the wild type. Circadian rhythms were assayed under LL and in DD, after plants have been entrained under LD cycles or WC cycles. Additionally, free-running conditions of monochromatic Rc or Bc after LD entrainment were analyzed. Only the line *elf3-225* displayed arrhythmic *Gl:LUC* expression, both under LL and in DD (Figure 4.6). The line *elf3-225* has an encoded stop codon (residue 550) and is likely an *elf3* loss of function allele.

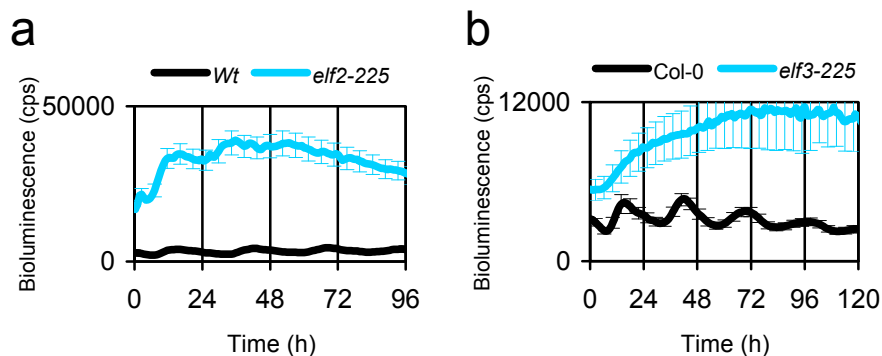


Figure 4.6. *elf3-225* is a loss of function allele.
(a) Free-running profile of *Gl:LUC* for Col-0 and *elf3-225* under LL.
(b) Free-running profile of *Gl:LUC* for Col-0 and *elf3-225* in DD.
 Error bars indicate S.E.M., and they are plotted every sixth read to clarify traces.

All the *elf3*-TILLING alleles, except the *elf3-225*, showed robust rhythms of *Gl:LUC*. For each experiment, the difference in phase and period between each line and the corresponding wild type was plotted to identify alleles with phase and period phenotypes (Figures 4.7 to 4.12). First, free-running-circadian rhythms of *Gl:LUC* in *elf3* lines was tested under LL. For the LD to LL experiments, plants were grown for 7 days under LD and then transferred to free-running LL. Under these conditions, the *elf3*-lines 210, 211, 214, and 218 displayed short periodicity, whereas *elf3-219* and *elf3-220* displayed long-period rhythms. Several *elf3* lines displayed late phase of *Gl:LUC* expression: *elf3-204*, 205, 210, 211, 213, 214, 217, and 231. On the contrary, *elf3-212* showed early phase of *Gl:LUC* expression. (Figure 4.7, Table 4.2). Next, *elf3* lines were subjected to WC entrainment under LL followed by free running LL at a constant temperature (WC to LL). Under these conditions, *elf3-210* and *elf3-218*

displayed short-circadian periodicity, whereas *elf3*-lines 204, 219, and 224 displayed long-period rhythms. Under WC to LL, the phase of *GI:LUC* in *elf3*-lines 204, 205, 220, 224, and 231 was late compared to the wild type, whereas *elf3-217* displayed an early-phase phenotype (Figure 4.8, Table 4.2). Thus, under LL, short-period rhythms for *elf3-210* and *elf3-218*, and long-period rhythms for *elf3-219*, were found, regardless of the entrainment condition. For phase, *elf3*-lines 204, 205, and 231 showed a late phase of *GI:LUC* expression under LL in both entrainment conditions. In summary, seven *elf3* lines showed phenotypic differences under free-running LL.

The free-running-circadian rhythms of *GI:LUC* in *elf3* lines were assayed in DD. For the LD to DD experiment, *elf3* lines were entrained for 7 days under LD and then released to DD. Under this condition, *elf3-205* and *elf3-222* displayed short periodicity of *GI:LUC*, whereas no line displayed long-period rhythms. Late-circadian phase was found for lines *elf3-226* and *elf3-227*, whereas *elf3-215* and *elf3-220* displayed early-circadian phase of *GI:LUC* expression (Figure 4.9, Table 4.2). Next, circadian rhythms in DD were assayed for plants grown under WC cycles under LL (WC to DD). The *elf3*-lines 215, 218, 220, 226, and 231 displayed short periodicity in DD. Also, *elf3*-lines 201, 218, 219, 223, 226, and 231 displayed late phase of *GI:LUC* expression in the WC to DD experiment (Figure 4.10, Table 4.2). Thus, under LD to DD conditions, fewer *elf3* lines displayed circadian phenotypes. The line *elf3-226* showed late-circadian phase under both DD conditions. The line *elf3-218* that displayed short periodicity under LL, also showed short-periodicity under WC to DD.

Since some of the *elf3* lines show circadian phenotypes under LL, I tested circadian rhythms of *GI:LUC* rhythms in *elf3* lines under Rc and Bc, after LD entrainment. Under Rc, *elf3*-lines 214, 218, and 219 displayed a short period, whereas *elf3-231* displayed a long period. For phase, *elf3-211* and *elf3-217* had an early phase of *GI:LUC* expression (Figure 4.11, Table 4.2). Under Bc, *elf3*-lines 201, 207, 209, 211, and 218 displayed short periodicity, whereas *elf3-212* and *elf3-219* displayed long periodicity. For circadian phase, *elf3-202* and *elf3-212* displayed early phase of *GI:LUC* expression (Figure 4.12, Table 4.2)

Figure legend for Figure 4.7 to Figure 4.12.

(a) Period vs. Phase differences of *elf3*-TILLING lines to the corresponding wild type, *er-105* (left panel) and *Col-0* (right panel), respectively. The graphs show differences in period- and phase-mean values between each *elf3*-TILLING line and the corresponding wild type. Error bars depict SEM of period and phase estimates of each *elf3*-TILLING lines and the wild type. Grey areas around x and y axis indicate values similar to wild type. Lines identified with the corresponding number have statistically significant period and/or phase changes compared to the wild type. Color code assigns location of residue change within the encoded ELF3 domains according to legend.

(b) Normalize luminescence traces of *Gl:LUC* for *elf3*-TILLING lines with statistically significant period or phase differences. Color code for *elf3*-TILLING lines is same as panel (a). Error bars indicate SEM, and are plotted every sixth read to clarify traces.

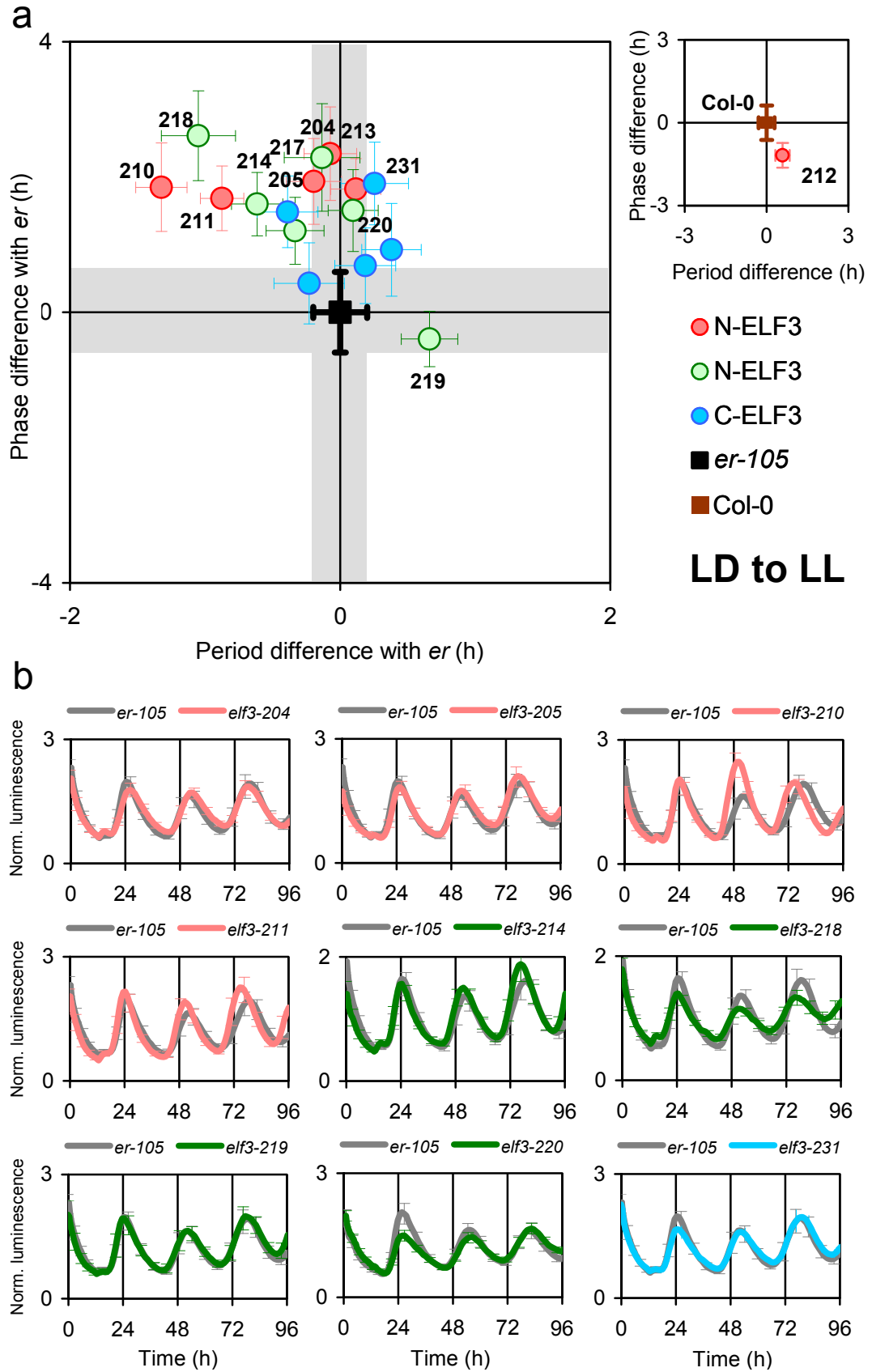


Figure 4.7. Circadian rhythms of *GI:LUC* in *elf3*-TILLING-lines under LL after LD entrainment. Please see figure legend text on page 86. Period and phase values are listed in Appendix 1 Table 1.

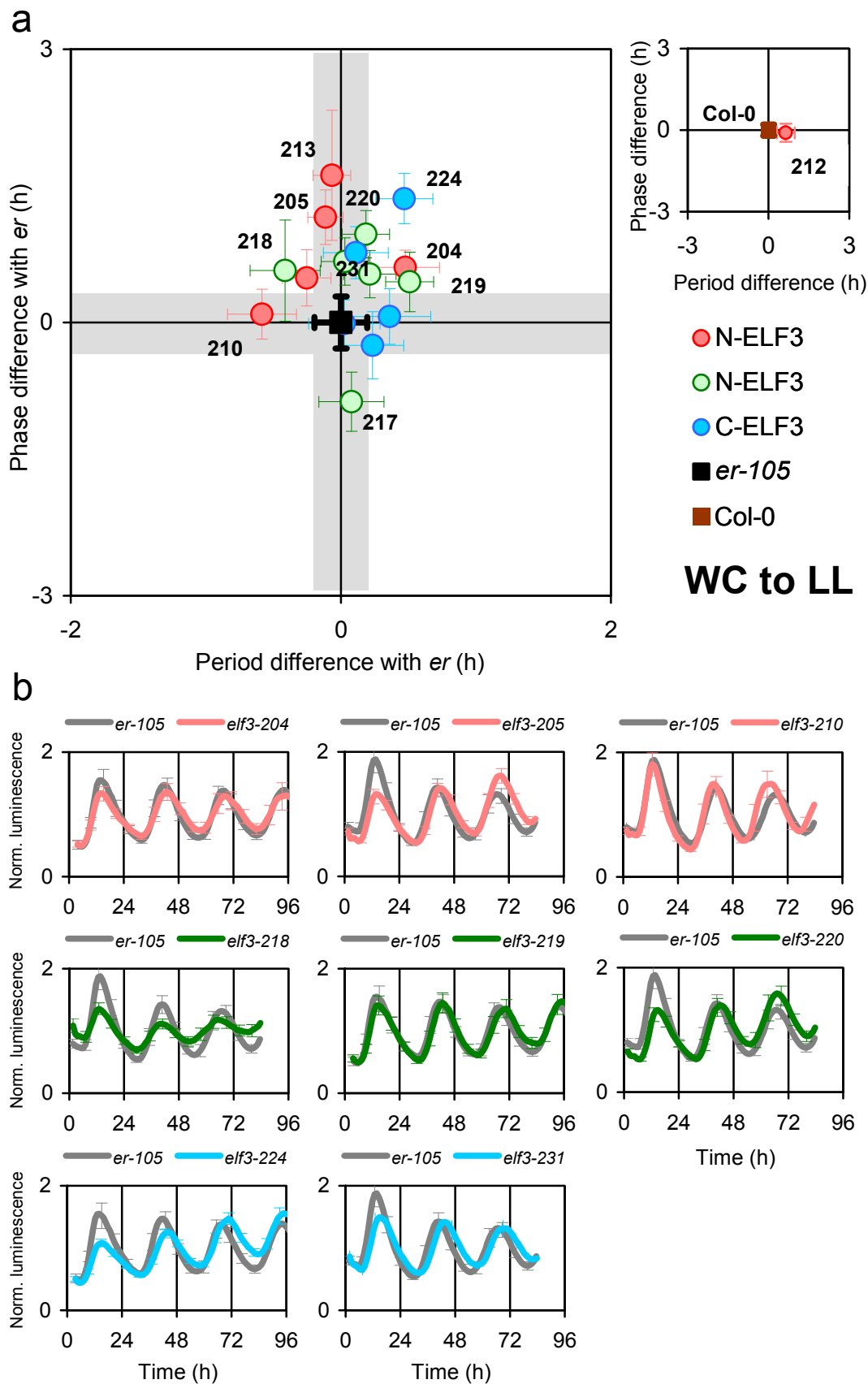


Figure 4.8. Circadian rhythms of *GI:LUC* in *elf3*-TILLING-lines under LL after WC entrainment. Please see figure legend text on page 86. Period and phase values are listed Appendix 1 Table 2.

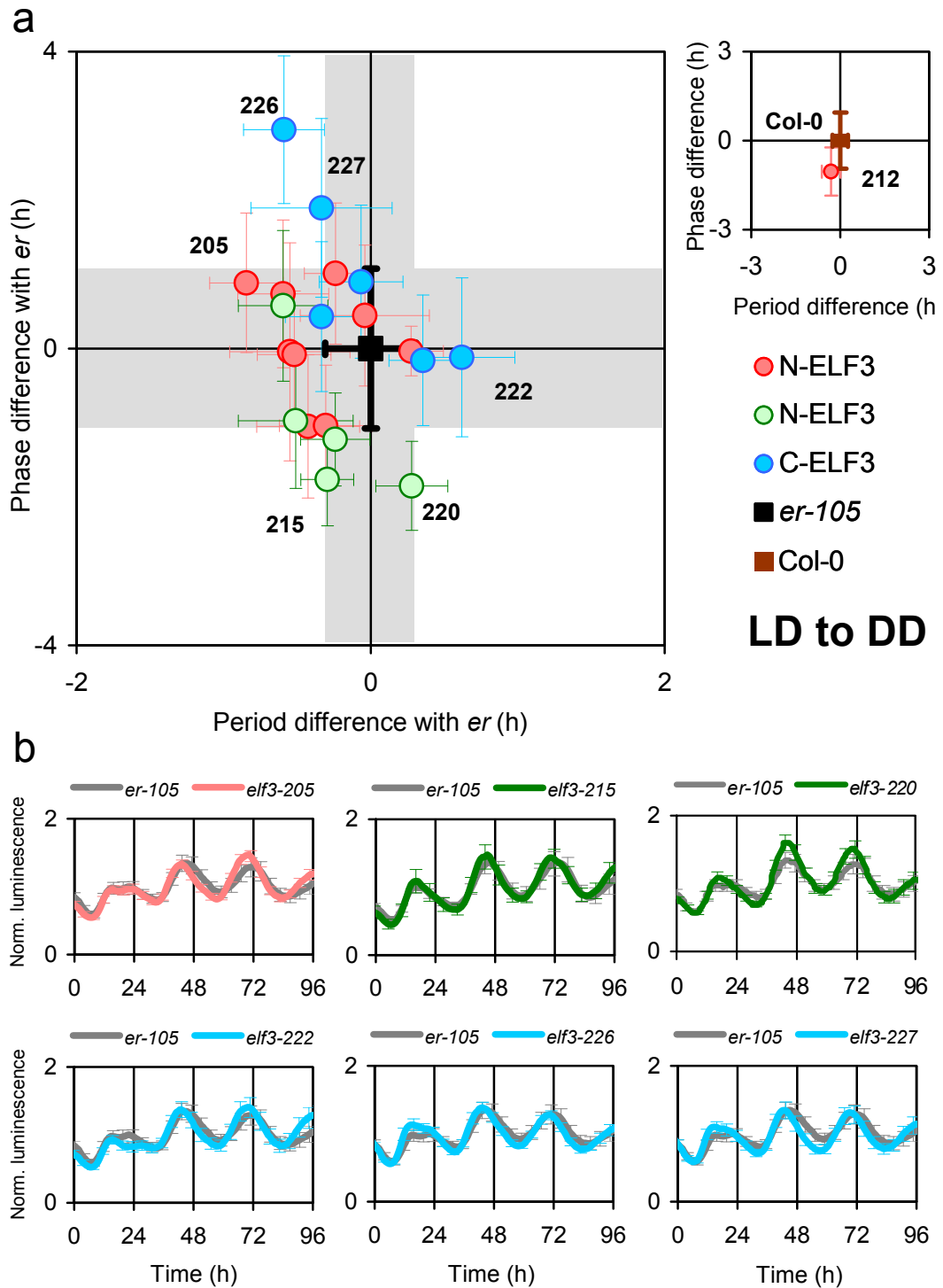


Figure 4.9. Circadian rhythms of *GI:LUC* in *elf3*-TILLING-lines in DD after LD entrainment. Please see figure legend text on page 86. Period and phase values are listed Appendix 1 Table 3.

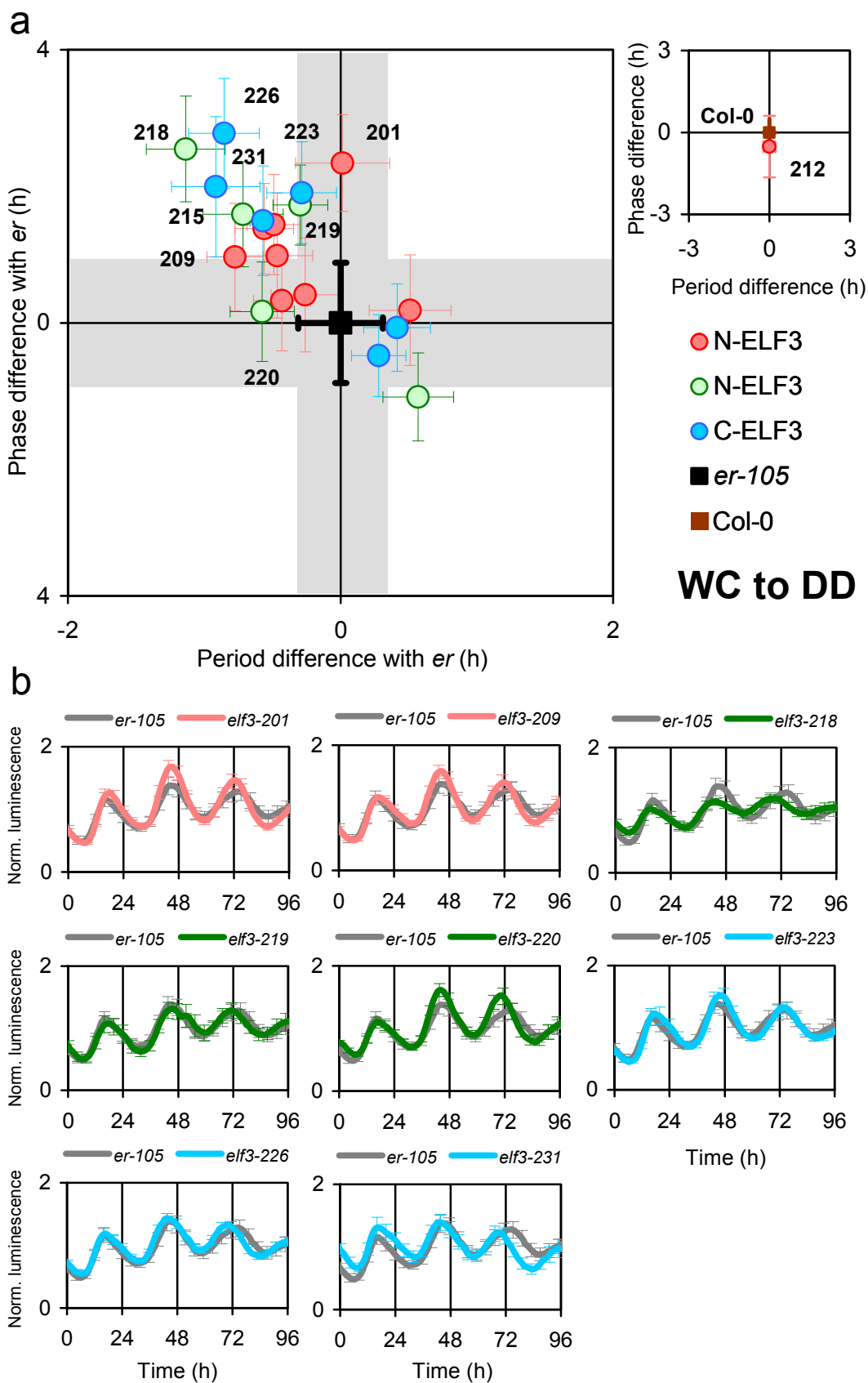


Figure 4.10. Circadian rhythms of *Gl:LUC* in *elf3*-TILLING-lines in DD after WC entrainment.
Please see figure legend text on page 86. Period and phase values are listed Appendix 1 Table 4.

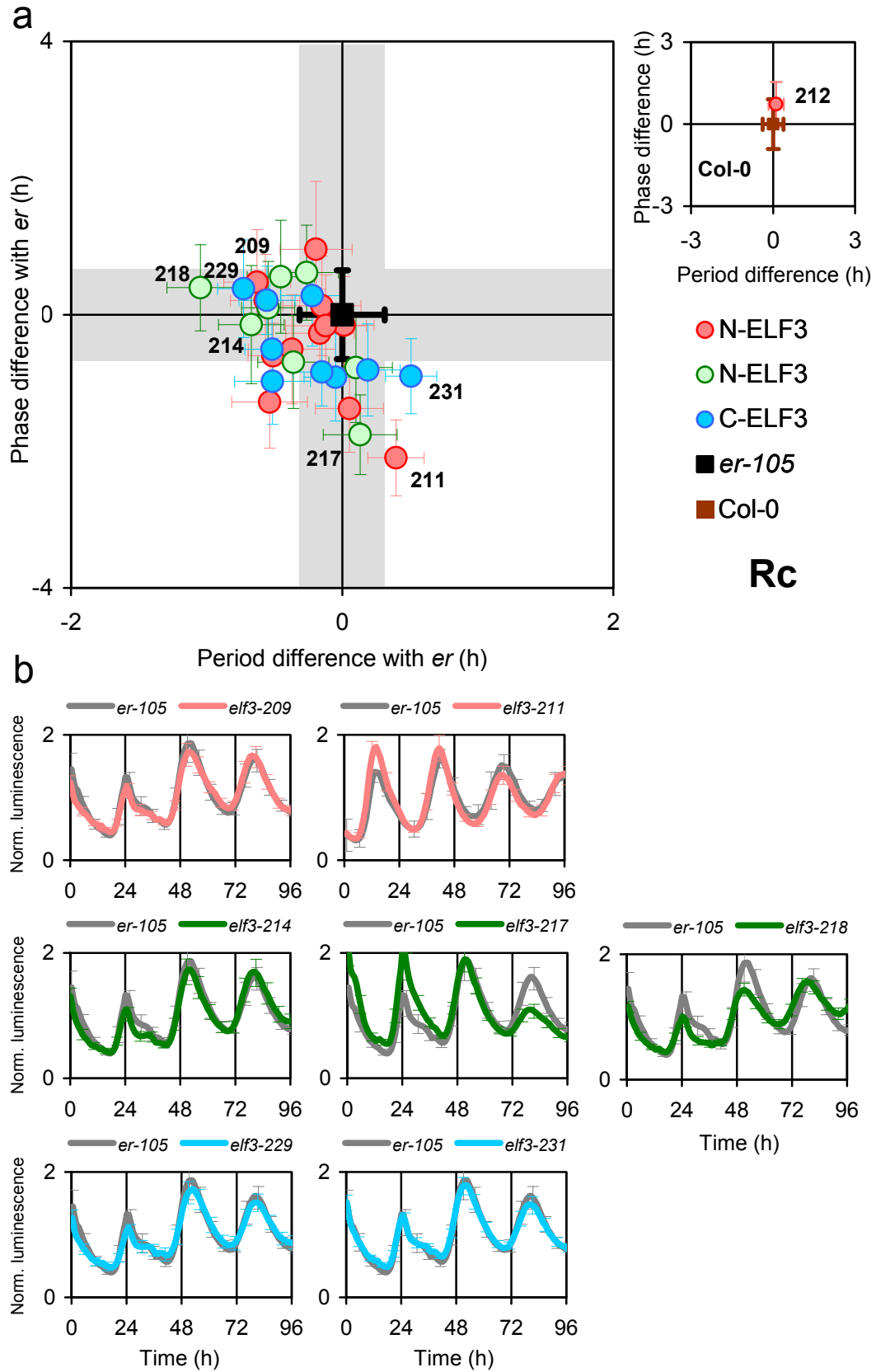


Figure 4.11. Circadian rhythms of *Gl:LUC* in *elf3*-TILLING-lines Rc. Please see figure legend text on page 86. Period and phase values are listed Appendix 1 Table 5.

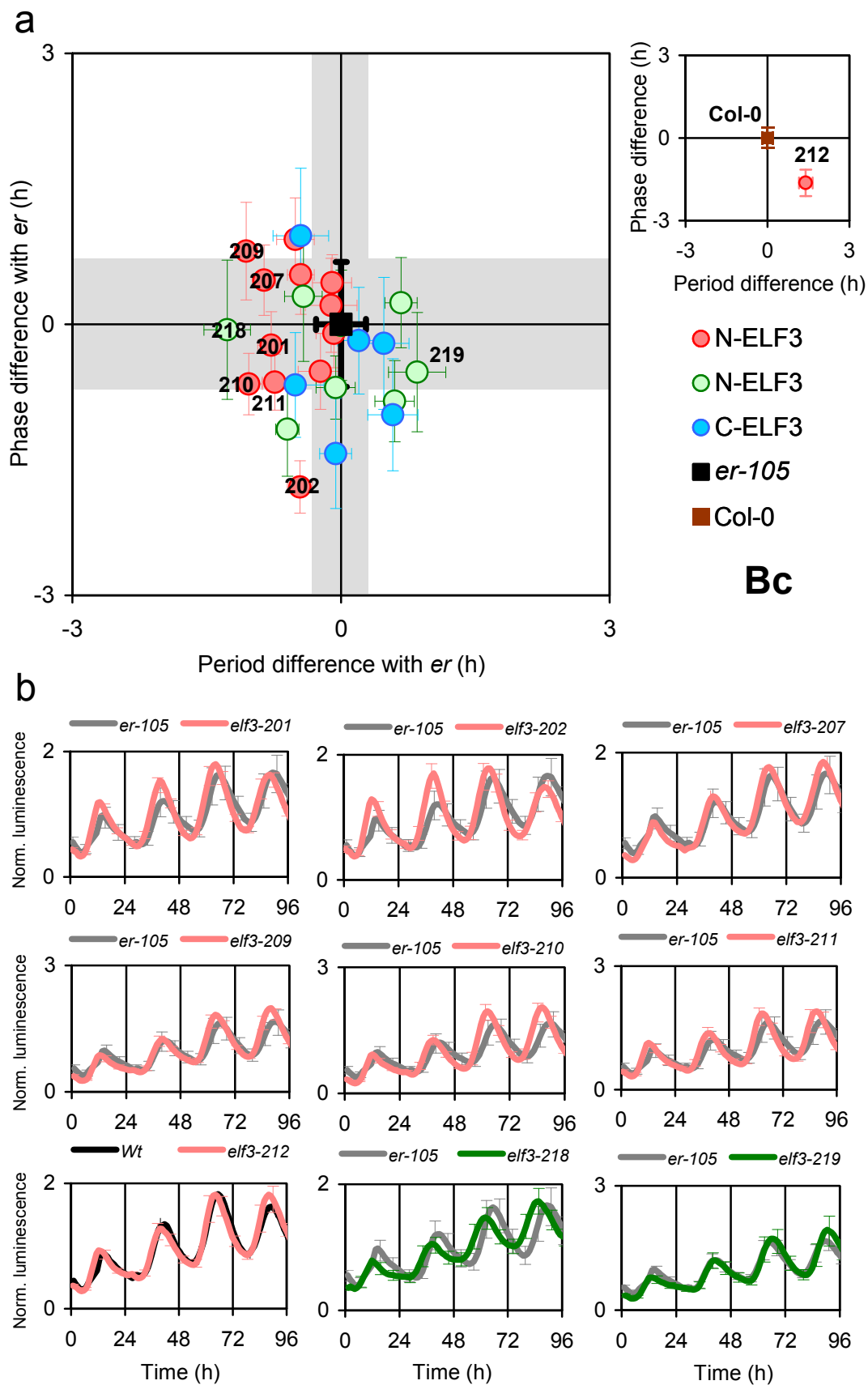


Figure 4.12. Circadian rhythms of *Gl:LUC* in *elf3*-TILLING-lines under Bc. Please see figure legend text on page 86. Period and phase values are listed Appendix 1 Table 6.

Table 4.2 Summary of period and phase phenotypes of *elf3*-TILLING lines under different entrainment and free-running conditions.

<i>elf3</i> allele	Period						Phase						Allelic test (LL)	
	Short			Long			Early			Late				
	LD to LL	WC to LL	LD to DD	WC to DD	Rc	Bc	LD to LL	WC to LL	LD to DD	WC to DD	Rc	Bc	Period	Phase
201	—	—					—	—						
202	—	—					—	—						
203	—	—	—	—			—	—	—	—				
204														
205														
206	—	—	—	—			—	—	—	—				
207	—	—					—	—	—	—				
208	—	—					—	—	—	—				
209	—	—					—	—	—	—				
210														
211														
212														
213														
214														
215														
216														
217														
218														
219														
220														
221														
222														
223														
224														
225	arrhythmic						arrhythmic						arrhythmic	
226														
227														
228														
229														
230														
231														

— indicates that period or phase values were not determined under the corresponding condition.

In order to confirm that the phenotypes of some of the *elf3* alleles was due to the missense mutation and not due to a linked second site mutation, I tested *GI:LUC* circadian rhythms of trans-heterozygous plants from crosses of the *elf3* line and the null allele *elf3-1*. Thus, these plants have one missense-active-mutant allele over the null allele, and are heterozygous from potential second-site mutations. Under LL, F1 trans-heterozygous plants from the cross of *elf3-1* and *elf3-225* displayed arrhythmic *GI:LUC* expression (Figure 4.13B). This confirms that *elf3-225* is a null allele. The trans-heterozygous plants from *er-105* and *elf3-1* displayed a similar *GI:LUC* expression that the cross between Col-0 and *elf3-1* (Figure 4.13A). This suggests that the *erecta* mutation does not confer a circadian phenotype. The phenotypes of *elf3-210*, *elf3-211*, *elf3-212* and *elf3-218* homozygous lines were similar of the F1 crosses of each line and *elf3-1* (Figure 4.13). These latter results confirm that these lines have an *elf3*-dependent phenotypic difference to the wild type. Taken together, line *elf3-210* and *elf3-218* display short periodicity, whereas *elf3-211* and *elf3-212* display long period.

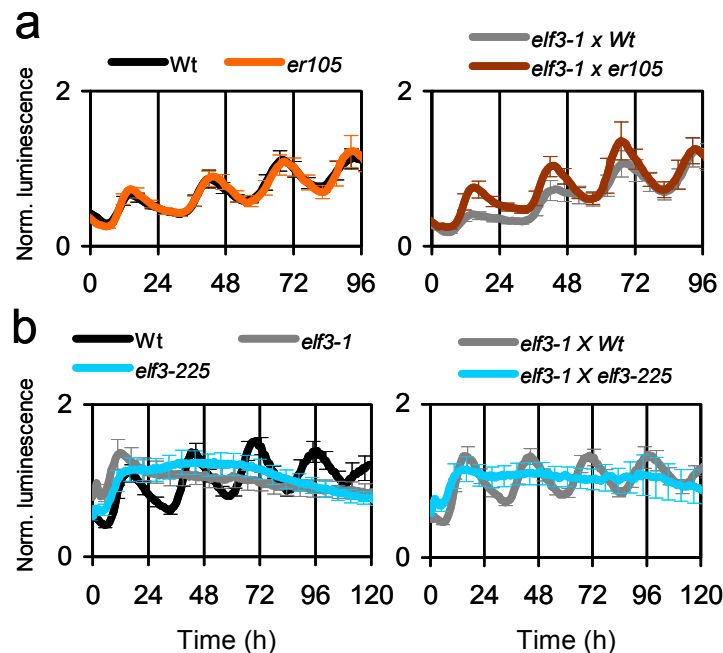


Figure 4.13. Allelic test for *er105* and *elf3-225*.

(a) Free-running profile of *er-105* and wild type (left panel), *elf3-1* x *er-105* F1 and *elf3-1* x wild type F1 (central panel).

(b) Free-running profile of *elf3-225* and wild type (left panel), *elf3-1* x *elf3-225* F1 and *elf3-1* x wild type F1 (central panel).

Error bars indicate SEM, and they are every sixth count to clarify traces.

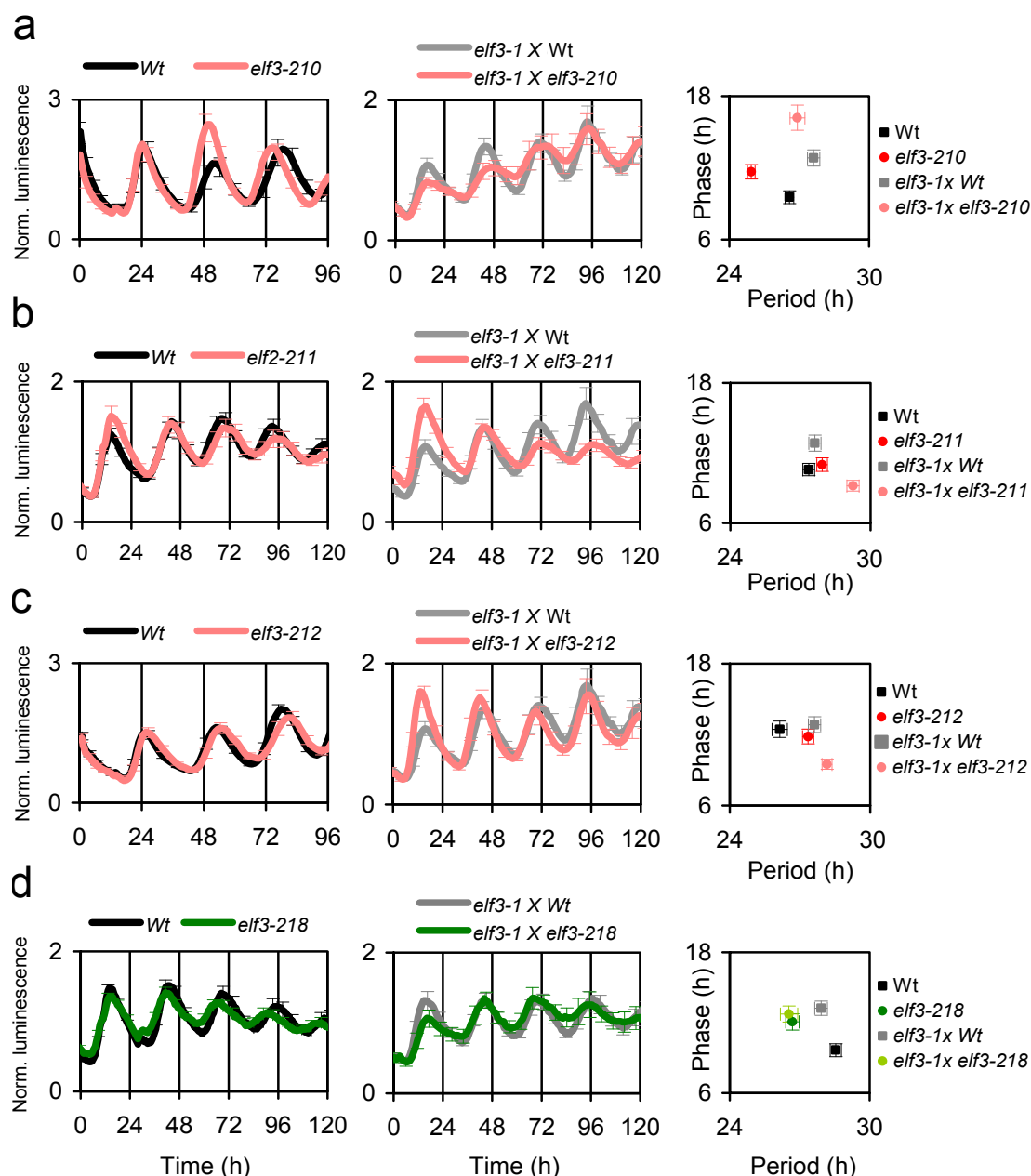


Figure 4.14. Allelic test of *elf3* lines 210, 211, 212 and 218.

(a) Free-running profile of *elf3-210* and wild type (left panel), *elf3-1 x elf3-210* F1 and *elf3-1 x wild type* F1 (central panel). Period vs. phase values for left and central panel (right panel).

(b) Free-running profile of *elf3-211* and wild type (left panel), *elf3-1 x elf3-211* F1 and *elf3-1 x wild type* F1 (central panel). Period vs. phase values for left and central panel (right panel)

(c) Free-running profile of *elf3-212* and wild type (left panel), *elf3-1 x elf3-212* F1 and *elf3-1 x wild type* F1 (central panel). Period vs. phase values for left and central panel (right panel)

(d) Free-running profile of *elf3-218* and wild type (left panel), *elf3-1 x elf3-218* F1 and *elf3-1 x wild type* F1 (central panel). Period vs. phase values for left and central panel (right panel)

Error bars indicate SEM. For free-running profiles SEM is plotted every sixth count to clarify traces.

4.3 Discussion

The loss of *ELF3* led to clock arrest under constant conditions, seen as arrhythmicity of all outputs (Covington *et al.*, 2001; Thines and Harmon, 2010). The phenotypical severity of *elf3* null alleles reduces the ability to assign a biological function to ELF3 protein. The over-expression of *ELF3-OX* led to a long-periodicity phenotype and an attenuated light-input to the oscillator (Covington *et al.*, 2001). This indicates that *ELF3* functions to lengthen circadian rhythms and to buffer light-signals to the clock. Hence, in the case of attenuated ELF3 function the opposite effect would be expected, *i.e.*, short periodicity and increased of light-signaling effects to the clock.

A forward genetic approach led to the identification of a new allele of *elf3* (Kolmos, 2007). The *elf3-12* allele retained circadian rhythmicity, albeit with short-periodicity phenotype. This indicates that attenuated ELF3 function was present in *elf3-12*. ELF3-12 protein function was sufficient for the normal control of flowering time and hypocotyl elongation (Kolmos, 2007). This suggests that the developmental defects observed in *elf3* null alleles are caused by circadian arrhythmicity and not only because of a defect in light signaling.

The attenuated function of *elf3-12* could be caused by a decrease capacity to produce *ELF3* transcript or ELF3 protein. The expression of ELF3 in the *elf3-12* was similar to the wild type (Bujdoso, personal communication). Hence, I tested if *ELF3-12* transcript could lead to viable protein expression. When ELF3-12-YFP fusion protein were expressed under ELF3 promoter in *N. benthamiana*, a similar ELF3-YFP accumulation than that of ELF3 wild type was observed. Also, ELF3-12-YFP cytoplasmic signal seemed to be increased as compared to the ELF3-YFP (Figure 4.1). In Chapter 3, I showed that co-expression of ELF4 and ELF3, enhances ELF3 nuclear localization (Figure 3.5). A decrease of TOC1 nuclear-pool was also observed for *toc1-weak* alleles affected in PRR5 binding (Wang *et al.*, 2010). Similarly, a defect on ELF3-ELF4 interaction in the presence of the *elf3-12* mutation could explain the increase of cytoplasmic localization, and by extension, the attenuated ELF3-12 function. In a Y2-H assay, I observed that ELF3-12 and ELF4 can still physically interact (Figure 4.1). However, it is possible that the Y-2H experiment is not sensitive enough to detect a weaker binding affinity of ELF3-12 and ELF4. Thus, future experiments may underlie a defect of ELF3-12 protein to physically associate with ELF4.

The *elf3-12* mutation was found to have a light-dependent short-periodicity (Figure 4.2 A-D). This phenotype is opposite to that of YFP-ELF3 MC lines that did not have the phyB-binding domain (ELF3N) and displayed long-period rhythms (Figure 3.8 and 3.9). In a Y2-H assay, ELF3-12 was found to bind PHYB (Figure 4.1). Moreover, *elf3-12* short-periodicity was enhanced by *PHYB-OX* and *PHYA-OX*. These observations are consistent with a direct negative role of phyB to modulate ELF3 action on periodicity. In the phase-resetting assay, *elf3-12* displayed pronounced phase advances induced by RL pulses at the end of the subjective night (Figure 4.2 E). Thus, *elf3-12* displayed hypersensitivity to light-input signals to the clock.

The isolation of new *elf3* weak alleles could expand the characterization of ELF3 protein function. Within the collection of 31 *elf3* point-mutation alleles, only *elf3-225* displayed arrhythmicity of *G:LUC* expression. Since *elf3-225* encodes for a truncated ELF3 protein with an early stop codon at residue 550, it is likely a null allele. This confirms the essential role of the C-terminus of ELF3 protein for circadian function. The rest of *elf3* alleles displayed robust *G:LUC* rhythms. Several *elf3* lines with residue changes within the ELF3N domain were found to display circadian phenotypes under LL. *elf3-210* displayed short periodicity in the LD to LL and WC to LL experiments (Figure 4.7 and 4.8). This short-periodicity could be confirmed by allelic test, although the period difference was less pronounced (Figure 4.13), this could be due to the action of other locus on periodicity in this line. Conversely, *elf3-212* displayed a statistically significant long-period phenotype under Bc (Figure 4.12). In the LD to LL and the WC to LL experiments, *elf3-212* also displayed long-periodicity, but this was not statistically significant (Appendix 1 Tables 1 and 2). The allelic test confirmed a slight long-periodicity and an early-phase under LL (Figure 4.13). Hence, *elf3-210* and *elf3-212* could serve to study the role of the ELF3N domain in light-input to the clock.

Within the lines encoding residue changes within the ELF3M domain, *elf3-218* and *elf3-219* displayed short and long periodicity, respectively, in several experiments. For *elf3-218*, short-period rhythms were observed under all conditions tested but LD to DD (Figure 4.7 to 4.12, Table 4.2). This phenotype was confirmed in the allelic test (Figure 4.13). The phenotype of *elf3-218* resembled *elf3-12* short-periodicity phenotype (Figure 4.2), but *elf3-218* also displayed short-period in the WC to DD experiment. Hence, it is possible that *elf3-218* encodes for a ELF3 protein with attenuated ELF4 binding. *elf3-219* displayed long-periodicity in the LD to LL, WC to LL assays and under Bc (Figure 4.7, 4.8 and 4.12). *elf3-219* encodes for change in a evolutionary-conserved serine (S303F, Table 4.1) located within a conserved region (residues 298-382) in the ELF3M domain. The functional importance of this conserved region was already

indicated by the circadian phenotypes of *elf3-12* allele (G326D). The ELF3-dependent phenotype of *elf3-219* should be confirmed with an allelic test.

The molecular mechanisms that set the phase of the circadian oscillator are not understood. The *phyB* mutant was found to display early-phase circadian rhythms after LD entrainment, but not after WC entrainment (Salome *et al.*, 2002). More recently, the *phyB* mutant was reported to have early phase of *GI:LUC* under white light (red+blue light), whereas it displayed late phase under Rc (Palagyi *et al.*, 2010). The *elf3*-lines 204, 205, and 213 displayed late phase under both LD to LL and WC to LL, but in DD (Table 4.2). *elf3-210* also displayed late phase of *GI:LUC* expression in the LD to LL experiment and in the allelic test (Figure 4.7 and 4.13). Hence, these three lines displayed have the opposite effect to that observed in *phyB* mutants (Palagyi *et al.*, 2010). *elf3-212* displayed an early-phase of *GI:LUC* under LD to LL, which was confirmed in the allelic test. These four alleles encode for residue changes within the ELF3N domain. Hence ELF3N could be involved in setting the phase of *GI:LUC* under LL. *elf3-231* displayed late phase both under LL and in DD (Table 4.2). Similarly, *elf3-226* also displayed late phase, but the phase change was only statistically significant in DD (Table 4.2). Both *elf3-226* and *elf3-231* encode for residue changes in the C-terminus of ELF3. Hence, it is possible that C terminus of ELF3 controls circadian phase independently of light. Further analysis of these *elf3* alleles may assist in determining if the role of ELF3 in circadian phase depends on phyB signaling.

Taken together, I propose that ELF4 and phyB compete for the activation and the repression of ELF3, respectively. ELF4 binding to the middle part of ELF3 would activate ELF3 by enhancing ELF3 nuclear. phyB binding to the N-terminus of ELF3 would negatively affect ELF3 capacity to lengthen periodicity. In the *elf3-12* a decrease of affinity for ELF4 would lead to an increase in phyB-mediated repression. This hypothesis is consistent with ELF3 being a multifunctional protein that sustains circadian rhythms and integrates light signals to the oscillator. Future experiments with the *elf3-12* mutant and other *elf3* weak alleles could assist in the understanding of the biochemical mechanism underlying ELF4 activation and phyB repression of ELF3 action.

Chapter 5 Final discussion and perspectives

5.1 Summary

ELF3 plays a pivotal role in the circadian clock mechanism and in the integration of light signals to the clock (McWatters *et al.*, 2000; Covington *et al.*, 2001; Thines and Harmon, 2010). However, at the start of this thesis, the molecular basis of ELF3 action was not understood. The functional characterization of ELF3 protein led me to identify three functional modules within ELF3 protein: (1) ELF3M (residues 261-484) mediates ELF4 binding. (2) ELF3N (residues 1-259) associates with phyB and COP1, and (3) ELF3C (residues 485-695) targets ELF3 nuclear localization and formation of nuclear bodies (NB). Therefore, ELF3 is a multifunctional protein (Figure 5.1).

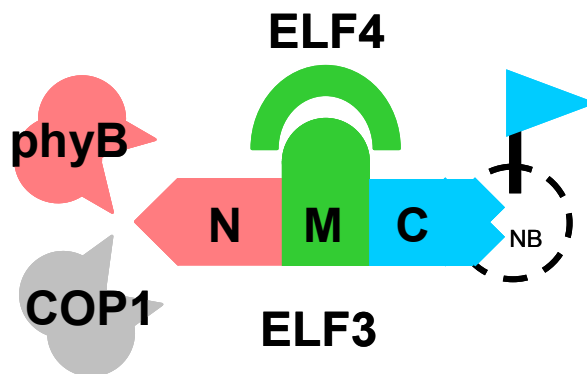


Figure 5.1. ELF3 is a multifunctional protein. The N-terminus of ELF3 (N, pink) mediates interaction with phyB and COP1. The middle domain of ELF3 (M, green) binds to ELF4. The C-terminus domain (C, blue) is required for localization into nuclear bodies (NB).

5.1.1 ELF4 acts as an effector for ELF3

In Chapter 3, I explored the genetic and physical interaction of ELF4 to ELF3. ELF3 and ELF4 were found to physically interact through the ELF3M domain (Figure 3.1). Notably, ELF4 protein localization is preferentially nuclear (Figure 3.10), whereas different fragments of ELF3 displayed distinct cytoplasmic and nuclear pools (Figure 3.4 and 3.6). This supports that ELF4 does not "move" ELF3, but rather, that ELF4 could serve as an anchor to dock ELF3 nuclear fraction. Consistently, I found that the ELF4-binding domain of ELF3 (the middle domain, ELF3M) was required for ELF3 signaling function (Figure 3.7). The levels of ELF3 nuclear protein were found to be stabilized under LL, whereas they gradually fade in DD (Liu *et al.*, 2001). ELF4

transcript accumulation is induced by light and it dampens in DD (Doyle *et al.*, 2002; Khanna *et al.*, 2003; Li *et al.*, 2011). Although, ELF4 protein levels were not measured, it is possible that there is more ELF4 protein under LL than in DD. Hence, stabilization of ELF3 protein under LL maybe mediated by higher levels of ELF4 protein under LL, as compared to DD.

ELF3-OX was found to restore the arrhythmic-clock phenotypes of *elf4* (Figure 3.2). This may further suggest that there is an active process that reduces the ELF3 nuclear pool (see below), and that ELF4 counteracts this process. In the *elf4* mutant, ELF3 would be preferential to a greater cytosolic fraction. In *elf4 ELF3-OX*, this active nuclear export process would not cope with the high amounts of ELF3, and there would be enough ELF3 protein to fulfill circadian function, even in the absence of *elf4* (Figure 5.2). In *ELF4-OX*, the ELF3 nuclear pool would be further stabilized leading to an enhanced capacity of ELF3 to lengthen circadian periodicity (Figure 3.2 and 3.3). Analogous processes have been found in other clock systems (Figure 1.6). For example, in the mouse clock, co-expression of BMAL and CLK led to re-localization of CLK in the nucleus (Kondratov *et al.*, 2003). Consistently, in *Bmal1* mutant fibroblasts, CLK protein was constitutively cytoplasmic (Gekakis *et al.*, 1998; Kondratov *et al.*, 2003). In *Drosophila*, the role of BMAL is taken by CYC that stabilizes nuclear-active CLK pool (Hung *et al.*, 2009). In *Neurospora*, WC-1 only localizes in the nucleus in the presence of WC-2, and they both assemble into WCC complex (Cheng *et al.*, 2002). Recent efforts in plants have observed the requirement of protein re-localization in normal clock function in Arabidopsis. For example, PRR5 increased TOC1 nuclear pool, and this protected TOC1 from ZTL-mediated targeted-proteasome degradation that would have occurred in the cytosol (Wang *et al.*, 2010). Also ZTL stabilization was found to be achieved by physical interaction with GI in the cytosol (Kim *et al.*, 2007). GI-ELF3 interaction was required for destabilization of GI by COP1-mediated proteosomal degradation (Yu *et al.*, 2008). Thus, protein re-localization mediated by protein-protein interactions is a common regulatory mechanism in circadian systems. Taken together, my observations are consistent with a role of ELF4 as an effector protein (Kolmos *et al.*, 2009) for its target ELF3. The effector activity of ELF4 would constrain ELF3 to a nuclear pool leading to an increase of ELF3 repressor activity.

5.1.2 The N-terminus of ELF3 is involved in Aschoff's rule

Interestingly, the N-terminal domain of ELF3 was found to be dispensable for ELF3 circadian function (Figure 3.7). Alone it preferentially localized in a cytoplasmic pool (Figure 3.4 and 3.6). Notably this N-terminal domain mediates physical interaction of ELF3 with phyB photoreceptor (Figure 3.8) (Liu *et al.*, 2001). As a result, I proposed that such protein-protein interactions modulate the repressive function of ELF3 activity, possibly by reducing the ELF3 nuclear pool. This active reduction of the ELF3 nuclear could serve as a mechanism for Aschoff's rule (Aschoff, 1979). In here, ELF3 and phyB play opposite roles, where ELF3 decelerates and phyB accelerates periodicity, respectively (Devlin and Kay, 2000b; Covington *et al.*, 2001). To physiologically test this hypothesis, I measured periodicity of *LHY:LUC* circadian rhythms in *YFP-ELF3* and *YFP-ELF3MC* and compared this to the wild type. This experiment indicated that *YFP-ELF3* period lengthening is suppressed under Rc, but not under Rc+Bc, Bc, and in DD (Figure 3.9). Interestingly, under Rc+Bc, *YFP-ELF3MC* was found to have a similar period length of *LHY:LUC* to that of *YFP-ELF3* (Figure 3.7 and 3.9, Table 3.1). However, under Rc and in DD, *YFP-ELF3MC* displayed a similar longer periodicity as compared to *YFP-ELF3* (Figure 3.9, Table 3.1). This indicates that ELF3N domain is required to repress ELF3 action in Aschoff's rule in a RL-dependent manner. Hence, physical association of phyB to ELF3N domain is likely to modulate ELF3 active levels. Furthermore, as *ELF4* activity in the dark mediates the correct timing of *PRR9* expression (Kolmos *et al.*, 2009), this could suggest that ELF4 binding to ELF3 disrupts phyB-mediated repression of ELF3. Below I will address the competitive roles of ELF4 and phyB on ELF3 function (Figure 5.4).

5.1.3 ELF3 localizes in nuclear bodies

The localization on nuclear bodies (NBs) is common for both clock and light-signaling proteins (Mas *et al.*, 2000; Chen, 2008; Yu *et al.*, 2008; Wang *et al.*, 2010). For ELF3, the ELF3C domain was found to be essential for localization in NBs. Notably, the NBs foci observed in *YFP-ELF3C* were different in size and number to the ones observed in *YFP-ELF3* full length. In particular, the *YFP-ELF3C* nuclear bodies were less abundant, but larger than those of *YFP-ELF3* (Figure 3.4 and 3.6). In transient expression in *N. benthamiana*, *ELF3C* nuclear bodies (Figure 3.4) were similar in size and shape to the ones observed for TOC1-*PRR5* interaction (Wang *et al.*, 2010); both experiments used a similar experimental set up. On the contrary,

YFP-ELF3 NBs resembled the nuclear bodies where ELF3, COP1, and GI were found to co-localize [Figure 3.4 and 3.6, (Yu *et al.*, 2008)]. Moreover, YFP-ELF3 NBs resemble the phyB NBs observed in phyB-GFP fusion proteins (Oka *et al.*, 2008). The YFP-ELF3MC construct generated few and small nuclear bodies (Figure 3.6). These observations suggest that ELF3 can localize into two different sub-cellular compartments. The interaction of ELF3 with phyB and COP1 through the ELF3N domain may mediate re-localization of ELF3 to the smallest, but more numerous YFP-ELF3 NBs.

5.1.4 *ELF3*, *ELF4*, and *LUX* form a transcriptional repressor complex

ELF3 and *ELF4* were proposed to act as transcriptional repressors of the morning genes *PRR9* and *PRR7* (Kolmos *et al.*, 2009). In *ELF3-OX* and *ELF4-OX*, the transcript accumulation of *PRR9* was severely reduced, whereas *PRR7* was not as severely affected (Figure 3.11). This indicates that *ELF3-ELF4* repressor complex preferentially targets *PRR9*. *ELF3* was found to associate to the Conserved Region 1 in the *PRR9* promoter as identified by phylogenetic shadowing (Figure 3.12). Others have also recently reported *ELF3* association to the *PRR9* promoter (Dixon *et al.*, 2011). The Conserved Region 1 is required for rhythmic expression of *PRR9*, and contains a LUX binding site (LBS) (Figure 3.12). The LBS mediates association of LUX (Helfer *et al.*, 2011). *elf3*, *elf4*, and *lux* mutants display similar phenotypes (Kolmos *et al.*, 2009; Thines and Harmon, 2010; Helfer *et al.*, 2011), leading me to test if these three genes act together in the circadian oscillator. Similar to the capacity of *ELF3-OX* to bypass the *elf4* mutant phenotype, *LUX-OX* restore *LHY:LUC* rhythmic expression in *elf4*. However, *LUX-OX* did not restore the *elf3* phenotype (Figure 3.14). This indicated that both *ELF3* and *LUX* are downstream of *ELF4*. As *LUX* appears to be nuclear localized regardless of the presence of *ELF4* and *ELF3* (Figure 4.13), a clear hierarchy exists in the cellular dynamics of this clock-sustaining co-repressor complex (Figure 5.2). First *ELF3* moves to the nucleus where it locates *ELF4*. *ELF4* retains *ELF3* in the nuclear compartment. In the nucleus, *ELF3* and *LUX* association to the *PRR9* promoter leads to repression of *PRR9* expression. Thus, three evening components of the circadian clock, *ELF4*, *ELF3*, and *LUX*, cooperatively act to sustain circadian oscillations (Figure 5.2)

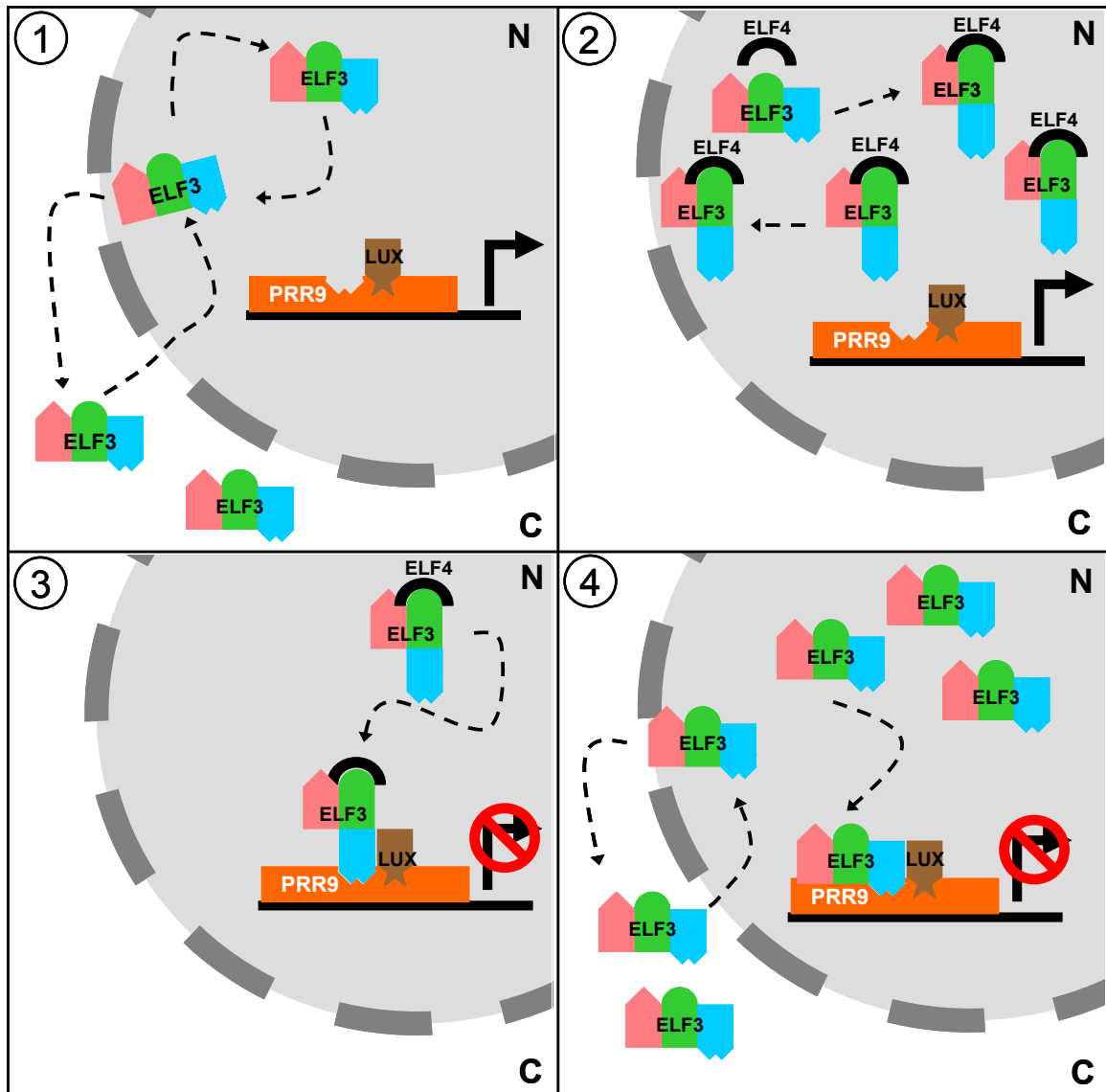


Figure 5.2. Model of the assembly of ELF3, ELF4, and LUX repressor complex.

1) ELF3 protein is imported to the nucleus. In the absence of ELF4, ELF3 is exported to the cytoplasm, and an active-ELF3 threshold is not achieved. Hence ELF3 does not associate to the *PRR9* promoter. LUX requires ELF3 for *PRR9* repression, and *PRR9* is not repressed.

2) Nuclear ELF3 pool is stabilized by ELF4 binding, and an active-ELF3 threshold is achieved.

3) ELF3, ELF4 and LUX association cooperatively promotes *PRR9* transcriptional repression.

4) Model for *elf4-1* ELF3-OX. The ELF3-active export process can not cope with high levels of ELF3. Hence, ELF3 reaches an active threshold, even in the absence of ELF4. ELF3 and LUX cooperatively mediate *PRR9* transcriptional repression.

5.1.5 Activation and repression in the *PRR9* promoter

The Conserved Region 1 in the *PRR9* promoter (Figure 3.12) mediates both 1) transcriptional repression by the ELF4/ELF3/LUX complex, where LUX binds to the LBS [Figure 3.12, (Helfer *et al.*, 2011)], as well as, 2) transcriptional activation by *CCA1* via the proximal EE (Portoles and Mas, 2010). The competition between activator and repressor complexes within such a promoter context has recently been found to be critical for *ELF4* expression (Li *et al.*, 2011). However, *CCA1* plays opposite roles in *ELF4* and *PRR9* expression. In the case of *ELF4*, *CCA1* mediates transcriptional repression by interfering in *FHY3* association to *ELF4* promoter (Li *et al.*, 2011). In the case of *PRR9*, *CCA1* mediates transcriptional activation (Farre *et al.*, 2005; Portoles and Mas, 2010). In here, *CCA1* could interfere in LUX and ELF3 association to *PRR9* promoter (Figure 5.3). Additionally, *PRR9* expression is light induced, and this acute response is severely reduced in *phyB* mutants, indicating that *phyB* is a positive regulator of *PRR9* expression (Ito *et al.*, 2003; Ito *et al.*, 2005). This positive regulation could be directly mediated by *phyB* attenuation of ELF3 repressive function (see section 5.1.4). In this context, *phyB* could displace ELF3 from *PRR9* promoter leading to a release of transcriptional repression (Figure 5.3). Thus, the competition of ELF3-ELF4-LUX repression complex with *CCA1* and *phyB* activation could be a molecular basis for rhythmic *PRR9* transcript accumulation.

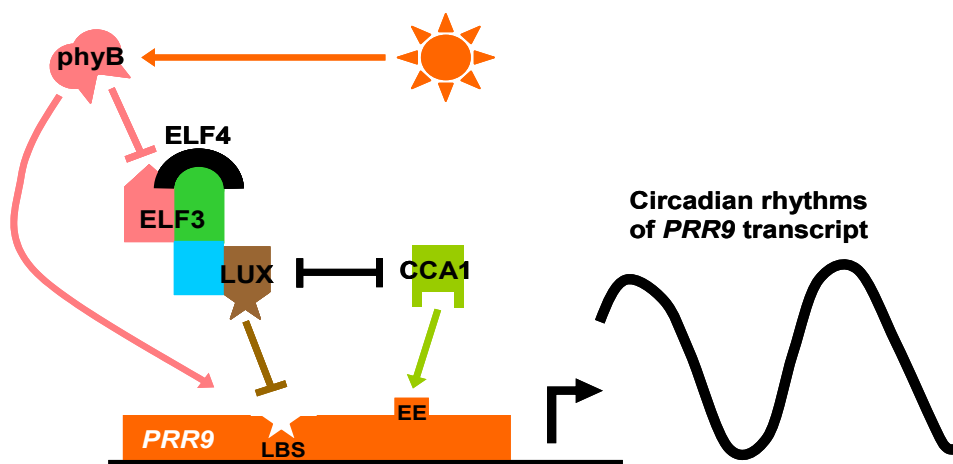


Figure 5.3. Activation and repression in the *PRR9* promoter. Competition between activation and repression complex could shape *PRR9* circadian expression. ELF3, ELF4 and LUX cooperatively mediate transcriptional repression; LUX associates via the LUX binding site (LBS). *CCA1* associates to the *PRR9* promoter via the evening element (EE) and mediates transcriptional activation. Light induction of *PRR9* expression depends on *phyB*. *phyB* binding to the N-terminus of ELF3 (pink) could indirectly activate *PRR9* by repressing ELF3.

5.1.6 *elf3-12* in the middle of phyB-ELF4 competition

The, *elf3-12* allele harbors a missense mutation within this ELF4 recognition domain (ELF3M), and it displays attenuated *ELF3* repressor activity (Figure 4.2). Missense alleles of *TOC1* (Wang *et al.*, 2010) and *ZTL* (Kim *et al.*, 2007) have been found to affect interaction with *PRR5* and *GI*, respectively, leading to attenuated clock function. Thus a similar mechanism could underlie *elf3-12* phenotype, where ELF3-12 would be affected in ELF4 binding. *elf3-12* displayed light-dependent short-period rhythms and hypersensitivity to RL-resetting pulses applied at the end of the subjective night. Hence, an increased light repression of ELF3 function seems to be present in *elf3-12*. Therefore, I hypothesize that ELF4 and phyB compete for activation and repression of ELF3 function (Figure 5.4), respectively. ELF3-phyB binding through the ELF3N seemed to be required for period-shortening under Rc (see section 5.1.2). ELF4-ELF3 binding through ELF3M (see section 5.1.1) would stabilize ELF3 nuclear pool by interfering in the ELF3-phyb interaction, leading to an enhanced capacity of ELF3 to lengthen circadian period (Figure 5.4). Therefore, ELF3 contains two functional modules that are required for repression (ELF3N) and for activation (ELF3M) of its function (Figure 5.4).

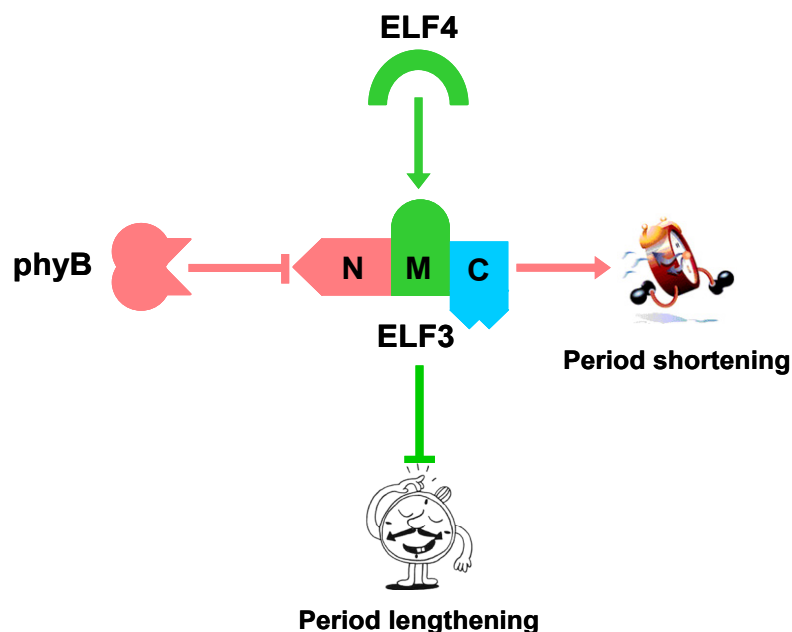


Figure 5.4. ELF4-phyB competition hypothesis. ELF3 has one activation domain ELF3M and one repression domain ELF3N. The competition of ELF4 and phyB for binding to ELF3 provides modulation of ELF3 function. ELF4 binds the ELF3M domain leading to enhanced ELF3 action to lengthen periodicity. phyB binds to the ELF3N domain leading to repression of ELF3 action and, thus, period shortening. Clock cartoons were obtained from www.google.com clock images.

5.2 Perspectives

5.2.1 ELF3-ELF4 interaction

ELF4-mediated stabilization of ELF3 nuclear-pool could be confirmed by measuring ELF3 nucleo-cytoplasmic ratio in the *elf4-1*, wild type, and *ELF4-OX* backgrounds. Additionally, the capacity of ELF4 to retain ELF3 in the nucleus could be examined by co-expressing ELF3 with increasing concentration of ELF4, and then, by measuring the ELF3 nucleo-cytoplasmic ratio in these samples. This approach was used to assess the PRR5-mediated TOC1 stabilization (Wang *et al.*, 2010). The expectation of this experiment would be that increasing ELF4 levels would enhance ELF3 nuclear distribution.

The *elf3-12* mutation maps to a highly-evolutionary conserved box (Kolmos, 2007) defined within the ELF3M region, which mediates ELF3-ELF4 binding (Figure 3.1 and Figure 5.5). Additionally, two weak *elf4* alleles were found to confer short periodicity, similarly to *elf3-12* (Kolmos *et al.*, 2008). The encoded proteins *elf3-12*, and these *elf4* weak alleles, could be affected in the ELF3-ELF4 binding capacity (Figure 5.5). Ultimately, combination of these mutations and/or additional mutagenesis of ELF3-conserved box and ELF4 protein, could assist in obtaining an ELF3, an ELF4, or an ELF3-ELF4 combination that abolishes ELF3-ELF4 interaction (Figure 5.5). The binding capacity could be assessed by FRET, similarly to Figure 4.1. For this assay, ELF3 and ELF4 fusion proteins could be expressed under the control of their native promoters to achieve physiological levels or both proteins. Then, the analysis study circadian function in the absence of ELF3-ELF4 binding could lead to the confirmation of the functional relevance of ELF3-ELF4 interaction. I expect that the failure of ELF4 activation of ELF3 severely affects ELF3-clock function and by extension lead to clock arrest (Figure 5.5).

The observation that both ELF3 and ELF4 display nuclear and cytoplasmic pools may indicate an additional cytoplasmic function of ELF3 and ELF4. In order to separate a putative cytoplasmic function from the known nuclear function, fusion proteins of ELF3 and ELF4 to nuclear localization signals (NLS) and nuclear export signals (NES) could be used to assay restoring of *elf3* and *elf4* phenotype, respectively. For example, it could be expected that an ELF3-NLS protein would be constitutively nuclear and able to mediate ELF3 function in the absence of ELF4. By extension, an ELF3-NLS protein might be insensitive to phyB action. On the contrary, an ELF3-NES protein that would be constrained in the cytoplasm could not restore *elf3*

phenotype. In a different experiment, an ELF4-NLS could mediate ELF3-nuclear stabilization and hence restore *elf4* phenotype. On the contrary, an exclusively cytoplasmic form of ELF4 (ELF4-NES) would fail to stabilize nuclear ELF3, and by extension would not restore *elf4* phenotype. This approach would further test ELF4 action on ELF3 nuclear stabilization.

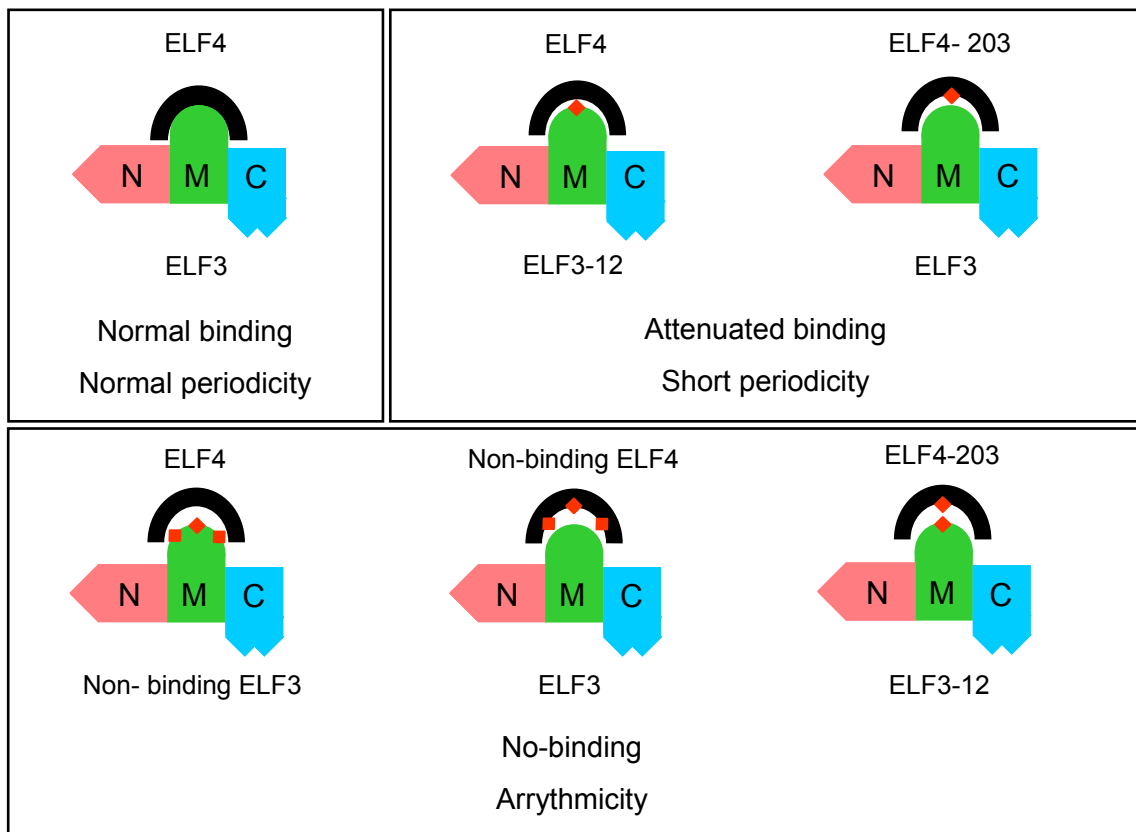


Figure 5.5. ELF3-ELF4 interaction essential for circadian function. ELF3-ELF4 binding is mediated by the ELF3M domain (green). This interaction requires electrostatic interaction between ELF3 and ELF4 conserved residues. In *elf3-12* and *elf4-203* weak alleles, the residue change leads to attenuated ELF3-ELF4 binding, resulting in short-periodicity of circadian rhythms. In the case of a ELF3 mutant, an ELF4 mutant, or a mutant combination that abolish ELF3-ELF4 interaction, arrhythmicity of circadian rhythms would be expected.

5.2.2 Functional analysis of ELF3 nuclear bodies

ELF3 was found to localize in NBs (Figure 3.4 and 3.6). It could be interesting to explore the functionality of these NBs. First, co-expression experiments could determine if YFP-ELF3 full NBs contain COP1 or phyB. Second, reporter constructs for other NBs could be used to assay if ELF3 co-localizes in known sub-nuclear structures. For example, the spliceosome has been found to form a NB (Lorkovic *et al.*, 2004). The YFP-ELF3C NBs were found to be different from the ones of YFP-ELF3, suggesting

that they are different sub-nuclear structures. The YFP-ELF3C line could be used for the isolation of additional proteins co-localizing within YFP-ELF3 NBs. For this, YFP-ELF3 plant material could be cross-linked, and then, the YFP tag could be used to isolate YFP-ELF3C complex. Proteins contained in such complex could be identified by mass-spectrometry. Overall, such experiments could assist to determine if clock and light-signaling protein localize in a sub-nuclear structure where clock- and light-transcriptional regulation may take place.

5.2.3 ELF3-ELF4 as transcriptional repressors

The mechanism of ELF4 stabilization of ELF3 nuclear pool is analogous to what has been described for the three essential complexes BMAL-CLK, CYC-CLK, and the WCC, in other clock systems (Cheng *et al.*, 2002; Kondratov *et al.*, 2003; Hung *et al.*, 2009). However, ELF3-ELF4 complex seems to mediate transcriptional repression, whereas the other three complexes are mediate transcriptional activation. ELF3 associates to *PRR9* and this correlates with repression of *PRR9* transcript accumulation (Figures 3.11 and 3.12). Consistently, both *ELF3-OX* and *prp9* loss of function led to circadian-period lengthening, whereas *elf3-12* and *PRR9-OX* led to circadian-period shortening. Since *PRR9-OX* retains circadian rhythms, the high levels of *PRR9* found in *elf3*, *elf4* and *lux* mutants (Kolmos *et al.*, 2009; Dixon *et al.*, 2011; Helfer *et al.*, 2011) do not explain alone their arrhythmicity phenotypes. One important genetic test would be to generate *elf3 prp9* double mutant and compared their circadian phenotypes to *elf3*. It could be expected that *elf3 prp9* mutant displays arrhythmicity, but the levels of *CCA1* and *LHY* increase compared to those of *elf3*. Moreover, ELF3 has been found to be required for GI targeted degradation, and hence, high levels of GI in *elf3* mutants may be partially responsible for its clock arrest. Generating *elf3 gi* double mutant could genetically test this possibility. It would be expected that high levels of TOC1 protein in the absence of GI, would lead to clock arrest in these double mutants. Finally, generating the *elf3 prp9 gi* triple mutant would reduce the clock network to the core loop by affecting the morning and evening loops, and the *ELF3-ELF4-LUX* complex. Testing circadian function in this triple mutant could determine the importance of multiple feed-back loops for circadian function.

Other targets of *ELF3-ELF4* and *LUX* complex could be mis-regulated in their corresponding null alleles. Notably, I did not find association of ELF3 to the *PRR7* promoter, consistent with a recent report (Dixon *et al.*, 2011). In addition, LUX association to the *PRR7* promoter was not found (Helfer *et al.*, 2011). Other

transcriptional target of ELF3 could be identified by the isolation of ELF3-DNA complexes by ChIP, followed by DNA sequencing [ChIP-Seq, (Kaufmann *et al.*, 2010)] or DNA hybridization to Arabidopsis arrays [ChIP-ChIP, (Kaufmann *et al.*, 2010)]. Additionally, a complementation line of ELF3 fused to the glucocorticoid receptor (ELF3-GR) could be used to identify direct targets of ELF3 transcriptional regulation (Sчена *et al.*, 1991). ELF3-GR would be constrained in the cytoplasm until application of dexamethasone. For the experiment, ELF3-GR plants could be treated with a protein-synthesis inhibitor and dexamethasone. Changes in gene expression after ELF3 nuclear action could be identified by microarray hybridization or RNA-seq. Genes up or down-regulated would be the direct targets of ELF3 action.

Arabidopsis clock components can often act as transcriptional activators and repressors. In section 5.1.6, I discussed such a dual role for CCA1. It is unknown if ELF3 can also act as a transcriptional activator. *elf3* mutants display arrhythmic-marginal levels of *LHY* expression. In my experiments, I observed rhythmic low levels of *LHY:LUC* in *elf3-12*, *elf4-1* *ELF3-OX* and *YFP-ELF3MC*. Hence, ELF3 could mediate both rhythmicity and total transcript accumulation of *LHY*. To test this hypothesis, ELF3 association to *LHY* promoter could be tested.

5.2.4 Mechanism of cooperative LUX and ELF3 action

Both ELF3 and LUX associate to the Conserved Region 1 of the *PRR9* promoter, and both associations correlate to transcriptional repression of *PRR9*. Moreover, both *ELF3-OX* and *LUX-OX* could bypass the circadian dysfunction of *elf4*. *LUX-OX* could not restore *elf3* arrhythmicity phenotype. It remains to be determined whether *ELF3-OX* could restore *lux* phenotype. Since there is not a *lux* null allele in *Ws* background, transgenic lines expressing an antisense microRNA (*amirLUX*) were generated both in both in the wild type and *ELF3-OX* backgrounds (Figure 5.6A). Preliminary characterization of *LHY:LUC* rhythms support a cooperative role of *LUX* and *ELF3* to sustain rhythmicity of *LHY:LUC* (Figure 5.6). The reduction of *LUX* levels by *amirLUX* in the wild type led to a reduction in the periodicity and the amplitude of *LHY:LUC* (Figure 5.6 C). This phenotype resembled that of *elf3-12* (Figure 4.2), suggesting that low levels of *LUX* lead to an attenuated *ELF3* function. Recently, it was reported that LUX repress its own expression by association to a LBS present in its promoter. In *ELF3-OX* a down-regulation of LUX transcript was found (Figure 5.6B). This is consistent with a cooperative-repressive action of *ELF3* and *LUX*. In the *ELF3-OX amirLUX* double-transgenic the oscillations of *LHY* became arrhythmic with

an increase in *LHY LUC* (Figure 5.6D). This suggests that *LUX* is required for *ELF3-OX* function. Further characterization of these *amirLUX* lines will assist to characterize *ELF3-LUX* genetic interaction.

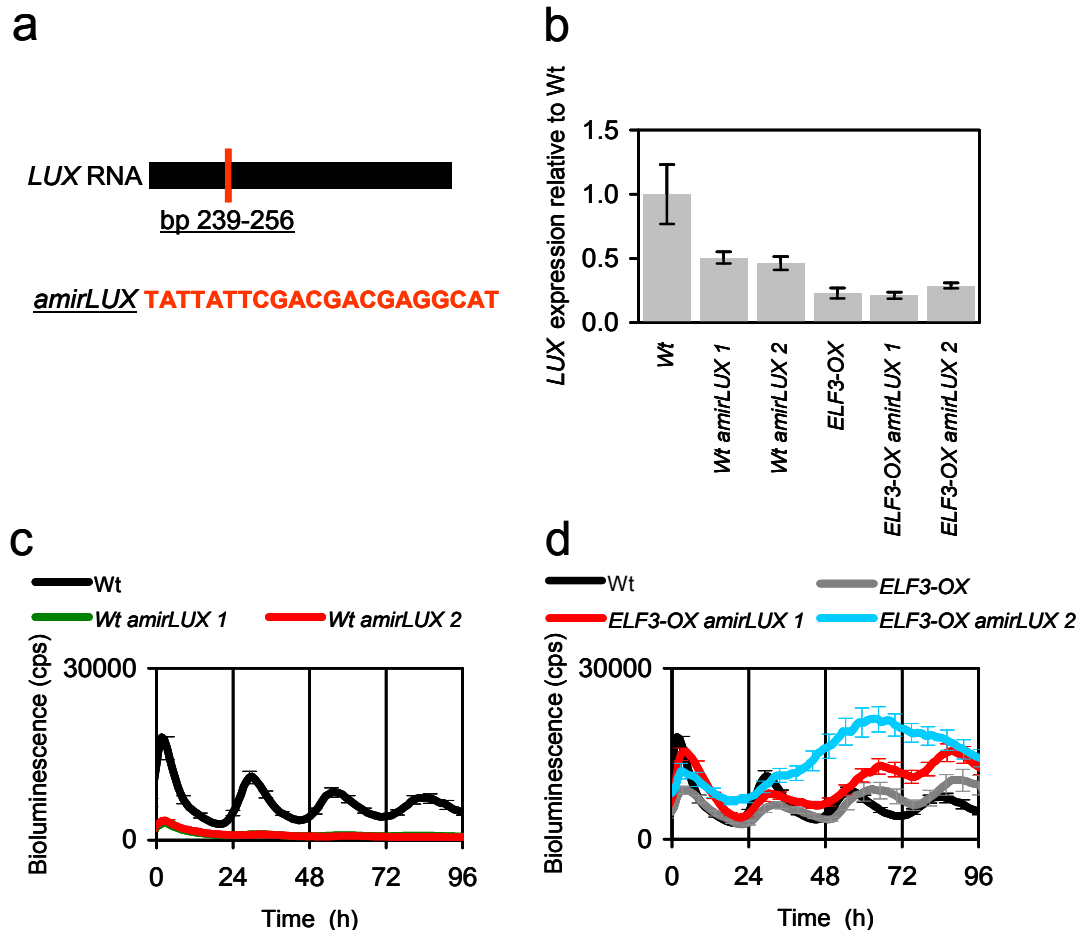


Figure 5.6. Understanding *LUX-ELF3* cooperative action.

a, sequence of *LUX* antisense microRNA (*amirLUX*).

b, *LUX* expression relative to Wt of two independent *amirLUX* lines in the wild type, and in the *ELF3-OX* background. Tissue samples for RNA extraction were collected at ZT 8.

c and **d**, free-running profile of *LHY:LUC* in (c) Wt and two Wt *amirLUX* lines, and (b) in the Wt, *ELF3-OX*, and two *ELF3-OX amirLUX* lines (d)

It was expected that *ELF3* could physically associate to *LUX*. This interaction could not be detected in a Y2-H assay (data not shown). However, my results together the observation that *LUX* and *ELF3* associate to the same region of the *PRR9* promoter [Figure 3.12, (Helfer *et al.*, 2011)], strongly suggest that *ELF3* and *LUX* could interact *in planta*. Transgenic resources generated here could test this. Since *YFP-ELF3MC* line led to complementation of *elf3* circadian arrhythmicity, it is likely that *ELF3 LUX*-binding-domain in *ELF3* is contained within this *ELF3MC* region. To test this possibility, co-immunoprecipitation experiments could be performed with *LUX*,

ELF3MC, and different ELF3MC sub-fragments. Within the ELF3MC fragment there is a highly conserved proline-rich region (Figure 4.4). Such proline-rich regions have been found to mediate interaction with GARP transcription factors (Tamai *et al.*, 2002). It is tempting to speculate that the proline-rich region of ELF3 mediates association with LUX.

The hierarchy of ELF3-ELF4-LUX complex formation could be tested within the *PRR9* promoter (Figure 5.2). The combination of ChIP experiments with the quantification of *PRR9* circadian transcript-accumulation could correlate the hierarchy of ELF3-ELF4-LUX complex assembly to in the repression of *PRR9* expression. If ELF4 affects ELF3 recruitment to the *PRR9* promoter, a reduced association of ELF3 would be expected in the *elf4* (Figure 5.2); this would correlate with higher levels of *PRR9*. If ELF3 requires LUX to associate to the *PRR9* promoter, a reduced association would be expected in the presence of low levels of LUX in *ELF3-OX amirLUX* lines; this also would be correlated with higher levels of *PRR9*. In my model, LUX association to the *PRR9* promoter does not depend on ELF3 and ELF4 (Figure 5.2); this could be tested in the *elf3 YPF-LUX* and *elf4 YPF-LUX* lines, respectively. Since LUX requires ELF3 for circadian function, high levels of *PRR9* would be expected in *elf3 YPF-LUX*.

5.2.5 ELF3 biochemical activity

The enzymatic activity of ELF3 remains unknown. ELF3 associates with the *PRR9* promoter and it is required for LUX action. Hence, ELF3 could be act as a transcriptional co-repressor. ELF3 has a glutamine rich region within its C-terminus [Figure 4.4, (Hicks *et al.*, 2001)], and the ELF3C domain was found to be required for circadian function (Figure 3.7). In animal circadian systems, the core component CLK has a glutamine-rich region that is required for its HAT activity (Doi *et al.*, 2006). However, a HAT activity of ELF3 is not expected since ELF3 seems to be involved in transcriptional repression. ELF3 essential role could lead to the recruitment of chromatin remodeling complexes to the *PRR9* promoter.

Recently, histone methylation function has been linked to circadian function in Arabidopsis. *JMD5* encodes for a histone methyltransferase, and it is co-expressed with ELF3 at dusk (Jones *et al.*, 2010). *jmd5* mutants displayed a weak light-dependent short-periodicity phenotype (Jones *et al.*, 2010). ELF3 could associate with JMD5 to mediate transcriptional repression at dusk. This scenario could be tested by examine ELF3-JMD5 physical interaction and JMD5 association to the *PRR9* promoter.

Additionally, co-localization studies of ELF3 and members of chromatin remodeling complexes could be performed.

5.2.6 Towards a mechanism for Aschoff's rule

The functional relevance of ELF3-phyB interaction has not been determined (Carre, 2002). In my thesis, I have found that ELF3 associated to phyB through ELF3N domain (Figure 3.8), and that this domain was not required for ELF3 circadian function (Figure 3.7). I proposed a hypothesis where phyB-ELF3 binding attenuates ELF3 action on lengthening circadian periodicity. This hypothesis could provide one mechanism for Aschoff's rule in Arabidopsis. To physiologically expand on this, the free-running period of *YFP-ELF3*, *YFP-ELF3MC*, and *elf3-12* under increasing intensities of Rc, Bc and Rc+Bc could be compared. For this, fluence-rate curves could be constructed.

One biochemical mechanism for Aschoff's rule could be found in the context of transcriptional regulation at the *PRR9* locus. On one hand, *PRR9* expression is repressed by ELF3-ELF4 complex. *ELF3-OX*, *ELF4-OX* and *prp9* displayed long-period rhythms [Figure 3.2, (Ito *et al.*, 2003)]. On the other hand, *PRR9* expression is activated by light through a phyB-dependent process (Ito *et al.*, 2003; Ito *et al.*, 2005). *PRR9-OX* and *elf3-12* both displayed short-periodicity phenotypes [(Matsushika *et al.*, 2002a), Figure 4.2]. Moreover, the *elf3-12* short period phenotype was light-dependent and was enhanced by *PHYB-OX* (Figure 4.3). Hence, phyB might activate *PRR9* expression by direct interaction with ELF3 and subsequent inactivation of ELF3-ELF3 repressor complex. This acceleration would thus be by repressing a repressor. To test this scenario, ChIP experiments could be performed with *YFP-ELF3* and *YFP-ELF3MC* lines at subjective night (zt \approx 14-16), comparing association to *PRR9* promoter in the darkness or under extended light. After some hours in DD (zt \approx 14-16), phyB action would be marginal, and hence YFP-ELF3 would efficiently bind to *PRR9* promoter. In extended light, phyB action would persist, and this would be seen as a reduced YFP-ELF3 association to the *PRR9* promoter. If YFP-ELF3MC can not be repressed by phyB, there would not be a difference in its association to the *PRR9* promoter in DD or under extended light.

5.2.7 ELF4-phyB competition for ELF3

I have proposed a mechanism where ELF4 and phyB compete for binding to ELF3 (Figure 5.3), and this leads to modulation of ELF3 action. This could be tested by

co-immunoprecipitation experiments where ELF3-phyB or ELF3-ELF4 would be expressed at constant levels, and ELF4 and phyB levels would be gradually increased, respectively. If ELF4 interferes with ELF3-phyB binding, their association would be reduced by ELF4 in a dose-dependent fashion. Conversely, ELF4-ELF3 interaction could be reduced by phyB in a similar fashion. Weak alleles of *elf3*, such as *elf3-12* and *elf3-218*, and weak alleles of *elf4* (Kolmos *et al.*, 2009) could be tested in these experiments to see how they affect ELF4-phyB competition. In this line, it was reported that *toc1* weak alleles diminished the interaction with PRR5 and ZTL (Wang *et al.*, 2010). Isolation of ELF3 alleles defective in phyB interaction would be very interesting. For example, *elf3-212* could be such an allele, since it encodes a residue-change in the ELF3N domain, and it displayed long-period rhythms (Figures 4.5 and Table 4.1).

The timing ELF3-phyB interaction within the circadian day has not been determined. PHYB and ELF3 transcript accumulation is circadian regulated with the highest expression at subjective day and at dusk, respectively (Covington *et al.*, 2001; Toth *et al.*, 2001). phyB NB formation was circadian regulated and preceded the dawn light-on signal (Kircher *et al.*, 1999). ELF3 protein-abundance is rhythmic and it is highest at zt14-16 (Liu *et al.*, 2001). ELF3 was found to bind both inactive (Pr) and active (Pfr) form of phyB (Kolmos, 2007). Hence, ELF3 could conceptually bind phyB both in the nucleus (phyB Pfr) and in the cytoplasm (phyB Pr). If phyB interferes with ELF3 repression of *PRR9*, a nuclear interaction would be expected. This could be tested by co-immunoprecipitation of ELF3-phyB complex in nuclear extracts collected at different times of the day. An ELF3-phyB interaction would be expected both at dusk and at dawn, when both proteins are present in the nucleus. A cytoplasmic ELF3-phyB complex could restrict ELF3 action in the nucleus. This could be tested by co-immunoprecipitation of ELF3-phyB complex in cytosolic fractions collected at different times of the day. The identification of a temporal dynamics of ELF3-phyB binding in both cytoplasm and nucleus would be useful to understand the repressive role of phyB on ELF3 action.

Chapter 6 References

- Ahmad, M., Jarillo, J.A., and Cashmore, A.R.** (1998a). Chimeric proteins between cry1 and cry2 Arabidopsis blue light photoreceptors indicate overlapping functions and varying protein stability. *Plant Cell* **10**, 197-207.
- Ahmad, M., Jarillo, J.A., Smirnova, O., and Cashmore, A.R.** (1998b). The CRY1 blue light photoreceptor of Arabidopsis interacts with phytochrome A in vitro. *Mol Cell* **1**, 939-948.
- Alabadi, D., Oyama, T., Yanovsky, M.J., Harmon, F.G., Mas, P., and Kay, S.A.** (2001). Reciprocal regulation between TOC1 and LHY/CCA1 within the Arabidopsis circadian clock. *Science* **293**, 880-883.
- Allen, T., Koustenis, A., Theodorou, G., Somers, D.E., Kay, S.A., Whitelam, G.C., and Devlin, P.F.** (2006). Arabidopsis FHY3 specifically gates phytochrome signaling to the circadian clock. *Plant Cell* **18**, 2506-2516.
- Anderson, S.L., Somers, D.E., Millar, A.J., Hanson, K., Chory, J., and Kay, S.A.** (1997). Attenuation of phytochrome A and B signaling pathways by the Arabidopsis circadian clock. *Plant Cell* **9**, 1727-1743.
- Andronis, C., Barak, S., Knowles, S.M., Sugano, S., and Tobin, E.M.** (2008). The clock protein CCA1 and the bZIP transcription factor HY5 physically interact to regulate gene expression in Arabidopsis. *Mol Plant* **1**, 58-67.
- Aschoff, J.** (1979). Circadian rhythms: influences of internal and external factors on the period measured in constant conditions. *Z Tierpsychol* **49**, 225-249.
- Batschauer, A., Banerjee, R., and Pokorny, R.** (2007). *Cryptochromes*. (Blackwell Publishing Ltd).
- Baudry, A., Ito, S., Song, Y.H., Strait, A.A., Kiba, T., Lu, S., Henriques, R., Pruneda-Paz, J.L., Chua, N.H., Tobin, E.M., Kay, S.A., and Imaizumi, T.** (2010). F-box proteins FKF1 and LKP2 act in concert with ZEITLUPE to control Arabidopsis clock progression. *Plant Cell* **22**, 606-622.
- Bauer, D., Viczian, A., Kircher, S., Nobis, T., Nitschke, R., Kunkel, T., Panigrahi, K.C., Adam, E., Fejes, E., Schafer, E., and Nagy, F.** (2004). Constitutive photomorphogenesis 1 and multiple photoreceptors control degradation of phytochrome interacting factor 3, a transcription factor required for light signaling in Arabidopsis. *Plant Cell* **16**, 1433-1445.
- Boffelli, D., McAuliffe, J., Ovcharenko, D., Lewis, K.D., Ovcharenko, I., Pachter, L., and Rubin, E.M.** (2003). Phylogenetic Shadowing of Primate Sequences to Find Functional Regions of the Human Genome. *Science* **299**, 1391-1394.
- Cao, S., Ye, M., and Jiang, S.** (2005). Involvement of GIGANTEA gene in the regulation of the cold stress response in Arabidopsis. *Plant Cell Rep* **24**, 683-690.
- Carre, I.A.** (2002). ELF3: a circadian safeguard to buffer effects of light. *Trends Plant Sci* **7**, 4-6.
- Chen, M.** (2008). Phytochrome nuclear body: an emerging model to study interphase nuclear dynamics and signaling. *Curr Opin Plant Biol* **11**, 503-508.
- Chen, M., Galvao, R.M., Li, M., Burger, B., Bugea, J., Bolado, J., and Chory, J.** (2010). Arabidopsis HEMERA/pTAC12 initiates photomorphogenesis by phytochromes. *Cell* **141**, 1230-1240.
- Cheng, P., Yang, Y., Gardner, K.H., and Liu, Y.** (2002). PAS domain-mediated WC-1/WC-2 interaction is essential for maintaining the steady-state level of WC-1 and the function of both proteins in circadian clock and light responses of Neurospora. *Mol Cell Biol* **22**, 517-524.
- Chou, M.L., and Yang, C.H.** (1999). Late-flowering genes interact with early-flowering genes to regulate flowering time in Arabidopsis thaliana. *Plant Cell Physiol* **40**, 702-708.
- Corbesier, L., Vincent, C., Jang, S., Fornara, F., Fan, Q., Searle, I., Giakountis, A., Farrona, S., Gissot, L., Turnbull, C., and Coupland, G.** (2007). FT Protein Movement Contributes to Long-Distance Signaling in Floral Induction of Arabidopsis. *Science* **316**, 1030-1033.
- Covington, M.F., and Harmer, S.L.** (2007). The circadian clock regulates auxin signaling and responses in Arabidopsis. *PLoS Biol* **5**, e222.
- Covington, M.F., Maloof, J.N., Straume, M., Kay, S.A., and Harmer, S.L.** (2008). Global transcriptome analysis reveals circadian regulation of key pathways in plant growth and development. *Genome Biol* **9**, R130.
- Covington, M.F., Panda, S., Liu, X.L., Strayer, C.A., Wagner, D.R., and Kay, S.A.** (2001). ELF3 modulates resetting of the circadian clock in Arabidopsis. *Plant Cell* **13**, 1305-1315.

- Davis, A.M., Hall, A., Millar, A.J., Darrah, C., and Davis, S.J. (2009). Protocol: Streamlined sub-protocols for floral-dip transformation and selection of transformants in *Arabidopsis thaliana*. *Plant Methods* **5**, 3.
- de Montaigu, A., Toth, R., and Coupland, G. (2010). Plant development goes like clockwork. *Trends Genet* **26**, 296-306.
- Devlin, P.F. (2002). Signs of the time: environmental input to the circadian clock. *J Exp Bot* **53**, 1535-1550.
- Devlin, P.F., and Kay, S.A. (2000a). Flower arranging in *Arabidopsis*. *Science* **288**, 1600-1602.
- Devlin, P.F., and Kay, S.A. (2000b). Cryptochromes are required for phytochrome signaling to the circadian clock but not for rhythmicity. *Plant Cell* **12**, 2499-2510.
- Devlin, P.F., and Kay, S.A. (2001). CIRCADIAN PHOTOPERCEPTION. *Annu. Rev. Physiol.* **63**, 677-694.
- Ding, Z., Doyle, M.R., Amasino, R.M., and Davis, S.J. (2007). A complex genetic interaction between *Arabidopsis thaliana* TOC1 and CCA1/LHY in driving the circadian clock and in output regulation. *Genetics* **176**, 1501-1510.
- Dixon, L.E., Knox, K., Kozma-Bognar, L., Southern, M.M., Pokhilko, A., and Millar, A.J. (2011). Temporal repression of core circadian genes is mediated through EARLY FLOWERING 3 in *Arabidopsis*. *Curr Biol* **21**, 120-125.
- Dodd, A.N., Salathia, N., Hall, A., Kevei, E., Toth, R., Nagy, F., Hibberd, J.M., Millar, A.J., and Webb, A.A. (2005). Plant circadian clocks increase photosynthesis, growth, survival, and competitive advantage. *Science* **309**, 630-633.
- Doi, M., Hirayama, J., and Sassone-Corsi, P. (2006). Circadian regulator CLOCK is a histone acetyltransferase. *Cell* **125**, 497-508.
- Dowson-Day, M.J., and Millar, A.J. (1999). Circadian dysfunction causes aberrant hypocotyl elongation patterns in *Arabidopsis*. *Plant J* **17**, 63-71.
- Doyle, M.R., Davis, S.J., Bastow, R.M., McWatters, H.G., Kozma-Bognar, L., Nagy, F., Millar, A.J., and Amasino, R.M. (2002). The ELF4 gene controls circadian rhythms and flowering time in *Arabidopsis thaliana*. *Nature* **419**, 74-77.
- Dunlap, J.C., Loros, J.J., and DeCoursey, P.J. (2004). Chronobiology Biological Timekeeping.
- Farre, E.M., Harmer, S.L., Harmon, F.G., Yanovsky, M.J., and Kay, S.A. (2005). Overlapping and distinct roles of PRR7 and PRR9 in the *Arabidopsis* circadian clock. *Curr Biol* **15**, 47-54.
- Finkelstein, R., Gampala, S.S., Lynch, T.J., Thomas, T.L., and Rock, C.D. (2005). Redundant and distinct functions of the ABA response loci ABA-INSENSITIVE(ABI)5 and ABRE-BINDING FACTOR (ABF)3. *Plant Mol Biol* **59**, 253-267.
- Fukamatsu, Y., Mitsui, S., Yasuhara, M., Tokioka, Y., Ihara, N., Fujita, S., and Kiyosue, T. (2005). Identification of LOV KELCH PROTEIN2 (LKP2)-interacting factors that can recruit LKP2 to nuclear bodies. *Plant Cell Physiol* **46**, 1340-1349.
- Fukushima, A., Kusano, M., Nakamichi, N., Kobayashi, M., Hayashi, N., Sakakibara, H., Mizuno, T., and Saito, K. (2009). Impact of clock-associated *Arabidopsis* pseudo-response regulators in metabolic coordination. *Proc Natl Acad Sci U S A* **106**, 7251-7256.
- Gekakis, N., Staknis, D., Nguyen, H.B., Davis, F.C., Wilsbacher, L.D., King, D.P., Takahashi, J.S., and Weitz, C.J. (1998). Role of the CLOCK protein in the mammalian circadian mechanism. *Science* **280**, 1564-1569.
- Gendrel, A.-V., Lippman, Z., Martienssen, R., and Colot, V. (2005). Profiling histone modification patterns in plants using genomic tiling microarrays. *Nat Meth* **2**, 213-218.
- Graf, A., Schlereth, A., Stitt, M., and Smith, A.M. (2010). Circadian control of carbohydrate availability for growth in *Arabidopsis* plants at night. *Proc Natl Acad Sci U S A*.
- Green, R.M., Tingay, S., Wang, Z.Y., and Tobin, E.M. (2002). Circadian rhythms confer a higher level of fitness to *Arabidopsis* plants. *Plant Physiol* **129**, 576-584.
- Greene, E.A., Codomo, C.A., Taylor, N.E., Henikoff, J.G., Till, B.J., Reynolds, S.H., Enns, L.C., Burtner, C., Johnson, J.E., Odden, A.R., Comai, L., and Henikoff, S. (2003). Spectrum of Chemically Induced Mutations From a Large-Scale Reverse-Genetic Screen in *Arabidopsis*. *Genetics* **164**, 731-740.
- Gwinner, E. (2003). Circannual rhythms in birds. *Current Opinion in Neurobiology* **13**, 770-778.
- Hall, A., Bastow, R.M., Davis, S.J., Hanano, S., McWatters, H.G., Hibberd, V., Doyle, M.R., Sung, S., Halliday, K.J., Amasino, R.M., and Millar, A.J. (2003). The TIME FOR

- COFFEE gene maintains the amplitude and timing of Arabidopsis circadian clocks. *Plant Cell* **15**, 2719-2729.
- Hanano, S., and Davis, S.J.** (2007). Mind the clock. *Plant Signal Behav* **2**, 477-479.
- Hanano, S., Domagalska, M.A., Nagy, F., and Davis, S.J.** (2006). Multiple phytohormones influence distinct parameters of the plant circadian clock. *Genes Cells* **11**, 1381-1392.
- Hanano, S., Stracke, R., Jakoby, M., Merkle, T., Domagalska, M.A., Weisshaar, B., and Davis, S.J.** (2008). A systematic survey in Arabidopsis thaliana of transcription factors that modulate circadian parameters. *BMC Genomics* **9**, 182.
- Harmer, S.L.** (2009). The circadian system in higher plants. *Annu Rev Plant Biol* **60**, 357-377.
- Harmer, S.L., and Kay, S.A.** (2005). Positive and negative factors confer phase-specific circadian regulation of transcription in Arabidopsis. *Plant Cell* **17**, 1926-1940.
- Harmer, S.L., Hogenesch, J.B., Straume, M., Chang, H.S., Han, B., Zhu, T., Wang, X., Kreps, J.A., and Kay, S.A.** (2000). Orchestrated transcription of key pathways in Arabidopsis by the circadian clock. *Science* **290**, 2110-2113.
- Hazen, S.P., Schultz, T.F., Pruneda-Paz, J.L., Borevitz, J.O., Ecker, J.R., and Kay, S.A.** (2005). LUX ARRHYTHMO encodes a Myb domain protein essential for circadian rhythms. *Proc Natl Acad Sci U S A* **102**, 10387-10392.
- Heintzen, C., Nater, M., Apel, K., and Staiger, D.** (1997). AtGRP7, a nuclear RNA-binding protein as a component of a circadian-regulated negative feedback loop in Arabidopsis thaliana. *Proc Natl Acad Sci U S A* **94**, 8515-8520.
- Helfer, A., Nusinow, D.A., Chow, B.Y., Gehrke, A.R., Bulyk, M.L., and Kay, S.A.** (2011). LUX ARRHYTHMO Encodes a Nighttime Repressor of Circadian Gene Expression in the Arabidopsis Core Clock. *Current Biology In Press, Corrected Proof*.
- Hicks, K.A., Albertson, T.M., and Wagner, D.R.** (2001). EARLY FLOWERING3 encodes a novel protein that regulates circadian clock function and flowering in Arabidopsis. *Plant Cell* **13**, 1281-1292.
- Hicks, K.A., Millar, A.J., Carre, I.A., Somers, D.E., Straume, M., Meeks-Wagner, D.R., and Kay, S.A.** (1996). Conditional circadian dysfunction of the Arabidopsis early-flowering 3 mutant. *Science* **274**, 790-792.
- Hiltbrunner, A., Nagy, F., and Schäfer, E.** (2007). *Phytochromes*. (Blackwell Publishing Ltd).
- Hong, C.I., Ruoff, P., Loros, J.J., and Dunlap, J.C.** (2008). Closing the circadian negative feedback loop: FRQ-dependent clearance of WC-1 from the nucleus. *Genes Dev* **22**, 3196-3204.
- Hubbard, K.E., Robertson, F.C., Dalchau, N., and Webb, A.A.** (2009). Systems analyses of circadian networks. *Mol Biosyst* **5**, 1502-1511.
- Hung, H.C., Maurer, C., Zorn, D., Chang, W.L., and Weber, F.** (2009). Sequential and compartment-specific phosphorylation controls the life cycle of the circadian CLOCK protein. *J Biol Chem* **284**, 23734-23742.
- Huq, E., Tepperman, J.M., and Quail, P.H.** (2000). GIGANTEA is a nuclear protein involved in phytochrome signaling in Arabidopsis. *Proc Natl Acad Sci U S A* **97**, 9789-9794.
- Ito, S., Nakamichi, N., Matsushika, A., Fujimori, T., Yamashino, T., and Mizuno, T.** (2005). Molecular dissection of the promoter of the light-induced and circadian-controlled APRR9 gene encoding a clock-associated component of Arabidopsis thaliana. *Biosci Biotechnol Biochem* **69**, 382-390.
- Ito, S., Matsushika, A., Yamada, H., Sato, S., Kato, T., Tabata, S., Yamashino, T., and Mizuno, T.** (2003). Characterization of the APRR9 pseudo-response regulator belonging to the APRR1/TOC1 quintet in Arabidopsis thaliana. *Plant Cell Physiol* **44**, 1237-1245.
- James, P., Halladay, J., and Craig, E.A.** (1996). Genomic libraries and a host strain designed for highly efficient two-hybrid selection in yeast. *Genetics* **144**, 1425-1436.
- Jang, S., Marchal, V., Panigrahi, K.C., Wenkel, S., Soppe, W., Deng, X.W., Valverde, F., and Coupland, G.** (2008). Arabidopsis COP1 shapes the temporal pattern of CO accumulation conferring a photoperiodic flowering response. *Embo J* **27**, 1277-1288.
- Jarillo, J.A., Capel, J., Tang, R.H., Yang, H.Q., Alonso, J.M., Ecker, J.R., and Cashmore, A.R.** (2001). An Arabidopsis circadian clock component interacts with both CRY1 and phyB. *Nature* **410**, 487-490.
- Jones, M.** (2009). Entrainment of the Arabidopsis Circadian Clock. *Journal of Plant Biology* **52**, 202-209.

- Jones, M.A., Covington, M.F., Ditacchio, L., Vollmers, C., Panda, S., and Harmer, S.L. (2010). Jumonji domain protein JMJD5 functions in both the plant and human circadian systems. *Proc Natl Acad Sci U S A*.
- Kalamvoki, M., and Roizman, B. (2010). Circadian CLOCK histone acetyl transferase localizes at ND10 nuclear bodies and enables herpes simplex virus gene expression. *Proceedings of the National Academy of Sciences* **107**, 17721-17726.
- Kaufmann, K., Muino, J.M., Osteras, M., Farinelli, L., Krajewski, P., and Angenent, G.C. (2010). Chromatin immunoprecipitation (ChIP) of plant transcription factors followed by sequencing (ChIP-SEQ) or hybridization to whole genome arrays (ChIP-CHIP). *Nat. Protocols* **5**, 457-472.
- Kevei, E., Gyula, P., Hall, A., Kozma-Bognar, L., Kim, W.Y., Eriksson, M.E., Toth, R., Hanano, S., Feher, B., Southern, M.M., Bastow, R.M., Viczian, A., Hibberd, V., Davis, S.J., Somers, D.E., Nagy, F., and Millar, A.J. (2006). Forward genetic analysis of the circadian clock separates the multiple functions of ZEITLUPE. *Plant Physiol* **140**, 933-945.
- Khanna, R., Kikis, E.A., and Quail, P.H. (2003). EARLY FLOWERING 4 functions in phytochrome B-regulated seedling de-etiolation. *Plant Physiol* **133**, 1530-1538.
- Kiba, T., Henriques, R., Sakakibara, H., and Chua, N.H. (2007). Targeted degradation of PSEUDO-RESPONSE REGULATOR5 by an SCFZTL complex regulates clock function and photomorphogenesis in *Arabidopsis thaliana*. *Plant Cell* **19**, 2516-2530.
- Kikis, E.A., Khanna, R., and Quail, P.H. (2005). ELF4 is a phytochrome-regulated component of a negative-feedback loop involving the central oscillator components CCA1 and LHY. *Plant J* **44**, 300-313.
- Kim, W.Y., Hicks, K.A., and Somers, D.E. (2005). Independent roles for EARLY FLOWERING 3 and ZEITLUPE in the control of circadian timing, hypocotyl length, and flowering time. *Plant Physiol* **139**, 1557-1569.
- Kim, W.Y., Fujiwara, S., Suh, S.S., Kim, J., Kim, Y., Han, L., David, K., Putterill, J., Nam, H.G., and Somers, D.E. (2007). ZEITLUPE is a circadian photoreceptor stabilized by GIGANTEA in blue light. *Nature* **449**, 356-360.
- Kircher, S., Kozma-Bognar, L., Kim, L., Adam, E., Harter, K., Schafer, E., and Nagy, F. (1999). Light quality-dependent nuclear import of the plant photoreceptors phytochrome A and B. *Plant Cell* **11**, 1445-1456.
- Kircher, S., Gil, P., Kozma-Bognar, L., Fejes, E., Speth, V., Husselstein-Muller, T., Bauer, D., Adam, E., Schafer, E., and Nagy, F. (2002). Nucleocytoplasmic partitioning of the plant photoreceptors phytochrome A, B, C, D, and E is regulated differentially by light and exhibits a diurnal rhythm. *Plant Cell* **14**, 1541-1555.
- Knowles, S.M., Lu, S.X., and Tobin, E.M. (2008). Testing time: can ethanol-induced pulses of proposed oscillator components phase shift rhythms in *Arabidopsis*? *J Biol Rhythms* **23**, 463-471.
- Kolmos, E. (2007). Genetic Analysis of two Evening Genes in the *Arabidopsis thaliana* Circadian Clock. PhD Thesis.
- Kolmos, E., Schoof, H., Plumer, M., and Davis, S.J. (2008). Structural insights into the function of the core-circadian factor TIMING OF CAB2 EXPRESSION 1 (TOC1). *J Circadian Rhythms* **6**, 3.
- Kolmos, E., Nowak, M., Werner, M., Fischer, K., Schwarz, G., Mathews, S., Schoof, H., Nagy, F., Bujnicki, J.M., and Davis, S.J. (2009). Integrating ELF4 into the circadian system through combined structural and functional studies. *Hfsp J* **3**, 350-366.
- Koncz, C., and Schell, J. (1986). The promoter of TL-DNA gene 5 controls the tissue-specific expression of chimaeric genes carried by a novel type of *Agrobacterium* binary vector. *Molecular and General Genetics MGG* **204**, 383-396.
- Kondratov, R.V., Chernov, M.V., Kondratova, A.A., Gorbacheva, V.Y., Gudkov, A.V., and Antoch, M.P. (2003). BMAL1-dependent circadian oscillation of nuclear CLOCK: posttranslational events induced by dimerization of transcriptional activators of the mammalian clock system. *Genes & Development* **17**, 1921-1932.
- Kume, K., Zylka, M.J., Sriram, S., Shearman, L.P., Weaver, D.R., Jin, X., Maywood, E.S., Hastings, M.H., and Reppert, S.M. (1999). mCRY1 and mCRY2 are essential components of the negative limb of the circadian clock feedback loop. *Cell* **98**, 193-205.
- Kyriacou, C. (2009). Clocks, cryptochromes and Monarch migrations. *Journal of Biology* **8**, 55.

- Lee, J., Lee, Y., Lee, M.J., Park, E., Kang, S.H., Chung, C.H., Lee, K.H., and Kim, K. (2008). Dual Modification of BMAL1 by SUMO2/3 and Ubiquitin Promotes Circadian Activation of the CLOCK/BMAL1 Complex. *Mol. Cell. Biol.* **28**, 6056-6065.
- Lee, J., He, K., Stolic, V., Lee, H., Figueroa, P., Gao, Y., Tongprasit, W., Zhao, H., Lee, I., and Deng, X.W. (2007). Analysis of transcription factor HY5 genomic binding sites revealed its hierarchical role in light regulation of development. *Plant Cell* **19**, 731-749.
- Lee, K.K., and Workman, J.L. (2007). Histone acetyltransferase complexes: one size doesn't fit all. *Nat Rev Mol Cell Biol* **8**, 284-295.
- Li, G., Siddiqui, H., Teng, Y., Lin, R., Wan, X., Li, J., Lau, O., Ouyang, X., Dai, M., Wan, J., Devlin, P., Deng, X., and Wang, H. (2011). Coordinated Transcriptional Regulation Underlying the Circadian Clock in Arabidopsis. *Nat Cell Biol.*
- Lin, C., Yang, H., Guo, H., Mockler, T., Chen, J., and Cashmore, A.R. (1998). Enhancement of blue-light sensitivity of Arabidopsis seedlings by a blue light receptor cryptochrome 2. *Proc Natl Acad Sci U S A* **95**, 2686-2690.
- Lin, R., Ding, L., Casola, C., Ripoll, D.R., Feschotte, C., and Wang, H. (2007). Transposase-derived transcription factors regulate light signaling in Arabidopsis. *Science* **318**, 1302-1305.
- Liu, X.L., Covington, M.F., Fankhauser, C., Chory, J., and Wagner, D.R. (2001). ELF3 encodes a circadian clock-regulated nuclear protein that functions in an Arabidopsis PHYB signal transduction pathway. *Plant Cell* **13**, 1293-1304.
- Locke, J.C., Kozma-Bognar, L., Gould, P.D., Feher, B., Kevei, E., Nagy, F., Turner, M.S., Hall, A., and Millar, A.J. (2006). Experimental validation of a predicted feedback loop in the multi-oscillator clock of Arabidopsis thaliana. *Mol Syst Biol* **2**, 59.
- Loop, S., Katzer, M., and Pieler, T. (2005). mPER1-mediated nuclear export of mCRY1/2 is an important element in establishing circadian rhythm. *EMBO Rep* **6**, 341-347.
- Lorkovic, Z.J., Hilscher, J., and Barta, A. (2004). Use of Fluorescent Protein Tags to Study Nuclear Organization of the Spliceosomal Machinery in Transiently Transformed Living Plant Cells. *Mol. Biol. Cell* **15**, 3233-3243.
- Lorrain, S., Allen, T., Duek, P.D., Whitelam, G.C., and Fankhauser, C. (2008). Phytochrome-mediated inhibition of shade avoidance involves degradation of growth-promoting bHLH transcription factors. *Plant J* **53**, 312-323.
- Lu, S.X., Knowles, S.M., Andronis, C., Ong, M.S., and Tobin, E.M. (2009). CIRCADIAN CLOCK ASSOCIATED1 and LATE ELONGATED HYPOCOTYL function synergistically in the circadian clock of Arabidopsis. *Plant Physiol* **150**, 834-843.
- Lu, S.X., Knowles, S.M., Webb, C.J., Celaya, R.B., Cha, C., Siu, J.P., and Tobin, E.M. (2010). The Jumonji C Domain-Containing Protein JM30 Regulates Period Length in the Arabidopsis Circadian Clock. *Plant Physiol* **155**, 906-915.
- Martin-Tryon, E.L., Kreps, J.A., and Harmer, S.L. (2007). GIGANTEA acts in blue light signaling and has biochemically separable roles in circadian clock and flowering time regulation. *Plant Physiol* **143**, 473-486.
- Mas, P., Devlin, P.F., Panda, S., and Kay, S.A. (2000). Functional interaction of phytochrome B and cryptochrome 2. *Nature* **408**, 207-211.
- Mas, P., Kim, W.Y., Somers, D.E., and Kay, S.A. (2003). Targeted degradation of TOC1 by ZTL modulates circadian function in Arabidopsis thaliana. *Nature* **426**, 567-570.
- Matera, A.G., Izaguirre-Sierra, M., Praveen, K., and Rajendra, T.K. (2009). Nuclear bodies: random aggregates of sticky proteins or crucibles of macromolecular assembly? *Dev Cell* **17**, 639-647.
- Matsushika, A., Imamura, A., Yamashino, T., and Mizuno, T. (2002a). Aberrant expression of the light-inducible and circadian-regulated APRR9 gene belonging to the circadian-associated APRR1/TOC1 quintet results in the phenotype of early flowering in Arabidopsis thaliana. *Plant Cell Physiol* **43**, 833-843.
- Matsushika, A., Makino, S., Kojima, M., Yamashino, T., and Mizuno, T. (2002b). The APRR1/TOC1 quintet implicated in circadian rhythms of Arabidopsis thaliana: II. Characterization with CCA1-overexpressing plants. *Plant Cell Physiol* **43**, 118-122.
- McCallum, C.M., Comai, L., Greene, E.A., and Henikoff, S. (2000). Targeting Induced Local Lesions IN Genomes (TILLING) for Plant Functional Genomics. *Plant Physiol.* **123**, 439-442.
- McWatters, H.G., Bastow, R.M., Hall, A., and Millar, A.J. (2000). The ELF3 zeitnehmer regulates light signalling to the circadian clock. *Nature* **408**, 716-720.

- McWatters, H.G., Kolmos, E., Hall, A., Doyle, M.R., Amasino, R.M., Gyula, P., Nagy, F., Millar, A.J., and Davis, S.J.** (2007). ELF4 is required for oscillatory properties of the circadian clock. *Plant Physiol* **144**, 391-401.
- Mehra, A., Baker, C.L., Loros, J.J., and Dunlap, J.C.** (2009). Post-translational modifications in circadian rhythms. *Trends Biochem Sci* **34**, 483-490.
- Menet, J.S., Abruzzi, K.C., Desrochers, J., Rodriguez, J., and Rosbash, M.** (2010). Dynamic PER repression mechanisms in the *Drosophila* circadian clock: from on-DNA to off-DNA. *Genes Dev* **24**, 358-367.
- Meyer, P., Saez, L., and Young, M.W.** (2006). PER-TIM interactions in living *Drosophila* cells: an interval timer for the circadian clock. *Science* **311**, 226-229.
- Michael, T.P., and McClung, C.R.** (2002). Phase-specific circadian clock regulatory elements in *Arabidopsis*. *Plant Physiol* **130**, 627-638.
- Michael, T.P., Mockler, T.C., Breton, G., McEntee, C., Byer, A., Trout, J.D., Hazen, S.P., Shen, R., Priest, H.D., Sullivan, C.M., Givan, S.A., Yanovsky, M., Hong, F., Kay, S.A., and Chory, J.** (2008). Network discovery pipeline elucidates conserved time-of-day-specific cis-regulatory modules. *PLoS Genet* **4**, e14.
- Michaels, S.D., and Amasino, R.M.** (2001). High Throughput Isolation of DNA and RNA in 96-Well Format Using a Paint Shaker. *Plant Mol. Biol. Rep.* **19**, 227-233.
- Millar, A.J., and Kay, S.A.** (1996). Integration of circadian and phototransduction pathways in the network controlling CAB gene transcription in *Arabidopsis*. *Proc Natl Acad Sci U S A* **93**, 15491-15496.
- Millar, A.J., Short, S.R., Chua, N.H., and Kay, S.A.** (1992). A novel circadian phenotype based on firefly luciferase expression in transgenic plants. *Plant Cell* **4**, 1075-1087.
- Millar, A.J., Straume, M., Chory, J., Chua, N.H., and Kay, S.A.** (1995a). The regulation of circadian period by phototransduction pathways in *Arabidopsis*. *Science* **267**, 1163-1166.
- Millar, A.J., Carre, I.A., Strayer, C.A., Chua, N.H., and Kay, S.A.** (1995b). Circadian clock mutants in *Arabidopsis* identified by luciferase imaging. *Science* **267**, 1161-1163.
- Mizoguchi, T., Wright, L., Fujiwara, S., Cremer, F., Lee, K., Onouchi, H., Mouradov, A., Fowler, S., Kamada, H., Putterill, J., and Coupland, G.** (2005). Distinct roles of GIGANTEA in promoting flowering and regulating circadian rhythms in *Arabidopsis*. *Plant Cell* **17**, 2255-2270.
- Nakamichi, N., Kita, M., Ito, S., Yamashino, T., and Mizuno, T.** (2005). PSEUDO-RESPONSE REGULATORS, PRR9, PRR7 and PRR5, together play essential roles close to the circadian clock of *Arabidopsis thaliana*. *Plant Cell Physiol* **46**, 686-698.
- Nakamichi, N., Kiba, T., Henriques, R., Mizuno, T., Chua, N.H., and Sakakibara, H.** (2010). PSEUDO-RESPONSE REGULATORS 9, 7, and 5 are transcriptional repressors in the *Arabidopsis* circadian clock. *Plant Cell* **22**, 594-605.
- Nozue, K., Covington, M.F., Duek, P.D., Lorrain, S., Fankhauser, C., Harmer, S.L., and Maloof, J.N.** (2007). Rhythmic growth explained by coincidence between internal and external cues. *Nature* **448**, 358-361.
- O'Neill, J.S., and Reddy, A.B.** (2011). Circadian clocks in human red blood cells. *Nature* **469**, 498-503.
- O'Neill, J.S., van Ooijen, G., Dixon, L.E., Troein, C., Corellou, F., Bouget, F.Y., Reddy, A.B., and Millar, A.J.** (2011). Circadian rhythms persist without transcription in a eukaryote. *Nature* **469**, 554-558.
- Oda, A., Fujiwara, S., Kamada, H., Coupland, G., and Mizoguchi, T.** (2004). Antisense suppression of the *Arabidopsis* PIF3 gene does not affect circadian rhythms but causes early flowering and increases FT expression. *FEBS Lett* **557**, 259-264.
- Oka, Y., Matsushita, T., Mochizuki, N., Quail, P.H., and Nagatani, A.** (2008). Mutant screen distinguishes between residues necessary for light-signal perception and signal transfer by phytochrome B. *PLoS Genet* **4**, e1000158.
- Onai, K., and Ishiura, M.** (2005). PHYTOCLOCK 1 encoding a novel GARP protein essential for the *Arabidopsis* circadian clock. *Genes Cells* **10**, 963-972.
- Ouyang, Y., Andersson, C.R., Kondo, T., Golden, S.S., and Johnson, C.H.** (1998). Resonating circadian clocks enhance fitness in cyanobacteria. *Proceedings of the National Academy of Sciences of the United States of America* **95**, 8660-8664.
- Palagyi, A., Terecskei, K., Adam, E., Kevei, E., Kircher, S., Merai, Z., Schafer, E., Nagy, F., and Kozma-Bognar, L.** (2010). Functional analysis of amino-terminal domains of the photoreceptor phytochrome B. *Plant Physiol* **153**, 1834-1845.

- Perales, M., and Mas, P.** (2007). A functional link between rhythmic changes in chromatin structure and the Arabidopsis biological clock. *Plant Cell* **19**, 2111-2123.
- Perales, M., Portoles, S., and Mas, P.** (2006). The proteasome-dependent degradation of CKB4 is regulated by the Arabidopsis biological clock. *Plant J* **46**, 849-860.
- Pfluger, J., and Wagner, D.** (2007). Histone modifications and dynamic regulation of genome accessibility in plants. *Curr Opin Plant Biol* **10**, 645-652.
- Picot, E., Krusche, P., Tiskin, A., Carre, I., and Ott, S.** (2010). Evolutionary analysis of regulatory sequences (EARS) in plants. *Plant J* **64**, 165-176.
- Pokhilko, A., Hodge, S.K., Stratford, K., Knox, K., Edwards, K.D., Thomson, A.W., Mizuno, T., and Millar, A.J.** (2010). Data assimilation constrains new connections and components in a complex, eukaryotic circadian clock model. *Mol Syst Biol* **6**, 416.
- Portoles, S., and Mas, P.** (2010). The functional interplay between protein kinase CK2 and CCA1 transcriptional activity is essential for clock temperature compensation in Arabidopsis. *PLoS Genet* **6**, e1001201.
- Pruneda-Paz, J.L., Breton, G., Para, A., and Kay, S.A.** (2009). A functional genomics approach reveals CHE as a component of the Arabidopsis circadian clock. *Science* **323**, 1481-1485.
- Qi, Y., and Katagiri, F.** (2009). Purification of low-abundance Arabidopsis plasma-membrane protein complexes and identification of candidate components. *The Plant Journal* **57**, 932-944.
- Reed, J.W., Nagpal, P., Bastow, R.M., Solomon, K.S., Dowson-Day, M.J., Elumalai, R.P., and Millar, A.J.** (2000). Independent action of ELF3 and phyB to control hypocotyl elongation and flowering time. *Plant Physiol* **122**, 1149-1160.
- Roden, L.C., and Ingle, R.A.** (2009). Lights, rhythms, infection: the role of light and the circadian clock in determining the outcome of plant-pathogen interactions. *Plant Cell* **21**, 2546-2552.
- Rosbash, M.** (2009). The implications of multiple circadian clock origins. *PLoS Biol* **7**, e62.
- Rozen, S., and Skaletsky, H.** (2000). Primer3 on the WWW for general users and for biologist programmers. *Methods Mol Biol* **132**, 365-386.
- Salome, P.A., Michael, T.P., Kearns, E.V., Fett-Neto, A.G., Sharrock, R.A., and McClung, C.R.** (2002). The out of phase 1 mutant defines a role for PHYB in circadian phase control in Arabidopsis. *Plant Physiol* **129**, 1674-1685.
- Schaffer, R., Ramsay, N., Samach, A., Corden, S., Putterill, J., Carre, I.A., and Coupland, G.** (1998). The late elongated hypocotyl mutation of Arabidopsis disrupts circadian rhythms and the photoperiodic control of flowering. *Cell* **93**, 1219-1229.
- Schena, M., Lloyd, A.M., and Davis, R.W.** (1991). A steroid-inducible gene expression system for plant cells. *Proc Natl Acad Sci U S A* **88**, 10421-10425.
- Schomburg, F.M., Patton, D.A., Meinke, D.W., and Amasino, R.M.** (2001). FPA, a Gene Involved in Floral Induction in Arabidopsis, Encodes a Protein Containing RNA-Recognition Motifs. *The Plant Cell Online* **13**, 1427-1436.
- Schoning, J.C., Streitner, C., Page, D.R., Hennig, S., Uchida, K., Wolf, E., Furuya, M., and Staiger, D.** (2007). Auto-regulation of the circadian slave oscillator component AtGRP7 and regulation of its targets is impaired by a single RNA recognition motif point mutation. *Plant J* **52**, 1119-1130.
- Schwerdtfeger, C., and Linden, H.** (2000). Localization and light-dependent phosphorylation of white collar 1 and 2, the two central components of blue light signaling in *Neurospora crassa*. *Eur J Biochem* **267**, 414-422.
- Sharrock, R.A., and Quail, P.H.** (1989). Novel phytochrome sequences in Arabidopsis thaliana: structure, evolution, and differential expression of a plant regulatory photoreceptor family. *Genes Dev* **3**, 1745-1757.
- Shen, H., Moon, J., and Huq, E.** (2005). PIF1 is regulated by light-mediated degradation through the ubiquitin-26S proteasome pathway to optimize photomorphogenesis of seedlings in Arabidopsis. *Plant J* **44**, 1023-1035.
- Shen, Y., Khanna, R., Carle, C.M., and Quail, P.H.** (2007). Phytochrome induces rapid PIF5 phosphorylation and degradation in response to red-light activation. *Plant Physiol* **145**, 1043-1051.
- Sigrist, C.J.A., Cerutti, L., de Castro, E., Langendijk-Genevaux, P.S., Bulliard, V., Bairoch, A., and Hulo, N.** (2010). PROSITE, a protein domain database for functional characterization and annotation. *Nucleic Acids Research* **38**, D161-D166.

- Somers, D.E., Devlin, P.F., and Kay, S.A.** (1998). Phytochromes and cryptochromes in the entrainment of the Arabidopsis circadian clock. *Science* **282**, 1488-1490.
- Southern, M.M., and Millar, A.J.** (2005). Circadian genetics in the model higher plant, *Arabidopsis thaliana*. *Methods Enzymol* **393**, 23-35.
- Spensley, M., Kim, J.Y., Picot, E., Reid, J., Ott, S., Helliwell, C., and Carre, I.A.** (2009). Evolutionarily conserved regulatory motifs in the promoter of the Arabidopsis clock gene LATE ELONGATED HYPOCOTYL. *Plant Cell* **21**, 2606-2623.
- Stemple, D.L.** (2004). TILLING [mdash] a high-throughput harvest for functional genomics. *Nat Rev Genet* **5**, 145-150.
- Strasser, B., Sanchez-Lamas, M., Yanovsky, M.J., Casal, J.J., and Cerdan, P.D.** (2010). *Arabidopsis thaliana* life without phytochromes. *Proc Natl Acad Sci U S A* **107**, 4776-4781.
- Strayer, C., Oyama, T., Schultz, T.F., Raman, R., Somers, D.E., Mas, P., Panda, S., Kreps, J.A., and Kay, S.A.** (2000). Cloning of the Arabidopsis clock gene TOC1, an autoregulatory response regulator homolog. *Science* **289**, 768-771.
- Suarez-Lopez, P., Wheatley, K., Robson, F., Onouchi, H., Valverde, F., and Coupland, G.** (2001). CONSTANS mediates between the circadian clock and the control of flowering in Arabidopsis. *Nature* **410**, 1116-1120.
- Tajima, T., Oda, A., Nakagawa, M., Kamada, H., and Mizoguchi, T.** (2007). Natural variation of polyglutamine repeats of a circadian clock gene ELF3 in Arabidopsis. *Plant Biotechnology* **24**, 237-240.
- Tamai, H., Iwabuchi, M., and Meshi, T.** (2002). Arabidopsis GARP transcriptional activators interact with the Pro-rich activation domain shared by G-box-binding bZIP factors. *Plant Cell Physiol* **43**, 99-107.
- Tamaru, T., Isojima, Y., van der Horst, G.T., Takei, K., Nagai, K., and Takamatsu, K.** (2003). Nucleocytoplasmic shuttling and phosphorylation of BMAL1 are regulated by circadian clock in cultured fibroblasts. *Genes Cells* **8**, 973-983.
- Tessadori, F., Schulkes, R.K., van Driel, R., and Fransz, P.** (2007). Light-regulated large-scale reorganization of chromatin during the floral transition in Arabidopsis. *Plant J* **50**, 848-857.
- Tessadori, F., van Zanten, M., Pavlova, P., Clifton, R., Pontvianne, F., Snoek, L.B., Millenaar, F.F., Schulkes, R.K., van Driel, R., Voesenek, L.A., Spillane, C., Pikaard, C.S., Fransz, P., and Peeters, A.J.** (2009). Phytochrome B and histone deacetylase 6 control light-induced chromatin compaction in Arabidopsis thaliana. *PLoS Genet* **5**, e1000638.
- Thines, B., and Harmon, F.G.** (2010). Ambient temperature response establishes ELF3 as a required component of the core Arabidopsis circadian clock. *Proc Natl Acad Sci U S A* **107**, 3257-3262.
- Toth, R., Kevei, E., Hall, A., Millar, A.J., Nagy, F., and Kozma-Bognar, L.** (2001). Circadian clock-regulated expression of phytochrome and cryptochrome genes in Arabidopsis. *Plant Physiol* **127**, 1607-1616.
- Untergasser, A., Nijveen, H., Rao, X., Bisseling, T., Geurts, R., and Leunissen, J.A.** (2007). Primer3Plus, an enhanced web interface to Primer3. *Nucleic Acids Res* **35**, W71-74.
- Valverde, F., Mouradov, A., Soppe, W., Ravenscroft, D., Samach, A., and Coupland, G.** (2004). Photoreceptor regulation of CONSTANS protein in photoperiodic flowering. *Science* **303**, 1003-1006.
- Van Norman, J.M., Frederick, R.L., and Sieburth, L.E.** (2004). BYPASS1 negatively regulates a root-derived signal that controls plant architecture. *Curr Biol* **14**, 1739-1746.
- van Zanten, M., Tessadori, F., McLoughlin, F., Smith, R., Millenaar, F.F., van Driel, R., Voesenek, L.A., Peeters, A.J., and Fransz, P.** (2010). Photoreceptors CRYPTOCHROME2 and phytochrome B control chromatin compaction in Arabidopsis. *Plant Physiol* **154**, 1686-1696.
- Viczian, A., Kircher, S., Fejes, E., Millar, A.J., Schafer, E., Kozma-Bognar, L., and Nagy, F.** (2005). Functional characterization of phytochrome interacting factor 3 for the Arabidopsis thaliana circadian clockwork. *Plant Cell Physiol* **46**, 1591-1602.
- Voinnet, O., Rivas, S., Mestre, P., and Baulcombe, D.** (2003). An enhanced transient expression system in plants based on suppression of gene silencing by the p19 protein of tomato bushy stunt virus. *Plant J* **33**, 949-956.

- Wang, L., Fujiwara, S., and Somers, D.E.** (2010). PRR5 regulates phosphorylation, nuclear import and subnuclear localization of TOC1 in the Arabidopsis circadian clock. *Embo J* **29**, 1903-1915.
- Wang, W., Barnaby, J.Y., Tada, Y., Li, H., Tor, M., Caldelari, D., Lee, D.U., Fu, X.D., and Dong, X.** (2011). Timing of plant immune responses by a central circadian regulator. *Nature* **470**, 110-114.
- Wang, Z.Y., and Tobin, E.M.** (1998). Constitutive expression of the CIRCADIAN CLOCK ASSOCIATED 1 (CCA1) gene disrupts circadian rhythms and suppresses its own expression. *Cell* **93**, 1207-1217.
- Yamamoto, Y., Sato, E., Shimizu, T., Nakamich, N., Sato, S., Kato, T., Tabata, S., Nagatani, A., Yamashino, T., and Mizuno, T.** (2003). Comparative genetic studies on the APRR5 and APRR7 genes belonging to the APRR1/TOC1 quintet implicated in circadian rhythm, control of flowering time, and early photomorphogenesis. *Plant Cell Physiol* **44**, 1119-1130.
- Yanovsky, M.J., Mazzella, M.A., and Casal, J.J.** (2000). A quadruple photoreceptor mutant still keeps track of time. *Curr Biol* **10**, 1013-1015.
- Yu, J.W., Rubio, V., Lee, N.Y., Bai, S., Lee, S.Y., Kim, S.S., Liu, L., Zhang, Y., Irigoyen, M.L., Sullivan, J.A., Zhang, Y., Lee, I., Xie, Q., Paek, N.C., and Deng, X.W.** (2008). COP1 and ELF3 control circadian function and photoperiodic flowering by regulating GI stability. *Mol Cell* **32**, 617-630.
- Zagotta, M.T., Hicks, K.A., Jacobs, C.I., Young, J.C., Hangarter, R.P., and Meeks-Wagner, D.R.** (1996). The Arabidopsis ELF3 gene regulates vegetative photomorphogenesis and the photoperiodic induction of flowering. *Plant J* **10**, 691-702.
- Zeilinger, M.N., Farre, E.M., Taylor, S.R., Kay, S.A., and Doyle, F.J., 3rd.** (2006). A novel computational model of the circadian clock in Arabidopsis that incorporates PRR7 and PRR9. *Mol Syst Biol* **2**, 58.

Appendix 1

Period and phase estimates from *elf3* TILLING lines. Figures 4.7 to 4.12, and Table 4.2

App1 Table 1 Period and phase values of *GI:LUC* for *elf3*-TILLING lines under LD to LL.

LD to LL <i>elf3</i> allele	Period (h)			Circadian Phase (h)		
	Mean	SEM	Difference	Mean	SEM	Difference
201	—	—	—	—	—	—
202	—	—	—	—	—	—
203	—	—	—	—	—	—
204	26.84	0.20	-0.07	12.36	0.69	<u>2.35</u>
205	26.72	0.21	-0.19	11.95	0.64	<u>1.94</u>
206	—	—	—	—	—	—
207	—	—	—	—	—	—
208	—	—	—	—	—	—
209	—	—	—	—	—	—
210	25.59	0.19	<u>-1.32</u>	11.86	0.66	<u>1.85</u>
211	26.04	0.16	<u>-0.87</u>	11.70	0.48	<u>1.69</u>
212	26.73	0.23	0.59	11.47	0.64	<u>-1.18</u>
213	27.03	0.19	0.12	11.83	0.46	<u>1.82</u>
214	26.30	0.19	<u>-0.61</u>	11.61	0.47	<u>1.60</u>
215	—	—	—	—	—	—
216	26.58	0.22	-0.33	11.22	0.50	1.21
217	26.78	0.28	-0.13	12.30	0.80	<u>2.29</u>
218	25.86	0.28	<u>-1.05</u>	12.62	0.67	<u>2.61</u>
219	27.57	0.21	<u>0.66</u>	9.62	0.41	-0.40
220	27.01	0.19	0.10	11.52	0.61	<u>1.51</u>
221	—	—	—	—	—	—
222	—	—	—	—	—	—
223	—	—	—	—	—	—
224	27.29	0.22	0.38	10.94	0.69	0.93
225	arrhythmic			arrhythmic		
226	27.10	0.23	0.19	10.70	0.56	0.69
227	26.68	0.26	-0.23	10.44	0.60	0.43
228	26.52	0.23	-0.39	11.50	0.53	1.49
229	—	—	—	—	—	—
230	—	—	—	—	—	—
231	27.17	0.25	0.26	11.92	0.61	<u>1.91</u>
<i>er105</i>	26.91	0.20		10.01	0.60	
<i>col0</i>	26.14	0.30		12.65	0.63	

For this experiment plants were entrained for 7 days under LD cycles at constant temperature, and then circadian rhythms were assayed under LL. Period and phase mean values were calculated by averaging two independent experiments. SEM, pooled standard error of the mean pooled from the two experiments. Difference indicates deviation from wild type values: *Col0* was used as wild type for line *elf3-212*, and *er-105* was used as wild type for the rest of the lines. Underlined values indicate statistically significant differences (pvalue < 0.05). — indicates not determined. Color code defines position of residue change within ELF3 domains: ELF3N (pink), ELF3M (green), and ELF3C (blue). From Figure 4.7.

App1 Table 2 Period and phase values of *GI:LUC* for *elf3*-TILLING lines under WC to LL.

WC to LL <i>elf3</i> allele	Period (h)			Circadian Phase (h)		
	Mean	SEM	Difference	Mean	SEM	Difference
201	—	—	—	—	—	—
202	—	—	—	—	—	—
203	—	—	—	—	—	—
204	26.82	0.25	<u>0.48</u>	15.02	0.19	<u>0.61</u>
205	26.23	0.13	-0.11	15.57	0.30	<u>1.16</u>
206	—	—	—	—	—	—
207	—	—	—	—	—	—
208	—	—	—	—	—	—
209	—	—	—	—	—	—
210	25.76	0.26	<u>-0.58</u>	14.50	0.28	0.09
211	26.09	0.18	-0.25	14.90	0.31	0.49
212	26.63	0.18	0.64	14.86	0.33	-0.09
213	26.28	0.14	-0.07	16.03	0.72	<u>1.62</u>
214	26.37	0.17	0.03	15.08	0.26	0.67
215	—	—	—	—	—	—
216	26.56	0.19	0.21	14.94	0.26	0.53
217	26.42	0.24	0.08	13.54	0.33	-0.87
218	25.93	0.26	-0.41	14.98	0.56	0.57
219	26.85	0.18	<u>0.51</u>	14.86	0.33	0.45
220	26.53	0.18	0.19	15.38	0.26	0.97
221	—	—	—	—	—	—
222	—	—	—	—	—	—
223	—	—	—	—	—	—
224	26.81	0.21	<u>0.47</u>	15.77	0.28	<u>1.36</u>
225	arrhythmic			arrhythmic		
226	26.58	0.23	0.24	14.16	0.37	-0.25
227	26.37	0.27	0.03	14.40	0.26	-0.01
228	26.71	0.31	0.36	14.48	0.31	0.07
229	—	—	—	—	—	—
230	—	—	—	—	—	—
231	26.46	0.24	0.11	15.18	0.29	0.77
<i>er105</i>	26.34	0.20		14.41	0.29	
<i>col0</i>	25.99	0.17		14.95	0.21	

For this experiment plants were entrained for 7 days under WC cycles under constant light, and then circadian rhythms were assayed under LL. Period and phase mean values were calculated by averaging two independent experiments. SEM, pooled standard error of the mean pooled from the two experiments. Difference indicates deviation from wild type values: *Col0* was used as wild type for line *elf3-212*, and *er-105* was used as wild type for the rest of the lines. Underlined values indicate statistically significant differences (pvalue < 0.05). — indicates not determined. Color code defines position of residue change within ELF3 domains: ELF3N (pink), ELF3M (green), and ELF3C (blue). From Figure 4.8.

App1 Table 3 Period and phase values of *GI:LUC* for *elf3*-TILLING lines under LD to DD.

LD to DD <i>elf3</i> allele	Period (h)			Circadian Phase (h)		
	Mean	SEM	Difference	Mean	SEM	Difference
201	27.31	0.44	-0.04	12.46	0.95	0.45
202	26.80	0.41	-0.55	11.97	1.47	-0.04
203	—	—	—	—	—	—
204	26.93	0.35	-0.43	10.97	0.97	-1.05
205	26.51	0.25	<u>-0.85</u>	12.90	0.94	0.89
206	—	—	—	—	—	—
207	—	—	—	—	—	—
208	26.76	0.31	-0.60	12.75	1.00	0.73
209	27.11	0.21	-0.24	13.03	0.95	1.01
210	—	—	—	—	—	—
211	27.22	0.22	0.28	11.98	0.34	-0.04
212	27.05	0.32	-0.31	12.38	0.82	-1.04
213	26.83	0.25	-0.52	11.94	0.86	-0.08
214	—	—	—	—	—	—
215	27.06	0.18	-0.30	10.25	0.63	<u>-1.77</u>
216	—	—	—	—	—	—
217	—	—	—	—	—	—
218	26.84	0.39	-0.51	11.04	0.91	-0.98
219	27.11	0.24	-0.24	10.79	0.63	-1.23
220	27.63	0.25	0.28	10.17	0.60	-1.85
221	26.76	0.31	-0.59	12.59	1.02	0.57
222	27.97	0.36	<u>0.62</u>	11.90	1.07	-0.12
223	27.71	0.23	0.35	11.86	0.88	-0.16
224	27.29	0.29	-0.07	12.92	1.03	0.90
225	arrhythmic			arrhythmic		
226	26.76	0.28	<u>-0.59</u>	14.97	1.00	<u>2.95</u>
227	27.02	0.25	-0.34	12.45	1.01	0.43
228	—	—	—	—	—	—
229	—	—	—	—	—	—
230	—	—	—	—	—	—
231	27.02	0.48	-0.34	13.91	1.21	1.90
<i>er105</i>	27.35	0.31		12.02	1.08	
<i>col0</i>	26.94	0.26		13.42	0.95	

For this experiment plants were entrained for 7 days under LD cycles at constant temperature, and then circadian rhythms were assayed in DD. Period and phase mean values were calculated by averaging two independent experiments. SEM, pooled standard error of the mean pooled from the two experiments. Difference indicates deviation from wild type values: *Col0* was used as wild type for line *elf3-212*, and *er-105* was used as wild type for the rest of the lines. Underlined values indicate statistically significant differences (pvalue < 0.05). — indicates not determined. Color code defines position of residue change within ELF3 domains: ELF3N (pink), ELF3M (green), and ELF3C (blue). From Figure 4.9.

App1 Table 4 Period and phase values of *GI:LUC* for *elf3*-TILLING lines under WC to DD.

WC to DD <i>elf3</i> allele	Period (h)			Circadian Phase (h)		
	Mean	SEM	Difference	Mean	SEM	Difference
201	27.65	0.35	0.01	14.01	0.71	<u>2.34</u>
202	27.37	0.25	-0.26	12.08	0.84	0.41
203	—	—	—	—	—	—
204	27.17	0.26	-0.47	12.66	0.92	0.98
205	27.07	0.22	-0.56	13.05	0.66	1.38
206	—	—	—	—	—	—
207	—	—	—	—	—	—
208	27.20	0.21	-0.43	12.00	0.74	0.33
209	26.86	0.21	<u>-0.78</u>	12.64	0.79	0.97
210	—	—	—	—	—	—
211	28.14	0.30	0.51	11.86	0.81	0.19
212	27.20	0.22	0.00	11.17	1.13	-0.52
213	27.14	0.20	-0.49	13.11	0.74	1.44
214	—	—	—	—	—	—
215	26.91	0.29	-0.72	13.26	0.77	1.59
216	—	—	—	—	—	—
217	—	—	—	—	—	—
218	26.49	0.29	<u>-1.14</u>	14.22	0.78	<u>2.55</u>
219	27.34	0.20	-0.30	13.39	0.59	<u>1.72</u>
220	27.06	0.24	<u>-0.58</u>	11.83	0.73	0.16
221	28.20	0.26	0.57	10.59	0.65	-1.09
222	28.05	0.25	0.41	11.60	0.64	-0.07
223	27.35	0.26	-0.29	13.58	0.75	<u>1.91</u>
224	27.91	0.20	0.28	11.19	0.60	-0.48
225	arrhythmic			arrhythmic		
226	26.78	0.26	<u>-0.86</u>	14.45	0.81	2.78
227	27.06	0.09	-0.57	13.17	0.81	1.50
228	—	—	—	—	—	—
229	—	—	—	—	—	—
230	—	—	—	—	—	—
231	26.72	0.33	-0.92	13.67	1.03	2.00
<i>er105</i>	27.63	0.31		11.67	0.88	
<i>col0</i>	27.20	0.23		11.69	0.50	

For this experiment plants were entrained for 7 days under WC cycles under constant light, and then circadian rhythms were assayed in DD. Period and phase mean values were calculated by averaging two independent experiments. SEM, pooled standard error of the mean pooled from the two experiments. Difference indicates deviation from wild type values: *Col0* was used as wild type for line *elf3-212*, and *er-105* was used as wild type for the rest of the lines. Underlined values indicate statistically significant differences (p value < 0.05). — indicates not determined. Color code defines position of residue change within ELF3 domains: ELF3N (pink), ELF3M (green), and ELF3C (blue). From Figure 4.10.

App1 Table 5 Period and phase values of *GI:LUC* for *elf3*-TILLING lines under LD to Rc.

Rc <i>elf3</i> allele	Period (h)			Circadian Phase (h)		
	Mean	SEM	Difference	Mean	SEM	Difference
201	27.68	0.27	-0.19	12.53	1.00	0.95
202	27.34	0.28	-0.53	10.30	0.68	-1.28
203	27.37	0.18	-0.51	10.98	0.48	-0.60
204	27.71	0.25	-0.16	11.31	0.65	-0.27
205	27.89	0.22	0.01	11.42	0.72	-0.16
206	27.73	0.29	-0.15	11.71	0.73	0.13
207	27.93	0.25	0.05	10.20	0.64	-1.38
208	27.76	0.30	-0.12	11.42	0.74	-0.16
209	27.25	0.25	-0.63	12.05	0.77	0.48
210	27.51	0.32	-0.37	11.07	0.80	-0.51
211	28.27	0.21	0.40	9.48	0.56	-2.10
212	27.58	0.28	0.11	12.46	0.73	0.34
213	27.31	0.26	-0.57	11.78	0.68	0.20
214	27.21	0.24	-0.67	11.43	0.87	-0.15
215	27.52	0.26	-0.36	10.88	0.68	-0.70
216	27.61	0.23	-0.26	12.19	0.70	0.61
217	28.01	0.27	0.13	9.82	0.59	-1.76
218	26.83	0.25	-1.05	11.97	0.63	0.40
219	27.42	0.25	-0.45	12.13	0.83	0.56
220	27.33	0.20	-0.55	11.68	0.68	0.10
221	27.98	0.27	0.10	10.80	0.81	-0.78
222	28.07	0.24	0.19	10.77	0.68	-0.81
223	27.32	0.21	-0.56	11.79	0.50	0.21
224	27.83	0.23	-0.05	10.66	0.64	-0.92
225	arrhythmic			arrhythmic		
226	27.73	0.21	-0.15	10.74	0.50	-0.84
227	27.36	0.28	-0.51	10.60	0.63	-0.98
228	27.36	0.20	-0.52	11.07	0.56	-0.51
229	27.15	0.19	-0.73	11.96	0.72	0.38
230	27.66	0.24	-0.22	11.86	0.74	0.28
231	28.38	0.19	0.51	10.68	0.55	-0.90
<i>er105</i>	27.88	0.31		11.58	0.65	
<i>col0</i>	27.47	0.38		11.85	0.91	

For this experiment plants were entrained for 7 days under LD cycles at constant temperature, and then circadian rhythms were assayed under Rc. Period and phase mean values were calculated by averaging two independent experiments. SEM, pooled standard error of the mean pooled from the two experiments. Difference indicates deviation from wild type values: *Col0* was used as wild type for line *elf3-212*, and *er-105* was used as wild type for the rest of the lines. Underlined values indicate statistically significant differences (pvalue < 0.05). Color code defines position of residue change within ELF3 domains: ELF3N (pink), ELF3M (green), and ELF3C (blue). From Figure 4.11.

App1 Table 6 Period and phase values of *G1:LUC* for *elf3*-TILLING lines under LD to Bc.

Bc <i>elf3</i> allele	Period (h)			Circadian Phase (h)		
	Mean	SEM	Difference	Mean	SEM	Difference
201	24.17	0.15	<u>-0.78</u>	16.42	0.37	-0.23
202	24.49	0.14	-0.46	14.85	0.29	<u>-1.80</u>
203	24.44	0.21	-0.51	17.59	0.46	0.94
204	24.50	0.15	-0.45	17.2	0.44	0.55
205	24.85	0.22	-0.10	17.11	0.31	0.46
206	24.87	0.2	-0.08	16.55	0.38	-0.10
207	24.09	0.13	<u>-0.86</u>	17.14	0.39	0.49
208	24.72	0.25	-0.23	16.13	0.42	-0.52
209	23.89	0.13	<u>-1.06</u>	17.46	0.54	0.81
210	23.92	0.15	<u>-1.03</u>	15.99	0.34	-0.66
211	24.21	0.14	<u>-0.74</u>	16.01	0.31	-0.64
212	25.38	0.25	<u>1.40</u>	16.3	0.48	<u>-1.63</u>
213	24.84	0.29	-0.11	16.86	0.52	0.21
214	24.53	0.21	-0.42	16.96	0.72	0.31
215	24.95	0.26	0.00	16.64	0.61	-0.01
216	25.62	0.18	0.67	16.89	0.5	0.24
217	24.35	0.13	-0.60	15.49	0.52	-1.16
218	23.68	0.26	<u>-1.27</u>	16.59	0.77	-0.06
219	25.80	0.32	0.85	16.12	0.66	-0.53
220	25.55	0.22	0.60	15.8	0.45	-0.85
221	24.89	0.22	-0.06	15.95	0.35	-0.70
222	25.15	0.24	0.20	16.47	0.59	-0.18
223	25.53	0.28	0.58	15.65	0.62	-1.00
224	25.43	0.28	0.48	16.44	0.73	-0.21
225	arrhythmic			arrhythmic		
226	—	—	—	—	—	—
227	—	—	—	—	—	—
228	—	—	—	—	—	—
229	24.89	0.18	-0.06	15.22	0.61	-1.43
230	24.44	0.32	-0.51	15.98	0.58	-0.67
231	24.50	0.31	-0.45	17.63	0.75	0.98
<i>er105</i>	24.95	0.28		16.65	0.69	
<i>col-0</i>	23.98	0.21		17.93	0.37	

For this experiment plants were entrained for 7 days under LD cycles at constant temperature, and then circadian rhythms were assayed under Bc. SEM, standard error of the mean. Difference indicates deviation from wild type values: *Col0* was used as wild type for line *elf3-212*, and *er-105* was used as wild type for the rest of the lines. Underlined values indicate statistically significant differences (p value < 0.05). — indicates not determined. Color code defines position of residue change within ELF3 domains: ELF3N (pink), ELF3M (green), and ELF3C (blue). From Figure 4.12.

Acknowledgments

This thesis reflects my work in the Davis' group for the last three and a half years. I would like to acknowledge Prof. George Coupland for granting me within the IMPRS program in the Coupland Department. I am thankful to Prof. George Coupland and Prof. Ute Hoecker for being the reviewers of my thesis. Also thank you to Prof. Martin Hülskamp for chairing my defense. Thanks to Dr. Franziska Turck for being my second supervisor and my '*Beizitzer*'.

I her am most grateful to Seth Davis for giving me the opportunity to follow my research ideas in this project. I am also most grateful for his support, his guidance, our many discussions, and for sharing my enthusiasm for this project.

Thanks to Elsebeth Kolmos to introduce me to the Davis lab and for her support, particularly during the first year of my PhD. I think our collaboration has proved to be successful.

Thanks to Nora Bujdoso for her support and her collaboration during the last two years.

Thanks to Amanda Davis for her support especially during the last year and her invaluable contribution to keep the Davis lab running.

Thanks to Jieun Shin for her help, her kindness, and her friendship. I could not imagine a better bench-mate.

Thanks to Alfredo Sanchez for sharing the Davis lab experience and for his friendship during these years.

Thanks to Reena Saini her collaboration in the ELF3/4 project

And thanks to the rest of Davis lab former and current members for their contribution to a nice environment in the Davis lab. Thank to all for standing my music.

Thanks to Takayuki Shindo for his wise advice and discussions in the agro-infiltration and protein work.

Thanks to Markus Berns and Prof. George Coupland for their collaboration in the ELF3/4 project.

Thanks to the members of the Coupland Department for creating a great atmosphere.

I will be always grateful to Ana Assunção, Mark Aarts and Maarten Koornneef for their support during my MSc thesis, without it I would not be here.

Thanks to the 2007 IMPRS class for sharing the PhD experience and for their friendship. I hope we can find time for a farewell BBQ!

Thanks to the Spanish community of the MPIPZ for their friendship, especially to Maria Salinas for being always there.

Thanks to my concert-mates, especially to Kerstin Richau, for sharing many great musical-nights.

Me siento enormemente privilegiada por tener una maravillosa y numerosa familia que me ha apoyado durante tantos años. Muchas gracias a mis padres por ser un ejemplo diario de amor, sacrificio, coraje, y humanidad. Gracias también por apoyar mi vocación por la biología, sin vuestro apoyo no estaría ahora terminando esta tesis. A mi madre por aprender a usar Skype para estar más cerca y por sus cientos de horas de conversación. Muchas gracias a todos mis hermanos: Gloria, Tito, Encina, Peche, Carmen, Iciar y Nico. También a la Titi, y a todos mis cuñ@dos y sobrin@s. Muchas gracias a todos por hacerme sentir cerca aun estando lejos.

Thanks to my wonderful Martin for sharing the last seven years of our lives. For endless love and friendship. For believing in us regardless of the distance. For thousands of Germanwings miles and hours on Skype. For wonderful weekends and holidays. And for many sacrifices you are doing for us. Still the best is just about to come. Milujem ta!

Erklärung

Köln, 2011

Ich versichere, dass ich die von mir vorgelegte Dissertation selbständig angefertigt, die benutzen Quellen und Hilfsmittel vollständig angegeben und die Stellen der Arbeit - einschließlich Tabellen, Karten und Abbildungen -, die anderen Werken mit Wortlaut oder dem Sinn nach entnommen sind, in jedem Einzelfall als Entlehnung kenntlich gemacht habe; dass diese Dissertation noch keiner anderen Fakultät oder universität zur Prüfung vorgelegen hat; dass sie noch nicht veröffentlicht worden ist, sowie dass ich eine solche Veröffentlichung vor Abschluss des Promotionsverfahrens nicht vornehmen werde. Die Bestimmungen der Promotionsordnung sind mir bekannt. Die von mir vorgelegte Dissertation ist von Prof. Dr. George Coupland betreut worden.

Max-Planck Institut für Planzenzüchtungsforschung,
Köln, 3 April 2011.

Eva Herrero Serrano

Curriculum vitae

Name Eva Herrero Serrano
Geburtsdatum und -ort 25. Juni 1981
Staatsangehörigkeit spanisch

Forschungserfahrung

Oktober 2007 – voraussichtlich bis Mai 2011

Max Planck Institut für Pflanzenzüchtungsforschung Köln, Deutschland

Projekt Dissecting the molecular basis of ELF3 action at dusk
Position Doktorandin in der International Max Planck Research School
Gruppenleiter Dr. S. J. Davis

Juni 2007 – September 2007

Centre for Plant Integrative Biology (CPIB), Universität Nottingham, UK

Projekt General features and modularity of the Arabidopsis predicted-interactome network
Position Praktikum im Master-Studium
Gruppenleiter Prof. C. Hodgman

Mai 2006 – Dezember 2006

Laboratory of Genetics, Universität Wageningen, NL

Projekt Identification of DNA binding proteins that interact with the promoter of an Arabidopsis zinc transporter
Position Masterstudent zur Anfertigung der Master-Arbeit
Gruppenleiter Dr. M.A. K. Aarts

April 2005 – August 2005

Agrotechnology and Food Innovations, Wageningen, NL

Projekt Improvement of pulp paper qualities using enzymes
Position Leonardo DaVinci Firmen-Praktikum
Gruppenleiter Dr. H. van der Valk

Juni 2003 – August 2003

NEIKER, Baskisches Institut für Agrarwissenschaftliche Forschung und Entwicklung, Abt. Pflanzenproduktion und Pflanzenschutz, Spanien

Projekt Praktikum in Kartoffel-, Mais- und Bohnenzucht
Position Praktikum als Bachelor-Student
Gruppenleiter Dr. J. I. Ruiz de Galarreta Gómez

Universitäre Ausbildung

October 2007 – voraussichtlich Mai 2011

IMPRS-Doktorandin am Max Planck Institut für Pflanzenzüchtungsforschung, Köln und der Universität Köln, Deutschland

September 2005 - September 2007

Master-Studium, Master-Abschluss in Pflanzenbiotechnologie, Universität Wageningen, Niederlande

Abschluss „cum laude“

September 2003 – August 2004

Bachelorabschluss in Biochemie, Universität von Navarra, Pamplona, Spanien

September 2003 – Juni 2004

Erasmus Studentin an der Vrije Universiteit Brussel, Brüssel, Belgien

Einjähriges akademisches Austauschjahr nach dem Inter-University Molecular Biology programme (IMB) mit Fokus auf Protein und Nukleinsäure-Chemie, Gentechnik und Mikrobiologie

September 1999 – Juni 2003

Bachelorabschluss in Biologie, Universität von Navarra, Pamplona, Spanien

Schwerpunkte Grundlegende Biologie und Gesundheit

Erhaltene Forschungsstipendien

2007 3 jähriges Doktorandenstipendium der Max Planck International Research

School, gefördert von der Max Planck Gesellschaft

2005 2 jähriges Stipendium für Vertiefungsstudien in Interessensgebieten des

Baskenlandes, gefördert durch die Regierung des Baskenlandes

Wissenschaftliche Publikationen

Eva Herrero*, Elsebeth Kolmos*, Nora Bujdoso, Ye Yuan, Mengmeng Wang, Markus Berns, George Coupland, Reena Saini, Mariusz Jaskolski, Alex Webb, Jorge Gonçalves & Seth J. Davis; **Effector activation of a co-repressor complex sustains the plant circadian oscillator**; submitted 2011

Elsebeth Kolmos*, Eva Herrero*, Nora Bujdoso, Andrew J. Millar, Reka Toth, Peter Gyula, Ferenc Nagy, Seth J. Davis; **Hypomorphic genetics supports a repressive role for EARLY FLOWERING 3 in the circadian clock**; submitted 2011

Ana G. L. Assunção, Eva Herrero, Ya-Fen Lin, Bruno Huettel, Sangita Talukdar, Cezary Smaczniak, Richard G. H. Immink, Mandy van Eldik, Mark Fiers, Nek Schat and Mark G.M. Aarts. ***Arabidopsis thaliana* transcription factors bZIP19 and bZIP23 regulate the adaption to zinc deficiency.** *Proceedings of the National Academy of Science*, 2010

Konferenzteilnahmen

International Conference of Arabidopsis Research

Yokohama, Japan, Juni 2010; Posterpräsentation und organisationsausschuß

Second Joint Retreat of PhD Students in Experimental Plant Sciences

Köln, Deutschland, April 2010; Posterpräsentation

IMPRS Retreat 2010

Deutschland, März 2010; Vortrag

IMPRS Retreat 2009

Monchau, Deutschland, März 2009; Vortrag

First Joint Retreat of PhD Students in Experimental Plant Sciences

Wageningen, Niederlande, October 2008; Posterpräsentation

IMPRS Retreat 2008

Königswinter, Deutschland, April 2008; Vortrag